

Goldschmidt 2012 Conference Abstracts

Mineralogical Magazine | www.minersoc.org

ADDENDUM

INDEX / TABLE OF CONTENT

A - Goldschmidt Abstracts 2012
pp. 161-164(7)

B - Goldschmidt Abstracts 2012
pp. 164-166(5)

C - Goldschmidt Abstracts 2012
pp. 167-171(10)

D - Goldschmidt Abstracts 2012
pp. 172-173(3)

E - Goldschmidt Abstracts 2012
pp. (0)

F - Goldschmidt Abstracts 2012
pp. 173-174(3)

G - Goldschmidt Abstracts 2012
pp. 175-177(5)

H - Goldschmidt Abstracts 2012
pp. 177(1)

I - Goldschmidt Abstracts 2012
pp. (0)

J - Goldschmidt Abstracts 2012
pp. 178-179(3)

K - Goldschmidt Abstracts 2012
pp. 179-181(5)

L - Goldschmidt Abstracts 2012
pp. 182-184(5)

M - Goldschmidt Abstracts 2012
pp. 184-188(9)

N - Goldschmidt Abstracts 2012
pp. 189(1)

O - Goldschmidt Abstracts 2012
pp. 189(1)

P - Goldschmidt Abstracts 2012
pp. 190(2)

Q - Goldschmidt Abstracts 2012
pp. 191(1)

R - Goldschmidt Abstracts 2012
pp. 191-193(4)

S - Goldschmidt Abstracts 2012
pp. 193-198(11)

T - Goldschmidt Abstracts 2012
pp. 199(1)

U - Goldschmidt Abstracts 2012
pp. (0)

V - Goldschmidt Abstracts 2012
pp. (0)

W - Goldschmidt Abstracts 2012
pp. 199-202(7)

X - Goldschmidt Abstracts 2012
pp. 203-204(3)

Y - Goldschmidt Abstracts 2012
pp. 204-206(4)

Z - Goldschmidt Abstracts 2012
pp. 206-208(5)

Adsorption behaviour of arsenic on goethite and schwertmannite

SABITA AACHARYA^{1*}, HIRONORI OHASHI², GAOWA NAREN¹,
YOSHIHIRO OKAUE¹, TAKUSHI YOKOYAMA¹

¹Faculty of Science, Kyushu University, Fukuoka, Japan

Sabita2010@chem.kyushu-univ.jp (* presenting author)

²Center for Research and Advancement in Higher Education, Kyushu University, Fukuoka, Japan

Introduction

Arsenic released by the oxidation and dissolution of the arsenic containing minerals occurs as a main pollutant in acid mine drainage (AMD) and acid sulfate soil (ASS) systems. Different types of iron minerals are formed by the oxidation or precipitation of AMD depending upon the pH and the precipitation conditions. These include goethite, schwertmannite, ferrihydrite, lepidocrocite and jarosite. Arsenic in AMD impacted areas are naturally attenuated by these minerals present in the system. Among the different iron minerals, goethite (FeOOH) and schwertmannite (Fe₈O₈(OH)_{8-2x}(SO₄)_x, where x ranges from 1 to 1.75) are the common precipitates predominant in AMD systems that retain significant amount of arsenic through adsorption, complexation or precipitation [1, 2]. Many studies related to arsenic adsorption on different iron oxides/hydroxides minerals are available. However, there are only a few studies related to arsenic adsorption onto schwertmannite and also the comparison of adsorption behaviour of arsenic [As(V) and As(III)] between goethite and schwertmannite has rarely been conducted. This study examines the adsorption behaviour of As(III) and As(V) between goethite and schwertmannite as a function of pH, concentration and contact time in order to compare the adsorption capacity and adsorption kinetics of these minerals. Both goethite and schwertmannite were synthesized by the method proposed by Schwertmann and Cornell [3]. Batch adsorption experiments were conducted to evaluate the adsorption behaviour of As(V) and As(III).

Results and Discussion

Both schwertmannite and goethite was found to have higher affinity towards arsenic however, amount of arsenic adsorbed on schwertmannite exceeds to that of goethite. Highest As(III) adsorption was observed on goethite as compared to As(V), whereas, the reverse phenomenon was observed in case of schwertmannite. Arsenic adsorbed on goethite as a function of the equilibrium arsenic concentration fits a Langmuir adsorption isotherm and that of schwertmannite fits a Freundlich adsorption isotherm. The kinetic study of arsenic on goethite and schwertmannite showed that the adsorption reaction seems to be faster for schwertmannite than goethite; however both the adsorption follows the pseudo second order reaction kinetics. Thus, goethite and schwertmannite acts as a good scavenger for arsenic that controls the mobility, bioavailability and fate of arsenic.

[1] Dixit and Hering (2003) *Environ. Sci. Technol* **37**, 4182-4189.

[2] Burton *et al.* (2009) *Environ.Sci.Technol* **43**, 9202-9207.

[3] Schwertmann and Cornell (1991) *Iron oxides in the Laboratory: preparation and Characterization*; VCH: New York.

A new theory of size dependent surface charging of nanoparticles

ABBAS ZAREEN^{*}, NORDHOLM STURE AND AHLBERG
ELISABET

University of Gothenburg, Department of Chemistry and Molecular Biology, Gothenburg, Sweden

zareen@chem.gu.se (* presenting author), ksjn@chem.gu.se,

ela@chem.gu.se

8h. Surface complexation modeling: Contemporary challenges and opportunities

There are some limitations in applying the traditional surface complexation (SC) theory to nanoparticles. For example, in the case of particles of diameter < 25 nm the curvature becomes important and the interface would not be properly modelled by the SC approach, since it is based on Poisson-Boltzmann (PB) theory in which the particle surface is considered as a planar wall. Moreover, ions are considered as point charges neglecting ion-ion correlations, which are important for highly charged surfaces. Corrected Debye-Hückel theory of surface complexation (CDH-SC) is developed [1] to circumvent some of the above mentioned shortcomings of the SC approach. In the CDH theory the particle is considered as a sphere, which can be of any size ranging from 1 nm upward and ions are modelled as charged hard spheres thus ion-ion correlations are included. Proton interaction with the surface site is described by a binding energy and vibrational frequency and not by an equilibrium constant as usually is done in the SC approach. The theoretical results show that experimentally determined pH_{PZC} of different metal oxides can be predicted. The theory has shown good agreement with the experimentally determined surface charging behavior of goethite and TiO₂ [2] at different ionic strength. A special feature of the CDH-SC theory is that the thickness of counter ion layer, which is formed around the charged particle surface at different pH values, can be calculated. The CDH-SC theory also predicts that the surface charge density of particles < 10 nm is much higher than for larger particles, which is in very good agreement with the Monte Carlo simulations as shown in Figure 1.

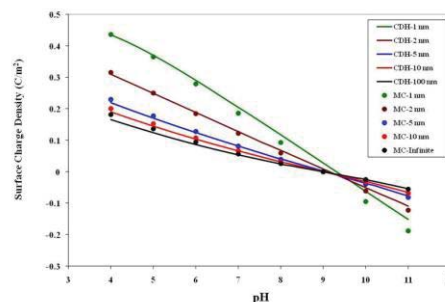


Figure: Size dependent surface charging calculated by CDH-SC theory and Monte Carlo simulations.

[1] Abbas *et al.* (2008) *J. Phys. Chem C* **112**, 5751-5723.

[2] Abbas *et al.* (2011) *Colloids and surfaces A: Physicochem. Eng Aspects* **384**, 254-261.

Binary Boundary Layers and Nd in Paleooceanography

CLAUDE ALLÈGRE^{1*}, ANTOINE COGEZ¹, LAURE MEYNADIER¹,
ERIC LEWIN² AND JEAN-LOUIS LE MOUËL³

¹ Equipe de Géochimie et Cosmochimie, Institut de Physique du Globe de Paris, Sorbonne Paris Cité, Univ Paris Diderot, UMR 7154 CNRS, F-75005 Paris, France, allegre@ipggp.fr (* presenting author)

² Institut des Sciences de la Terre (ISTerre), CNRS : UMR5275 – IFSITTAR – Université de Savoie – Université Joseph Fourier - Grenoble I, France

³ Equipe de Géomagnétisme, Institut de Physique du Globe de Paris, Sorbonne Paris Cité, Univ Paris Diderot, UMR 7154 CNRS, F-75005 Paris, France

Nd isotopic composition measured in oceanic sediment cores varies in space and time. The present modelling of those variations is not fully convincing yet. The residence time computed in a simple way yield numbers like 5000 to 8000 years. Since the mixing time for the ocean are 1500 years the Nd isotope should be uniform at a world scale, such as Sr isotopes. Various ad-hoc assumptions were developed to obtain a residence time of 500 years. The other lack in the various modelling is that rivers inputs are not included in the model even though they are the major source of chemical elements in ocean water.

We surmise that Nd isotopes registered in sediments reflect mainly the activity of two boundary layers : the upper boundary layer often known as the mixing layer and the lower boundary layer which is the interface between soft sediments and bottom seawater. We estimate that at least half of the Nd injected by the rivers into the mixing zone is trapped by the precipitation of Mn as coating around foraminiferae. The Nd residence time in this mixing layer is about 20 to 30 years for Nd. At the bottom of the ocean, part of the Mn oxides is dissolved and consequently some Nd is reinjected into the ocean increasing the Nd concentration in the bottom ocean. We calculate that during less than 1000 years Nd can be exchanged between bottom water and sediment at the water-sediment interface. The effective residence time for the whole system is 400 years.

On this dual structure is superimposed the lateral transfer by oceanic current both at the surface and at the bottom. Therefore the (Nd) signal registered in the sediment is a mixture between surface signal ultimately derived from rivers and transferred vertically to the bottom and lateral input from deep ocean current. The correlation between ϵNd surface and ϵNd bottom permit to distinguish the different geographic areas where the bottom current is a major process and those dominated by surface processes.

We developed a multibox model describing the global transfer of Nd isotopes in the ocean. To define the boxes we use both Ganachaud and Wunch paper (2000) and the Nd isotopes map established by Cögez et al. (this meeting). With this 19 boxes model we reproduce the Nd distribution in the different oceanic domains and constrain both bottom and surface currents intensities.

Trace metal loading of sediments in the apex of the New York Bight: implications for metal transport in a high energy environment

NOUREDDIN AMAACH^{1*}, STEPHEN AJA² AND CECILIA MCHUGH³,

¹Brooklyn College of the City University of New York (* presenting author), Brooklyn, U.S.A., angeoch@aol.com

²Brooklyn College of the City University of New York, Brooklyn, U.S.A., suaja@brooklyn.cuny.edu

³Queens College of the City University of New York, Queens, U.S.A., Cecilia.McHugh@qc.cuny.edu

Introduction

The Apex of the New York Bight (latitude 39°N to 41° N, longitude 72°W to 75°W) encompasses the expanse of shallow ocean constrained by the southern coast of Long Island and the coast of the state of New Jersey (U.S.A.); it extends up to 189 km to the edge of the continental shelf. Bight sediments were presumably deposited after the last glacial maximum. From about 1890 to 1971, the Bight Apex served as an ocean waste disposal center. The waste disposal sites included the sewage sludge site, the mud dump site, the cellar dirt site, acid waste site, the wreck site and a chemical waste dump site just outside the Bight limit; waste disposal in the Bight ceased in the 1990's. In this study, sediments from the Bight area were analyzed to evaluate their trace metal loading and to assess the potential for metal transport in this high energy environment.

Experimental Methods and Results

The sediments used in this study were collected by Harris (1976) and by McHugh (1997). Both set of sediment samples were size fractionated and the fine fractions examined by XRD. The different size fractions were split into duplicates and analyzed for their metal content by first conducting a leaching experiment with a 50% HNO₃, then the resulting filter cakes were digested using HF/HClO₄/HNO₃ solutions. Total whole digestions were also conducted on the duplicates in a single step. Using AAS techniques, the aqueous extracts were then analyzed for their Pb, Cu, Zn, Ni, Cd, Cr and Mn contents.

The mineralogy of the dumpsites was variable; at the mud dump site, the amounts of fine sand, very fine sand and silt and clay were nearly equal whereas in the sewage sludge site, the mineralogy was dominated by silt and clay. Illite was the main clay mineral present in the clay fractions. The trace metals, generally concentrated, in the clay fraction varied from one dump site to the other. In the sewage sludge site, trace metal levels have decreased from hundreds of ppm in 1976 to virtually zero ppm by 1997. In the mud dump site, on the other hand, the metal concentration had decreased 40% (Cd), 44% (Ni), 46% (Zn), 67% (Pb), 87% (Cu), and 88% (Cr) relative to 1976 levels. Apparently, sediment resuspension at the sewage sludge site, correlatable with wave activity, explains this significant recovery over time; in the mud dump site, on the other hand, the differentiated metal behavior suggests a selectivity in trace metal release from the sediments even in this high energy environment.

The $\delta^{34}\text{S}$ of dimethyl sulfide in the surface ocean

AMRANI A.^{1*}, SESSIONS A.², ADKINS J.², DALLESKA N.²,
DEKAS A.², JOHN S.², ORPHAN V.²

¹Earth Sciences Institute, Hebrew University, Jerusalem, Israel,
alon.amrani@mail.huji.ac.il (* presenting author)

²Division of Geological and Planetary Sciences, California Institute
of Technology, Pasadena, CA,

Dimethyl sulfide (DMS) is the major volatile breakdown product of dimethylsulfoniopropionate (DMSP), produced in the oceans by phytoplankton. Massive amounts (13-45 TgS/year) of DMS are released to the atmosphere and profoundly affect the global sulfur cycle. When DMS enters the atmosphere it is rapidly oxidized to sulphate, which is a significant constituent of sub-micrometer aerosols that influence the reflection of solar radiation from the Earth. We studied the $\delta^{34}\text{S}$ values of DMS in surface ocean water in order to constrain estimates of the marine DMS flux to the atmosphere. These are the first direct S-isotopic measurements of DMS in seawater using a new method for the analysis of $\delta^{34}\text{S}$ in individual compounds at trace amounts (picograms). DMS was analyzed by coupling a gas chromatograph to a multicollector inductively-coupled plasma mass spectrometer [1]. Results obtained by this technique show fairly uniform $\delta^{34}\text{S}$ DMS values in surface marine water of about 18-21‰ in all locations – Tasmania, Pacific Costa Rica, and San Pedro, CA. Variations of $\delta^{34}\text{S}$ values in the water column down to 80 m below the surface are relatively small (2-4‰) and appear to correlate with the mixed-layer boundary. This study shows that the $\delta^{34}\text{S}$ values of DMS are distinct from those of anthropogenic sources of sulfate, and therefore enable calculations of isotopic mass balance. However, DMS recoveries in our analyses were low (less than 50%), probably because of degradation of DMS during storage and inefficient transfer to the GC. Despite this, $\delta^{34}\text{S}$ values were quite accurate as determined by multiple purge-and-trap experiments of standard DMS solutions. The average $\delta^{34}\text{S}$ (n=10, stdev=1.1‰) is within 0.4‰ of the known DMS $\delta^{34}\text{S}$ value. Currently, we are improving the trapping, storage, and transfer of DMS to achieve better recovery, precision and accuracy. We use the Gulf of Aqaba, Israel as a natural laboratory to test our new methods and to study the $\delta^{34}\text{S}$ values of DMS in marine water in conjunction with sulphate $\delta^{34}\text{S}$ values in the marine boundary layer.

[1] Amrani, et al., (2009) *Analytical Chemistry*, **81**, 9027-9034.

Uranium mobilisation during the Panafrican metamorphism: implications on Cu-Co-(U) deposits, Domes region, NW Zambia

Anne-Sylvie André-Mayer¹, Aurélien Eglinger^{1*}, Olivier Vanderhaeghe¹, Michel Cuney¹, Cyril Durand², Jean-Louis Feybesse³

¹G2R, Université de Lorraine- *aurelien.eglinger@univ-lorraine.fr

²Géosystèmes, Université de Lille

³AREVA, BU Mines

Introduction

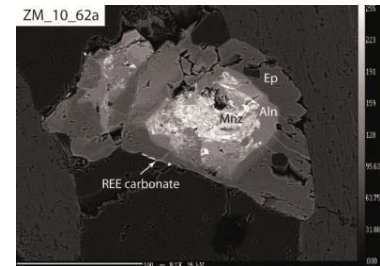
The Lufilian belt formed between the Congo and Kalahari cratons with the evolution of the Gondwana supercontinent during the Panafrican orogeny [1]. This orogenic belt hosts (i) world-class Cu-Co deposits within deformed Katanga metasedimentary rocks and (ii) uranium occurrences with estimated ages of 652.3 ± 7.3 Ma and 530.1 ± 5.9 Ma [2]. Remobilization of a previous syndiagenetic stock of uranium is the metallogenic model proposed in this area. This abstract will focus on the uranium sources.

Geological setting

In domes region, NW Zambia, the uranium deposits of the Katanga Copperbelt are typically hosted in the lower part of the Neoproterozoic Roan Group in sheared contacts between Lower Roan metasediments and gneissic dome. The lower Roan Group is represented by siliciclastic sequence (kyanite micaschist). The Gneiss Formation is characterized by paragneiss, migmatite and peraluminous granite. The uranium mineralization consists of mainly uraninite and brannerite [3].

Results

The petrography of accessory minerals from the gneissic dome is characterized by the presence of allanite, monazite, zircon, apatite, (Th-REE)-silicate and REE carbonate. Monazite grains present a corona texture with allanite and epidote rims (figure). Allanite crystals are strongly altered and filled with newly-formed (Th-REE)-silicate, REE carbonate and apatite.



Discussion

During a hydrothermal event within the gneissic dome rocks, uranium may be leached from refractory accessory minerals such as monazite and allanite. Mass balance calculation indicates that monazite alteration to allanite and allanite alteration to (Th-REE)-silicate and apatite can liberate about $500\text{-}650 \text{ t.km}^{-3}$ of U.

[1] Unrug (1996) *Episodes* **19**, 11-20. [2] Decrée et al. (2011) *Ore Geology Reviews* **40**, 81-89. [3] Cosi et al. (1992) *Precambrian Research*, **58**: 215-240.

Fate of Ni during post depositional transformation of Mn-rich marine sediments

AMY ATKINS^{1*}, SAMUEL SHAW¹ AND CAROLINE L. PEACOCK¹

¹School of Earth & Environment, University of Leeds, Leeds, UK, jhs5aa@leeds.ac.uk (* presenting author)

Birnessite is the dominant Mn oxide in marine ferromanganese-rich sediments. Scavenging of dissolved Ni to this mineral is an equilibrium process that exerts a strong control on the concentration of Ni in seawater and the associated sedimentary system.[1] In the modern oceans, Ni-enriched ferromanganese precipitates reflect the abundance of Ni in contemporaneous seawater, and the exchange of Ni between birnessite and the overlying water column plays a major role in Ni oceanic cycling. In turn, as oceanic sediments accumulate over time, ancient Mn-rich deposits potentially provide a record of palaeo Ni signatures, from which we can draw inferences about Ni cycling and the Ni concentration of palaeo seawater. Nickel is a bioessential element, where it participates in a variety of cellular processes, including bacterial methanogenesis, the growth of primitive life-forms and nitrogen metabolism by higher-order organisms.[2] As such, interpreting these Ni signatures in marine sediments might offer insight into the co-evolution of life and ocean chemistry.[3]

Interpretation of both modern and palaeo Ni signatures in marine Mn-rich sediments is not straightforward however, because under diagenesis and mild hydrothermal conditions, the phyllo-manganate birnessite transforms to the tectomanganate todorokite.[4-6] The fate of Ni during this transformation pathway is unclear, but will determine whether Ni remains sequestered by Mn oxides, and whether its initial equilibrium reaction with birnessite describes its partitioning between sediment and seawater, or whether there is a subsequent reaction during transformation that gives rise to a new relationship between sediment concentration and seawater abundance.

Here we present the results of novel experiments to transform hexagonal birnessite to todorokite at environmentally relevant conditions, and to determine the fate of Ni during the transformation process. Using a combination of X-ray Diffraction (XRD), Scanning Electron Microscopy (SEM), High-Resolution Transmission Electron Microscopy (HR-TEM) and X-ray Absorption Spectroscopy (XAS) we provide new insight into the transformation mechanism, and determine the molecular-level interaction of Ni with the precursor, intermediate and final mineral phases.

[1] Peacock and Sherman (2007) *Chem. Geol.* **238**, 94-106. [2] Mulrooney and Hausinger (2006) *FEMS Microbiol. Rev.* **27**, 239-261. [3] Konhauser et al. (2009) *Nature* **458**, 750-753. [4] Burns and Burns (1977) *Mineralogy of ferromanganese deposits*. In *Marine Manganese Deposits* (Elsevier, Amsterdam). [5] Bodeř et al. (2007) *Geochim. Cosmochim. Acta* **71**, 5698-5716. [6] Feng et al. (2010) *Geochim. Cosmochim. Acta* **74**, 3232-3245.

Assessing the metabolic potential of microbes in Opalinus Clay Rock

ALEXANDRE BAGNOUD¹, BERNHARD SCHWYN², RIZLAN BERNIER-LATMANI^{1,*}

¹Environmental Microbiology Laboratory, Ecole Polytechnique Fédérale de Lausanne, EPFL, Lausanne, Switzerland, alexandre.bagnoud@epfl.ch, rizlan.bernier-latmani@epfl.ch (* presenting author)

²National Cooperative for the Disposal of Radioactive Waste, NAGRA, Wettingen, Switzerland, bernhard.schwyn@nagra.ch,

Repositories for high level nuclear waste rely on the low water permeability and the long term stability of the host rock to safely dispose of radioactive waste. Opalinus Clay is the host rock being considered for nuclear waste disposal in Switzerland. While physicochemical processes that could impact the safety of the repository are studied extensively, little is known about the microbiological processes that could take place in these environments. Knowledge of the potential microbial processes sustainable during the long term storage of this waste would assist the evaluation of the storage system and possibly impact the final design.

Here, we chose three approaches to consider the metabolic potential of microbes in the Opalinus Clay. All approaches relied on access to Opalinus Clay formation via the Mont Terri underground rock laboratory in Switzerland. The first approach entailed collecting porewater from the rock and characterizing the microbial community based on 16S rRNA sequences as well as probing the metabolic potential via direct incubations with potential substrates. Results from that investigation show remarkable spatial heterogeneity in 16S rRNA distribution across the Mont Terri laboratory but relative temporal homogeneity.

The second approach entailed installing a downhole *in situ* bioreactor in Opalinus Clay and amending recirculating porewater with various substrates sequentially. The first substrate was H₂ and it was chosen because of its expected production in a repository via anoxic corrosion of the steel canisters containing nuclear waste. Porewater was continuously saturated with gaseous H₂ and chemical parameters such as sulfide, pH and dissolved oxygen measured online. Sampling of the recirculating porewater allows the collection of DNA and RNA when metabolic processes are clearly underway. Metagenomic and meta-transcriptomic analyses of the nucleic acids is expected to provide a glimpse of the shift in microbial community and metabolism as a result of H₂ amendment.

The final approach entailed collecting Opalinus Clay samples from drill cores deep within the formation, extracting DNA directly from the rock and carrying out metagenome sequencing. This approach was designed to probe more specifically the presence of surviving indigenous microbes and to characterize their metabolic potential and phylogenetic relationship to porewater microbes.

This multi-pronged strategy will yield a more thorough understanding of the potential for various microbial metabolisms in Opalinus Clay and help repository decision-makers account for the impact of microbial processes on their design.

Uranium(VI) reduction and uranium(IV) dynamics in a reduced alluvial aquifer: Insights from in-situ studies

J.R. BARGAR^{1*}, J. LEZAMA-PACHECO¹, N. JANOT¹, J.E. STUBBS², K.H. WILLIAMS³, P.E. LONG³, E. SUVOROVA⁴, M. STYLO⁴, D. ALESSI⁴, R. BERNIER-LATMANI⁴, K. CAMPBELL⁵, J. A. DAVIS³, P. FOX³, K. HANDLEY⁶, J.M. CERRATO⁷, AND D.E. GIAMMAR⁷.

¹Stanford Synchrotron Radiation Lightsource, SLAC, Menlo Park, CA, USA, bargar@slac.stanford.edu (* presenting author)

²University of Chicago, Chicago, IL, USA

³Lawrence Berkeley National Laboratory, Berkeley, CA, USA

⁴École Polytechnique Fédérale de Lausanne, Lausanne, Switzerland

⁵US Geological Survey, Boulder, CO, USA

⁶University of California, Berkeley, CA, USA

⁷Washington University, St. Louis, MO, USA

Microbially-driven metal reduction can profoundly alter uranium speciation and dynamics in aquifers. Under conditions where natural or amended organic carbon is present and dissolved oxygen is low or absent, bioreduction of U(VI) produces U(IV) and effects orders-of-magnitude decreases in uranium groundwater concentrations. Naturally (bio)reduced uranium occurs in contaminated aquifers at US Department of Energy legacy ore processing sites in the Western U.S., such as the Old Rifle, CO site, where it has been implicated as a factor maintaining persistent uranium groundwater plumes. Stimulated bioreduction of groundwater uranium via organic carbon amendment is also of interest as a method to manage uranium redox state and mobility in impacted aquifers. While a variety of U(IV) species have been identified in the lab, little is known about the speciation and dynamics of U(IV) in aquifer sediments. This dearth of information is due to both the relative inaccessibility of aquifer sediments and the typically low (<1 ppm) concentration of sediment-hosted uranium inventories.

We have conducted sediment column studies that directly access biogeochemical conditions in aquifer sediments at the Old Rifle, CO site to interrogate the chemical and physical forms of sediment-hosted U(IV) formed during acetate amendment field experiments. Sediments were examined using x-ray and electron microscopy, x-ray absorption spectroscopy (XAS), and chemical extractions. U(IV) was found to occur as monomeric U(IV) complexes and as uraninite. Grain coating mineralogy and the distribution of U(IV) in the sediments differ strikingly following reduction under metal- and sulfate-reducing conditions. Aging of sediment-hosted monomeric U(IV) complexes in the aquifer over a 12 month period resulted in their partial transformation into uraninite, with a concomitant increase in stability. This work establishes the importance of both monomeric U(IV) complexes and uraninite in subsurface sediments at the Old Rifle site. The body of this work provides a foundation from which the formation, dynamics, and stability of naturally reduced U(IV) in the Old Rifle aquifer can be investigated.

Sr-Nd-Hf isotopes Geochemistry of the Qitianling tin-bearing and the Yaogangxian tungsten-bearing granites, Southwest China: implications for W and Sn mineralization

XIANWU BI^{1*}, SHAOHUA DONG^{1,2}, RUIZHONG HU¹, YOUWEI CHEN¹, JIANTANG PENG¹, LINBO SHANG¹, XIAOYAN HU¹

¹State Key Laboratory of Ore Deposit Geochemistry, Institute of Geochemistry, Chinese Academy of Sciences, Guiyang 550002, China, bixianwu@vip.gyig.ac.cn

²Graduate School of Chinese Academy of Sciences, Beijing 100039, P.R.China

The Nanling granitic magma intrusive belt in South China is the important granitic belt in the world, which is characterized by intensive and widespread granitic plutonism associated with numerous tungsten and tin deposits. These Jurassic plutons consist predominantly of biotite granite with lesser amounts of two-mica granite, and they were previously considered to be typical S-type granites, but some have recently been identified as A-type. The Qitianling Sn-bearing granites and the Yaogangxian W-bearing granites are closed in space and time in the belt. This study aims to examine these two intrusions, Qitianling granite which is related to Sn mineralization and Yaogangxian granite which is related to W mineralization, to discuss the relationship between magma evolution and the mineralization of tungsten and tin.

The initial Sr isotopic compositions (I_{Sr}) ratios of the Qitianling granite range from 0.7047 to 0.71525, with $\epsilon_{Nd}(t)$ values from -7.8 to -6.6. Sr-Nd isotopic data of the Qitianling granites appear consistent with a binary mixing between a juvenile, mantle-derived magma and evolved crustal components for their origin. The initial Sr isotopic compositions (I_{Sr}) ratios from the Yaogangxian granite range between 0.71898 and 0.75090, with $\epsilon_{Nd}(t)$ values from -11.5 to -9.1. The Sr-Nd isotopic data of the Yaogangxian granites appear consistent with a evolved crustal components for their origin. We performed forty-four Hf analyses on zircons from Qitianling granites. All the $^{176}\text{Hf}/^{177}\text{Hf}$ of the zircons fit a relatively narrow range from 0.282381 to 0.282594, corresponding to clearly negative $\epsilon_{Hf}(t)$ values which between -10.2 to -2.8. Twenty-seven spots of in situ Hf isotope analysis have been determined on zircon from Yaogangxian granites. The $^{176}\text{Hf}/^{177}\text{Hf}$ of the zircons are ranging from 0.282215 to 0.282543, corresponding to clearly negative $\epsilon_{Hf}(t)$ values which between -16.0 to -5.1. Based upon the fact that these two intrusions had similar characteristics on tectonic setting, age of mineralization, we suggested that the different mineralization of these two intrusions were probably related to the differences on source regions.

This work was supported by the National Basic Research Program of China (2007CB411404)

Gas accumulating process of Xujiahe coal-bearing formation, central Sichuan basin

BIAN CONGSHENG^{1*}, WANG HONGJUN¹, WANG ZECHENG¹, XU ANNA¹, XU ZHAOHUI¹, JIANG QINGCHUN¹, GU ZHIDONG¹, LIU HAITAO¹

¹ PetroChina Research Institute of Petroleum Exploration & Development, Beijing, China, bcs_1981@petrochina.com.cn (*)

The Upper Triassic Xujiahe Formation contains a set of land clastic rocks with coal-bearing deposits, including six members from bottom to top, among which member I, III and V are source rock and caps and member II, IV and VI are reservoir rocks, which is low porosity and permeability. Many gas fields have been discovered now and the gas accumulating process is not clear and need further study.

Research on the burial history of central Sichuan area indicates that Xujiahe formation underwent rapid buried from Jurassic to early Cretaceous period to the depth of 4500-5000m, and the maturity of source rock reached 1.2-1.5% Ro, therefore, the source rock became thermal mature and generated mass gases. Meantime, the gas migrated from source rock to reservoir and accumulated. After late Cretaceous, the whole Xujiahe formation was elevated and eroded, and the total erosion thickness is beyond 1500 m. From then on, the gas generation process generally ceased.

The hydrocarbon inclusions are very important tools to study gas accumulation course. Amounts of gaseous hydrocarbon inclusions have been found in the micro-fractures of quartz. The homogenization temperature of coeval saline inclusions of the gaseous hydrocarbon inclusions ranges 90-100°C and 110-130°C, and the freezing point temperature are -5~0 and -20~-5°C. The low homogenization temperature and high freeze point temperature means that the hydrocarbon inclusions are formed during Jurassic period, when the source rock became thermal mature and generated mass gases. The high homogenization temperature and low freeze point temperature suggests that its are formed during uplifting period of Xujiahe formation, and the gas accumulation occurred in a large scale. This is because the occurrence of coal desorption and gas expansion in the process of uplift of Xujiahe formation, and the quantity of the gas in this period reaches 20-40% of maximum expulsive gas from the source rock.

[1] Zhao Wenzhi, et al., 2010. Petroleum exploration and development 37:2, 146-157.

[2] Carlos R., et al., 2002. AAPG Bull 86:10, 1310-1345.

[3] Dai Jingxing, et al., 1992. Scientific Sinica 2, 185-193.

(U-Th)/He thermochronology of the Mesozoic reactivation of the St. Lawrence Rift System.

LAURA BOUVIER^{1*}, DANIELE L. PINTI^{1*}, ALAIN TREMBLAY¹, WILLIAM G. MINARIK², MARY K. RODEN-TICE³, RAPHAEL PIK⁴

¹GEOTOP-UQAM, Montréal, QC, Canada

bouvier.laura@courrier.uqam.ca (presenting author)

pinti.daniele@uqam.ca

tremblay.a@uqam.ca

²GEOTOP-McGill University, Montréal, QC, Canada

william.minarik@mcgill.ca

³Plattsburgh State University of New York, Plattsburgh, USA

rodenmk@plattsburgh.edu

⁴CRPG - CNRS, Nancy, France

rpik@crpg.cnrs-nancy.

The St. Lawrence Rift System (SLRS) is a NE-trending half-graben, extending for more than 500 km along St. Laurent River valley. Reactivation of the SLRS is believed to have occurred along Late Proterozoic to Early Paleozoic normal faults related to the opening of the Iapetus Ocean. The absence of strata younger than the Ordovician however makes difficult to determine if the SLRS has been reactivated in more recent times. However, recent AFT dating [1] suggests a reactivation younger than Jurassic. (U-Th)/He thermochronometry on apatite was thus performed along three transects across the SLRS, from Québec city to the Charlevoix area in order to verify the occurrence of «young» episode of faulting.

The analyzed samples were taken from the hanging wall and footwall of the Montmorency and Saint-Laurent faults. Apatites were separated from five Mesoproterozoic granitic to charnockitic gneisses and an amphibolite of the Grenville Province. The ⁴He content was measured with a noble gas mass spectrometer in CRPG-Nancy and a quadrupole mass spectrometer at GEOTOP. Measurement of U and Th by ICP-MS was carried out at McGill University by nitric acid attack. Obtained U-Th/He ages were calibrated against measured samples of international standard Durango Apatite (31.4±0.5 Ma).

U-Th/He ages for the hanging wall were 138Ma at Cap-aux-Oies, 143Ma at Sault-au-Cochon and 127Ma at Montmorency Falls. These ages are compatible with previous AFT within uncertainties. U-Th/He ages for footwall are more dispersed: 259 Ma at Cap-aux-Oies, 180 Ma at Sault-au-Cochon, and 146Ma at Montmorency Falls. For each sampled fault, we observed discontinuous AFT and He ages on both sides, indicating the reactivation of these structures during Jurassic.

He ages are younger than AFT ages as expected, except for Cap-aux-Oies which shows a U-Th/He of 259Ma older than the AFT age of 195Ma. This suggests that other parameters, such as the fragmentation of apatite grains, possibly influence the chemical diffusion of helium giving erroneous U-Th/He age estimates.

[1] Tremblay A., Roden-Tice M., (2010), *GSA NE-SE Joint Meeting, Baltimore, Abs. Prog.*, 42, p. 79.

Moroccan Atlas lithospheric thinning and alkaline volcanism: induced by Edge-driven Convection?

CADOUX ANITA¹, MISSENARD YVES^{2*}

¹ Institut des Sciences de la Terre d'Orléans (ISTO) UMR 7327 - CNRS/Université d'Orléans, 45071 Orléans Cedex 2, France, acadoux@cnsr-orleans.fr

² UMR IDES 8148, Département des Sciences de la Terre, Université Paris Sud-11, 91405 Orsay Cedex, France, Yves.Missenard@u-psud.fr (* presenting author)

The Moroccan lithosphere is characterized by an anomalously thinned area, located beneath the Atlas domains, which forms a singular narrow NE-SW directed strip overlain by Cenozoic alkaline volcanism. The origin of this thinning and volcanism is still a matter of debate. The proposed models invoke processes either related to the Mediterranean slab, or mantle plumes. Here, we propose an alternative Edge Driven Convection (EDC) model involving small-scale convection at the boundary between the West-African craton and the Atlas lithosphere. Our comparison of the Atlas lithosphere velocity and volcanism episodes during the last 80 Ma points out that volcanism occurs when plate moves at velocities ca. <1 cm/yr, a velocity sufficiently low to trigger EDC. This is the first process which could explain the ~20 Ma volcanism shutdown separating the two volcanic episode of the Atlas. Additionally, it may successfully account for the lithosphere thinning location and geometry and volcanism geochemistry.

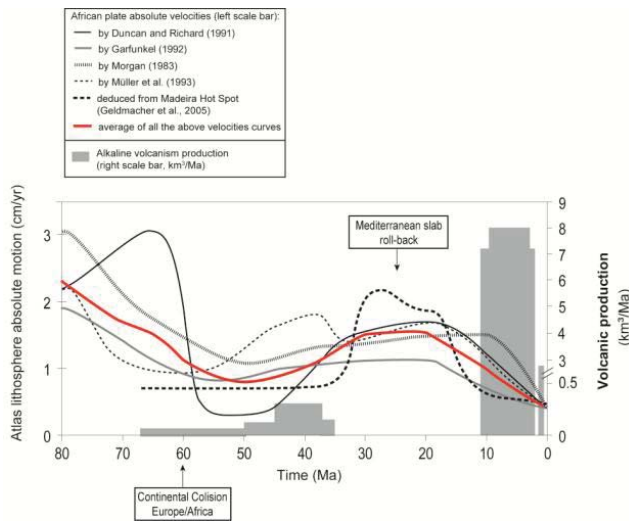


Figure 1: Atlas lithosphere absolute motion (cm/yr) in a fixed hotspot frame compared to volcanic production since the last 80 Ma (km³/Ma). The red curve represents the average velocity of the five models used in this study. The two main periods of volcanic activity in the Atlas and Sahara domains coincide with absolute velocities plate velocities lower than ca. 1 cm/yr. Modified after [1].

[1] Missenard & Cadoux (2012) *Terra Nova* **24**, 27-33.

A Geochemical and Isotopic Study of Nitrate Contamination in the Alter do Chão - Monforte Aquifer

M.ROSÁRIO CARVALHO^{1*}, M.CATARINA.R. SILVA¹, PAULA FERNANDES¹, ANA RITA LOPES², M.ROSÁRIO JESUS²

¹Universidade de Lisboa, Faculdade de Ciências, Dep. Geologia/CeGUL, Lisboa, Portugal, mdrcarvalho@fc.ul.pt

²INAG, Instituto Nacional da Água, Lisboa, Portugal, ana.rita@inag.pt

Abstract

The Alter do Chão - Monforte aquifer system (Alentejo region, Portugal) is composed by cambrian carbonate formations and Pre-Variscan basic igneous complex, which has been subjected to serpentinization-rodigitization processes. The aquifers are unconfined with a mixed karstic-fissured circulation [1] and represents one of the main water resources of this region, located in an area of intensive agriculture and cattle breeding.

The groundwaters show varied chemical composition, reflecting fast chemical changes associated with the water-rock interaction. The water circulating in the carbonate formations have slightly basic pH ($\approx 7-8$), and Ca-HCO₃ facies; waters from slates and granitic rocks belong to the Na/Ca-HCO₃ and Na-HCO₃-type, respectively; Mg-HCO₃-type waters, with very high pH (≈ 11), constitute most of the groundwaters discharging from the serpentinites. Some of the sampled waters shown evidence of contamination, with nitrate concentrations above 50 mg/L, and seasonal variation, probably as a result of dilution by rain.

In this study, we used traditional geochemical and isotopic techniques ($\delta^{15}\text{N}$ and $\delta^{18}\text{O}$ in nitrates), in order to distinguish the different sources of nitrate pollution of the aquifer. The results allowed to identify different N sources contributing to the N cycle in groundwater (cattle breeding, agriculture and urban) based on the fact that the main sources of nitrate in the area have distinct $\delta^{15}\text{N}$ and $\delta^{18}\text{O}$ values, typical of: manure and septic waste; fertilizer and rain; and soil N.

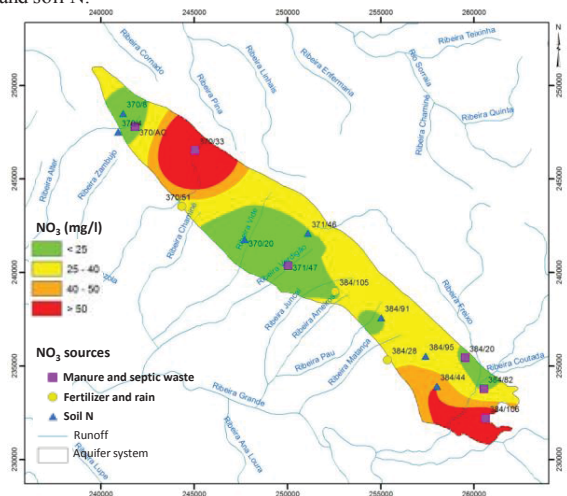


Figure 1: Nitrate distribution in the aquifer system and N source signature based on $\delta^{15}\text{N}$ and $\delta^{18}\text{O}$ - NO₃ signature.

References

[1] Fernandes, J, Francés, A (2009). Sistema Aquífero Monforte-Alter do Chão: resultados obtidos no âmbito do Estudo dos Recursos Hídricos Subterrâneos do Alentejo, ERHSA. AHR Tejo.

Geochemical discrimination between mineralized and barren mafic-ultramafic intrusions from Hongqiling Cu-Ni sulfide mines in Jilin province, NE China

SHELI CHAI^{1*}, JING CAI¹, YUAN CHAI², LINA GAO¹ AND CHAO ZHANG²

¹College of Geo-exploration Science and Technology, Jilin University, Changchun 10026, China (*Correspondence: chaisl@jlu.edu.cn)

²College of Earth Science, Jilin University, Changchun 13061, China

More than 50 mafic-ultramafic intrusions with the ages ranging from 216±5 Ma[1] to 232.75±0.95 Ma[2] dated with U-Pb zircon were identified within Hongqiling Cu-Ni sulfide mines including Sandaogang ore mine, Hongqiling ore mine and Chajian ore mine in Jilin province of NE China, and they hosted Cu-Ni ore reserves ranking the second in China. The intrusions were intruded into the Paleozoic Hulan Group of low to intermediate metamorphic grades as dikes extending northwardly, and they were divided into two groups: mineralized intrusions and barren intrusions based on whether Cu-Ni sulfide mineralization found in each intrusion or not. Mineralized intrusions were mainly composed of peridotite, pyroxenite, gabbro, with minor hornblendite and norite, and the intrusions enriched orthopyroxene and underwent weak or no deformation processes. The rock types of barren intrusions were to some extent similar with those of mineralized ones, but the intrusions were comparatively rich in clinopyroxene and suffered more tense deformation than mineralized ones. The bulk geochemical compositions show that Al₂O₃/CaO (1.3), Rb/Sr (4.6), Zr/Ti (3.5) and Th/Yb (8.27) ratios and Pb (327ppm), Zr (6.7ppm) and Th (21ppm) contents in mineralized intrusions were higher than those values in barren intrusions with Al₂O₃/CaO of 1.1, Rb/Sr of 1.2, Zr/Ti of 1.9, Th/Yb of 4.4, Pb of 55.4 ppm, Zr of 4.8 ppm and Th of 8.1 ppm, implying that crustal contamination was comparatively evident in the processes of formation of mineralized intrusions. Mineralized intrusions had higher contents of Au (72.2 ppb), Pd (44.3 ppb), Rh (3.9 ppb) and PGE (77.4 ppb) and ratios of Ni/Pd (55.6×10³), Cu/Pd (1346.6×10³) and Pd/Ir (44.2) than those values in barren intrusions with Au of 16.6 ppb, Pd of 31.8 ppb, Rh of 1.0 ppb, PGE of 68.9 ppb, Ni/Pd of 4.0×10³, Cu/Pd of 94.9×10³ and Pd/Ir of 36.4, suggesting that the magma related to Cu-Ni sulphide mineralization was once experienced sulphide mineral segregation before its emplacement. Olivine compositions of mineralized intrusions had a narrow forsterite ranges and the elevated Si and Ni contents; while olivine compositions of barren intrusions were low Si and Ni contents and a comparatively wide ranges of forsterite contents.

In conclusion, major element, trace element, REE and PGE geochemistry, together with olivine composition, can discriminate the mineralized mafic-ultramafic intrusions from the barren ones quite well. The deformation and sulfide segregation found in mafic-ultramafic intrusions may indicate that the mineralized intrusions were fractionated at shallower levels than the barren ones, so the barren intrusions may have a poor ore potential.

[1] Wu et al. (2004) *Journal of Asian Earth Sciences* 23(5), 781-797.

[2] Wang et al. (2011) *Journal of Jilin University (Earth Science Edition)* 41(sup.1), 126-132 (in Chinese with English abstract).

Petrological and Sr-Nd-Os isotopic constraints on the origin of the Fanshan ultrapotassic complex from the North China Craton

B. CHEN^{1,2*}, X.L. NIU², A.K. LIU², AND K. SUZUKI³

¹Institute of Geology and Exploration Engineering, Xinjiang University, Urumqi, China, binchen@pku.edu.cn (* presenting author)

²Key Laboratory of Orogenic Belts and Crustal Evolution, Peking University, Beijing, China

³Institute for Research on Earth Evolution, Japan Agency for Marine-Earth Science and Technology, Yokosuka, Japan

The Fanshan ultramafic-syenitic complex is located on the northern margin of North China Craton (NCC), with zircon U-Pb ages of 220 Ma. It is a concentrically zoned complex, with syenite in the core, surrounded by ultramafic rocks (e.g., clinopyroxenite, biotitite) and garnet-clinopyroxene syenite, respectively, towards the rim. Apatite-magnetite ore deposits are hosted in the ultramafic rock unit. Diopside, biotite, orthoclase, melanite, magnetite and apatite are the major minerals, with subordinate sphene and calcite. Petrological (e.g., cumulate textures) and geochemical data point to the formation of the complex through fractional crystallization and accumulation of ferromagnesian phases from a SiO₂-undersaturated ultrapotassic alkaline-peralkaline parent magma. The abundance of CaO-rich diopside, biotite, melanite, orthoclase and magnetite of the complex suggest high CaO, Fe₂O₃, and K₂O contents for the parent magma. The presence of interstitial primary calcite between the cumulus minerals in the ultramafic rocks and the occurrence of carbonatite veins indicate a CO₂-rich primary melt. Fluorapatite is a ubiquitous euhedral phase in different rocks and accumulates as ore-bodies, which indicates that the parent magma is enriched in CaO, P₂O₅ and F. In addition, the high TiO₂ contents of the clinopyroxenes, the occurrence of melanites and the pure orthoclase compositions of feldspars argue for the high temperature features of the magma (probably > 1000 °C). Rocks from the complex are highly enriched in light rare earth elements (LREE) and large ion lithophile elements (e.g., Sr up to 5000 ppm), depleted in high field strength elements (HFSE; e.g., Nb, Ta, Ti), and show relatively homogeneous Sr-Nd isotopic compositions with initial ⁸⁷Sr/⁸⁶Sr = 0.7051 – 0.7059 and ε_{Nd(t)} = –5.8 to –5.3. The geochemical data suggest that the Fanshan complex originated from a phlogopite-clinopyroxenite-rich lithosphere mantle source that had previously been metasomatized by melts from carbonated oceanic crust above a subduction zone. Highly radiogenic Os isotope compositions of the complex (with initial ¹⁸⁷Os/¹⁸⁸Os = 0.3 – 2.45) suggest that the parent magma has been contaminated by Precambrian mafic crustal rocks during magma emplacement in crustal levels.

The occurrence of the Fanshan complex, together with many other ultramafic/alkaline plutons of similar ages, on the northern margin of NCC suggests that the northern NCC entered into a large-scale extensional regime in late Triassic after the final amalgamation between Mongolian microcontinent and the NCC, which may signify the initiation of the Mesozoic lithospheric thinning in the NCC.

Geoinformation integration and singularity mapping for prediction of mineral resources in covered terranes

QIUMING CHENG^{1,2}

¹York University, Earth and Space Science and Engineering, Geography, Toronto, Canada, qiuming@yorku.ca

²State Key Lab of Geol. Processes and Mineral Resources (China Univ. of Geos.), Beijing and Wuhan, China

It is indisputable that finding mineral deposits in regions with transported or deeply weathered cover has become one of the most challenges of mineral exploration. The following difficulties are the critical issues need to be addressed in order to successfully conduct prediction of mineral deposits in covered terrane: missing information or inadequate information due to lack of direct geological observation and surface sampling is a common problem for proper prediction of location of mineral deposits according to conventional mineral exploration model; and weak or mixing geochemical and geophysical signals due to concealing effect of overburden is another barrier for extraction of footprints reflecting underlying mineralization. The above two main problems are addressed in a new framework developed in the current paper on the basis of geocomplexity theory for processing and integration of geoinformation. Firstly, it has been demonstrated that weak geochemical and geophysical anomalies observed on the earth surface and caused by concealed mineralization can be better identified by means of nonlinear information enhancing methods (e.g., local singularity analysis) and filtering methods (e.g., generalized self-similarity) applied to geochemical landscape and geophysical fields. Further, a cascade model has been proposed to integrate geological, geochemical and geophysical information for mapping singularities related to occurrence of mineral deposits. These methods have been successfully applied in delineation of targeting areas for discovering Fe and Cu mineral deposits of skarn types and W and Mo mineral deposits of hydrothermal types in three large regions in the Eastern Inner Mongolia (about 280,000 km²), Tianshan of Xinjiang (300,000 km²), and Wuyi district of Fujian (120,000 km²) in China where the regions are largely covered by Cenozoic to Eocene Epoch sediments and deserts or vegetation covers. A large number of mineral deposits of various types have been discovered in the three provinces but a few deposits have been found in the covered areas. There are comprehensive geodatasets available which include geological maps, aeromagnetic maps and gravity geophysical maps at 1:200,000 scale and some areas with maps at finer scale. Large portion of the areas are surveyed by sampling stream sediments at 1 sample per 4 km² and each sample analyzed for 39 major and trace elements. A downscaling strategy was applied to process and integrate geological, geochemical, aeromagnetic and gravity data for prediction of potential locations of intrusions and fault structures associated to mineralization, extents of contact metasomatic or hydrothermal alterations zones around inferred intrusions, and mineralization-associated local anomalies within the extents of alteration zones delineated. A final predictive map showing potential targeting areas are constructed by boosting processes using multiple layers of geoinformation.

Assessing the Role of Submarine Groundwater Discharge on the Rare Earth Element budgets of Two Estuaries

DARREN A. CHEVIS^{1*}, KAREN H. JOHANNESSON¹, DAVID J. BURDIGE², JAYE E. CABLE³, JONATHAN B. MARTIN⁴, ROGER P. KELLY⁵, S. BRADLEY MORAN⁵ AND CHRISTOPHER D. WHITE⁶

¹Department of Earth and Environmental Sciences, Tulane University, New Orleans, LA 70118

²Department of Ocean, Earth, and Atmospheric Sciences, Old Dominion University, Norfolk, VA 23529

³Department of Marine Science, University of North Carolina, Chapel Hill, NC 27599

⁴Department of Geological Sciences, University of Florida, Gainesville, FL 32611

⁵Graduate School of Oceanography, University of Rhode Island, Narragansett, RI 02882

⁶Craft and Hawkins Department of Petroleum Engineering, Louisiana State University, Baton Rouge, LA 70803

Understanding the sources and sinks of trace elements like the rare earth elements (REE) in the oceans has important implications for quantifying their global geochemical cycles, their application as paleoceanographic tracers, and in discerning the geochemical reactions that mobilize, sequester, and fractionate REEs in the environment. This is critical for neodymium (Nd) because radiogenic Nd isotopes are commonly used in paleoceanographic studies over glacial–interglacial to million year time scales. Our initial estimate of the SGD Nd flux to the Indian River Lagoon, FL, USA, was ~100 mmol/day based on a simple three-box mass balance model [1]. Using irrigation rates estimated from ²²²Rn measurements [2] and additional porewater samples analyzed for the REEs, more rigorous flux calculations show that SGD contribution may be more on the order of ~10 mmol/day of Nd to the overlying lagoon. This new estimate is equivalent to the riverine flux entering the system assuming 70% Nd removal from salt-induced, colloid coagulation in the surface estuaries. Biogeochemical reactions within the sediments appear to release Nd along with the other light REE and middle REE, whereas the sediments act a sink for heavy REE. We compare our REE data and results for the Indian River Lagoon subterranean estuary with another subterranean estuary in Rhode Island, USA, where we have recently initiated investigations of the local SGD REE fluxes.

[1] Johannesson et al. (2011) *Geochim. Cosmochim. Acta* **75** 825-843. [2] Smith et al. (2008) *Earth Planet. Sci. Lett.* **273** 312-322.

Towards a Mechanistic Understanding of Anaerobic Nitrate Dependent Iron Oxidation: Balancing Electron Uptake and Detoxification

JOHN D. COATES^{1*}, HANS K. CARLSON¹, IAIN C. CLARK¹,
RYAN A. MELNYK¹

¹Department of Plant and Microbial Biology, University of California, Berkeley, CA, USA, jdcoates@berkeley.edu
(*presenting author)

The anaerobic, nitrate-dependent oxidation of Fe(II) by subsurface microorganisms is an important part of biogeochemical cycling in the environment. However, the biochemical mechanisms involved in coupling iron oxidation to nitrate respiration are not well understood. The thermodynamics of nitrate-dependent Fe(II) oxidation are favorable, however, the success of an iron oxidizing microorganism depends on the extent to which electron donation from Fe(II) can be controlled and toxic reactions prevented or managed. Based on our own work and the evidence available in the literature, we propose a mechanistic model for anaerobic nitrate-dependent Fe(II) oxidation that is composed of mixed biotic and abiotic interactions. This model accounts for electron transfer and energy conservation. We suggest that anaerobic Fe(II) oxidizing microorganisms likely exist along a continuum including: 1) bacteria that inadvertently oxidize Fe(II) by abiotic or biotic reactions with enzymes or chemical intermediates in their metabolic pathways (e.g. denitrification) and suffer from toxicity or energetic penalty, 2) Fe(II) tolerant bacteria that gain little or no growth benefit from iron oxidation but can manage the toxic reactions, and 3) bacteria that efficiently accept electrons from Fe(II) to gain a growth advantage while preventing or mitigating the toxic reactions. The proposed mechanistic model of nitrate-dependent Fe(II) oxidation includes both enzymatically mediated components and abiotic interactions between Fe(II) and reactive intermediates possibly resulting in a net energy gain. These mechanisms may be mutually exclusive, but based on reactive species formed during metabolism and reaction kinetics, it is more likely that hybrid abiotic/biotic mechanisms are functioning. To the best of our knowledge such hybrid abiotic/biotic mechanisms represent a novel metabolic process in microbiology.

Update on the U-Th geochronology (inter-)calibration project

DANIEL J. CONDON¹, GIDEON M. HENDERSON², DAVID A. RICHARDS³, STEPHEN R. NOBLE¹, JON WOODHEAD⁴, NOAH MCLEAN¹, ANDREW MASON², MORTEN B. ANDERSEN⁵ AND JOHN HELLSTROM⁴

¹ NERC Isotope Geosciences Laboratory, UK, dcondon@bgs.ac.uk

² Department of Earth Science, Oxford University, UK

³ School of Geographical Sciences, University of Bristol, UK

⁴ School of Earth Sciences, University of Melbourne, Australia

⁵ School of Earth Sciences, University of Bristol, UK

The U-Th chronometer is routinely employed to determine the absolute age of carbonate materials (e.g., corals, speleothem) less than about 500,000 years old. The accuracy of U-Th dates (for closed system materials) is controlled by both the ²³⁴U and ²³⁰Th decay constants [1] and the calibration of the U-Th tracers against which the sample U-Th ratio is determined. U-Th tracers are themselves variably calibrated against either assumed secular equilibrium materials and/or metal-derived gravimetric reference solutions. Recent studies have demonstrated that some of the widely used secular equilibrium materials have variable U/Th and therefore calibration using such materials introduces additional, and poorly quantified, uncertainty. Calibration against metal derived U-Th gravimetric reference solution using certified/well characterised reference materials (e.g., CRM 112a, IRMM 3636) provides a calibration that is directly traceable to SI units [e.g., 1, 2] and does not rely upon assumptions of calibration materials being in elemental and isotopic secular equilibrium.

A project aimed at developing a series of U-Th 'age solutions', combined with gravimetric reference solutions for tracer calibration, has been initiated. The purpose of this project is to improve the inter-comparability of U-Th geochronology such that uncertainty related to calibration is quantified and minimised. This involves the development and calibration of a series of synthetic U-Th 'age solutions' prepared by mixing different amounts of high-purity mono-isotopic solutions (²³⁴U, ²³⁰Th etc.) in proportions that mimic commonly analysed materials (e.g., a last-interglacial speleothem) so that their analysis replicates the isotope ratio measurement protocols employed on typical samples. These solutions will augment natural carbonate standards as a means of interlaboratory comparison and assessment of long-term external reproducibility. The composition of the U-Th 'age solutions' will be determined by a multi-laboratory effort using tracers calibrated against metal derived U-Th gravimetric reference solutions and isotopic reference materials (e.g., IRMM 3636 ²³³U-²³⁶U double spike [2]). Aliquots of both the U-Th gravimetric reference solutions and the U-Th 'age solutions' will be made available to members of the U-Th community.

Work on this project commenced early 2012 and this poster will present a status update. This (inter-)calibration project is part of a broader community effort that has developed out of the PALSEA and EARTHTIME initiatives. For more information on this U-Th geochronology initiative, and to contribute to its development, please visit www.useries.org.

[1] Cheng (2000) *Chemical Geology* **169**, 17-33. [2] Richter (2000) *International Journal of Mass Spectrometry* **269**, 145-148.

Electrochemical study of FeS oxidation by dissolved oxygen

CRISTINA A. CONSTANTIN^{1*}, PAUL CHIRITA¹ AND MICHEL L. SCHLEGEL²

¹University of Craiova, Department of Chemistry, Calea Bucuresti 107I, Craiova Romania, cristina_a_constantin@yahoo.com (* presenting author) and paulxchirita@gmail.com

²CEA, DEN/DANS/DPC/SEARS/Laboratory for the Engineering of Surfaces and Lasers, F-91191 Gif-sur-Yvette, France, michel.schlegel@cea.fr

The identification of the processes controlling the rate of iron monosulfide (FeS) oxidative dissolution is central to understanding the behavior of FeS under the environmentally aggressive conditions of acid mine drainage.[1] The main objective of the present study was to investigate the reaction mechanism of FeS oxidation by identifying the rate determining step.

The electrochemical behavior of synthetic FeS in HCl solutions was studied by potentiodynamic techniques and electrochemical impedance spectroscopy. The electrochemical trials were performed at initial pH between 2.5 and 5.0 and temperatures from 30 to 55°C. The collected polarization curves and impedance spectra were used to study the effects of the pH and temperature on the oxidation of FeS by dissolved O₂. The polarization curves have provided the values of exchange currents (I₀), and the impedance spectra have provided values of charge transfer resistances (R_{ct}).

The interpretation of experimental results has shown that the reaction order with respect to hydrogen ions concentration is 0.7 at 30°C, with an apparent activation energy is 24.5 kJ mol⁻¹ (initial pH 2.5). The values obtained for the kinetic parameters are in good agreement with those reported in previous studies.[1,2] and suggest that the FeS oxidative dissolution is controlled by the diffusion of oxidant across a diffusion-limiting layer formed on FeS surface.[1,2] It is reasonable to consider that at pH below 3.5 the layer formed on FeS surface is a sulfur rich layer, while the layer formed to the higher values of pH could be one more rich in iron.[1]

The authors greatly appreciate support from IFA-CEA Program (Project CI-04).

References

[1] Belzile *et al.* (2004) *J. Geochem. Explor.* **84** 65-76. [2] Chirita *et al.* (2008) *J. Colloid Interface Sci.* **321**, 84-95.

Bioaccumulation of uranium in aquatic plants in the region of Horta da Vilariça (NE Portugal)

CRISTINA CORDEIRO^{1*}, PAULO FAVAS^{1,3}, JOÃO PRATAS^{2,3}

¹School of Life Sciences and the Environment, University of Trás-os-Montes e Alto Douro, Vila Real, Portugal, CGACordeiro@sapo.pt

²Department of Earth Sciences, Faculty of Sciences and Technology, University of Coimbra, Coimbra; Portugal.

³Geosciences Center, Faculty of Sciences and Technology, University of Coimbra, Coimbra, Portugal.

This work has as main objective to study the bioaccumulation of uranium (U) in aquatic plants in Horta da Vilariça, the uraniumiferous region. For this purpose we selected 15 sampling points with sampling of water, sediments and aquatic plants representative of the aquatic flora of the region. For the detection of U in water, sediment and plants used the method of fluorimetry. Analytical data of the sampling water indicate the main hydrochemical facies is sodium bicarbonate. The electrical conductivity ranges from 24.6 µS/cm to 274.0 µS/cm, with a mean of 93.7 µS/cm, and the pH ≈ 7. From those results we can assume that waters have low mineralization and are neutral. The concentration of U ranges from 0.6 µg/L to 5.56 µg/L, with a mean of 1.98 µg/L. We also analyzed 15 samples of sediments; the concentration of U ranges from 23909.5 µg/kg to 123.5 µg/kg with a mean of 3929.2 µg/kg, with therefore a high coefficient of variation of 1.52. In the sampling points were collected 26 species of aquatic plants for a total of 199 samples. Plants that have higher content U (mean) are *Scorpiurium deflexifolium* (34205.0 µg/kg), *Fontinalis antipyretica* (25612.4 µg/kg), *Nasturtium officinale* (roots) (7380.1 µg/kg) and *Roripa sylvestris* (aerial parts) (7280.5 µg/kg). However, comparing the mean levels of U in the water and the mean levels of U in plants, we can say that the remaining plants also exhibit the ability to concentrate U. In the case of plants with roots, by comparing the mean U content of sediments with mean U content in the roots of the plants, found that only *Nasturtium officinale*, *Eleocharis palustris*, *Mentha rotundifolia* and *Mentha pulegium* have the ability to concentrate U in the roots. The plant *Roripa sylvestris* has a higher mean content of U in the aerial parts over the roots, which shows ability to translocation and bioaccumulation.

The highest values of the bioconcentration factor (BCF = concentration of U in plant / concentration of U in water) are 23920 for the *Scorpiurium deflexifolium*; 16418 for *Fontinalis antipyretica*; *Nasturtium officinale* with 5125 (roots); and 4282 for *Roripa sylvestris* (aerial parts).

We can conclude that there are U levels with some relevance in the Horta da Vilariça. Local plants have some ability to concentrate U in their tissues, highlighting by the mean U contents and the BCF the following species *Scorpiurium deflexifolium*, *Fontinalis antipyretica*, *Nasturtium officinale* (roots), and *Roripa sylvestris* (aerial parts). However, we can not exclude other plants, since all reveal a U content in their tissues in quantities greater than the water where they grow.

The $^{10}\text{Be}(\text{meteoric})/^{9}\text{Be}$ ratio: the Renaissance Art of determining weathering rates

N. DANNHAUS¹, F. VON BLANCKENBURG^{*1}, J. BOUCHEZ¹, H. WITTMANN¹

¹German Research Center for Geosciences GFZ, Earth Surface Geochemistry, Potsdam, Germany, fvb@gfz-potsdam.de
(* presenting author)

A perfect clock of the stability of the Earth surface is one that combines a first isotope the flux of which depends on the release rate during erosion, and a second isotope produced at constant rate. The ratio of the meteoric cosmogenic nuclide ^{10}Be to stable ^{9}Be is such a system. We provide a quantitative framework for its use. With this new approach we contribute towards the renaissance of the long since known single-isotope $^{10}\text{Be}(\text{meteoric})$ system.

In a weathering zone some of the ^{9}Be , present typically in 2ppm concentrations in silicate minerals, is released and partitioned between a reactive phase (adsorbed to clay and hydroxide surfaces, given the high partition coefficients at intermediate pH), and into the dissolved phase. The combined mass flux of both phases is defined by the soil formation rate and a mineral dissolution rate – and is hence proportional to the chemical weathering rate and the denudation rate. At the same time, the surface of the weathering zone is continuously exposed to fallout of meteoric ^{10}Be . This ^{10}Be percolates into the weathering zone where it mixes with dissolved ^{9}Be . Both isotopes may exchange with the adsorbed Be, given that equilibration rate of Be is fast relative to soil residence times. Hence a $^{10}\text{Be}/^{9}\text{Be}(\text{reactive})$ ratio results from which the total denudation rate can be calculated. A prerequisite is that the flux of meteoric ^{10}Be is known from field experiments or from global production models [1]. In rivers, when reactive Be and dissolved Be equilibrate, a catchment-wide denudation rate can be determined from both sediment and a sample of filtered river water.

We have tested this approach in sediment-bound Be [2] and dissolved Be in water [3] of the Amazon and Orinoco basin. The reactive Be was extracted from sediment by combined hydroxylamine and HCl leaches. In the Amazon trunk stream, the Orinoco, Apure, and La Tigra river $^{10}\text{Be}/^{9}\text{Be}(\text{dissolved})$ agrees well with $^{10}\text{Be}/^{9}\text{Be}(\text{reactive})$, showing that in most rivers these two phases equilibrate. $^{10}\text{Be}/^{9}\text{Be}$ ratios range from 5×10^{-9} for the Brazilian shield rivers to 2×10^{-10} for the Beni river draining the Andes, corresponding to denudation rates of 0.01mm/yr for the shields and 0.5mm/yr for the Andes, compatible with denudation rates from in situ-produced cosmogenic ^{10}Be [2]. Once delivered to the ocean, this riverine Be, be it dissolved or reactive, will eventually drive $^{10}\text{Be}/^{9}\text{Be}$ ratios of ocean water and disclose global denudation rates – at the present and in the sedimentary record from the past [4].

- [1] Willenbring and von Blanckenburg, *Earth Sc. Reviews* 98, 2010
[2] Wittmann et al., *Geol. Soc. Am. Bull.*, 123, 2011
[3] Brown, E. et al., *Geochim Cosmochim. Acta* 56, 1992
[4] Willenbring and von Blanckenburg (2010) *Nature* 465

Early stages of amorphous calcium phosphate nucleation: a computational study

RAFFAELLA DEMICHELIS^{1*}, PAOLO RAITERI¹ AND JULIAN D. GALE¹

¹Curtin University, Department of Chemistry, Perth, WA, Australia, raffaella.demichelis@curtin.edu.au (* presenting author)

Calcium phosphate is present in several kinds of organic and mineral phases both in living organisms, where it represents one of the main constituents of hard tissues, and at the Earth's crust [1,2].

Crystalline calcium phosphate is generally found as apatite, fluoroapatite, and hydroxyapatite, but the nucleation process is postulated to occur via a non-classical mechanism, involving the formation of amorphous calcium phosphate (ACP) precursors [3]. The steps of this process and the influence of different factors, such as the pH, the ionic strength and the presence of other mineral compounds or organic molecules, are still a matter of debate. A high level of scientific interest has risen around this topic in the last few years, as it is likely to be the key for a better understanding of several pathologies and geochemical processes [1,2].

This work presents the investigation of the early stages of ACP nucleation with a molecular dynamics approach. The hypothesis of polymeric pre-nucleation clusters is considered [4]. The effect of ion concentration and pH on the aggregation of calcium, phosphate and orthophosphate ions is explored. Calculations have been run in presence of other mineral forming species too, including magnesium, sodium, chloride, carbonate and bicarbonate ions, in order to be as close as possible to the marine environment, where these processes mainly occur.

- [1] Dorozhkin & Epple (2002) *Angew. Chem.* **41**, 3130-3146. [2] Gilinskaya, Zanin & Rudina (2007) *Lithol. Miner. Resour.* **42**, 56-67. [3] Wang & Nancollas (2008) *Chem. Rev.* **108**, 4628-4669. [4] Demichelis, Raiteri, Gale, Quigley & Gebauer (2011) *Nat. Commun.* **2**, 590-1:8.

Hf-Nd isotope systematics in Archean komatiites and associated lava-flows

C. DUCHEMIN^{1*}, V. DEBAILLE¹, N. MATTIELLI¹,
C. CHAUVEL² AND N. ARNDT².

¹Laboratoire G-Time, Université Libre de Bruxelles, Brussels, Belgium.

(*correspondence: Claire.Duchemin@ulb.ac.be)

²ISTerre, UMR5275 CNRS, Université Joseph Fourier, 38041 Grenoble, France.

Komatiites are volcanic ultramafic rocks with high MgO content (>18Wt.%) which are mostly confined to Archean terranes. They are among rocks that make up the first few blocks of the Archean crust, and are indicative of the earliest mantle dynamic. While Archean rocks cover only 10% of the current crust, komatiites represent 1% of the Archean rocks assemblage.

Fred's Flow and Theo's Flow are two thick Archean differentiated flows (2.7 Ga) located in the Abitibi Greenstone Belt (Munro Township, Canada). Fred's Flow overlies Theo's Flow with an intermediate hyaloclastite level between the two. Fred's Flow has a komatiitic affinity, and is classified as Al-undepleted type, characterized by chondritic ratios of $(Al_2O_3/TiO_2) \sim 20$ and $(Gd/Yb)_N \sim 1$, with a moderate to strong depletion in LREE with $(La/Yb)_N = 0.6$. In contrast, Theo's Flow has an Fe-rich tholeiitic affinity, with a HREE depletion $(Gd/Yb)_N > 1$ and $(La/Yb)_N > 1$, a subchondritic ratio of $(Al_2O_3/TiO_2) \sim 9$, and can thus be classified as Al-depleted type.

The HREE depletion in Theo's Flow indicates that garnet was residual during partial melting of the mantle source. In contrast, Fred's Flow has flat HREE implying that melting conditions of the source would not be the same between the two flows. These observations suggest that Fred's and Theo's Flows formed either (1) from two distinct mantle sources, or (2) by successive partial melting events of a single mantle source with different depths and/or melting degrees. Theo's and Fred's Flows thus offer a unique combination of Al-depleted and Al-undepleted types that can be used to investigate the source of komatiites and compare the role of garnet in the earliest stages of the Mantle evolution.

The coupled or decoupled behavior of the ^{147}Sm - ^{143}Nd and ^{176}Lu - ^{176}Hf in lavas is a very sensitive indicator of the presence of garnet in their source. Some studies of the Lu-Hf system in komatiites [1,2,3], identified poor reproductibility of Hf isotopic data due to the unusual sample matrix and potential analytical problems, as specified in Blichert-Toft et al. [2].

Consequently, we will pay particular attention to analytical procedures when using Sm-Nd and Lu-Hf isotope systematics of komatiites to characterize their mantle source and melting conditions. To summarize, the aim of this study consists to present a careful comparison between Al-depleted and Al-undepleted komatiites and associated lava flows of the Abitibi Greenstone Belt in order to constrain the role of garnet in their respective sources.

[1] Blichert-Toft & Arndt (1999) *EPSL* **171**, 439-451. [2] Blichert-

Toft, Arndt & Gruau (2004) *Chemical Geology* **207**, 261-27.

[3] Blichert-Toft & Puchtel (2010) *EPSL* **297**, 598-606.

Potential of wild plant species in bioindication of metal-contaminated sites around mining areas

PAULO FAVAS^{1,3*}, JOÃO PRATAS^{2,3}

¹Dep. of Geology, University of Trás-os-Montes e Alto Douro, Ap.1013, 5000-801 Vila Real, Portugal, pjcf@utad.pt (*presenting author)

²Dep. of Earth Sciences, University of Coimbra, Largo Marquês de Pombal, 3001-401 Coimbra, Portugal

³Geosciences Center, University of Coimbra

The main objectives of this study were: to characterize the biogeochemical signature of some heavy metals and metalloids in soils and plants from abandoned mining areas (N Portugal); to identify plant species or parts of these, indicators of excessive chemical elements present in the soils; to select plant species for potential use in bioindication of contamination in mining areas with similar mineral paragenesis (wolframite/cassiterite/scheelite and sulphides).

The determination of total element contents in soils was performed using tri-acid digestion ($HF-HNO_3-HClO_4$) followed by ICP-MS (inductively coupled plasma-mass spectrometry) analysis using an Elan 6000 Perkin-Elmer spectrometer. The determination of element contents in plants was performed using acid digestion ($HNO_3-H_2O_2$) followed by ICP-MS. The analytical methods for element concentrations was assessed using reference material, which was included in the triplicate analyses.

Based on the ratio of maximum concentration obtained for each element and the biogeochemical background in the plant samples, the types of physiological barriers present were determined and concluded on the bioindicator capacity of each species.

Given the types of physiological barriers present and the correlation coefficients between the levels in soil and plant material, found on the bioindicator capacity of each species. Thus, focusing on the absence of physiological barriers or the presence of high barriers, and the correlation coefficients with a level of confidence exceeding 99.9%, it appears that either the leaves or the branches of *Halimium umbellatum* (L.) Spach, may be useful as biogeochemical indicators of As and W; the leaves of *Erica arborea* L. may be useful in contamination indicating of Bi, Sn, W and Pb and especially their woody parts may also have application in bioindication of Pb; the leaves of *Pinus pinaster* Aiton and the aerial parts of *Pteridium aquilinum* (L.) Kuhn show potential to biogeochemistry indicate of W; the leaves of *Quercus faginea* Lam. can give indications on the content of Sn in soils.

Reconstructing Mediterranean-Atlantic exchange during the Miocene Messinian Salinity Crisis

RACHEL FLECKER^{1*}, RUŽA IVANOVIĆ², TANJA KOUWENHOVEN³, MARCUS GUTJAHR⁴, ROB ELLAM⁵, JÖRG RICKLI⁶

¹University of Bristol, Bristol, UK, r.flecker@bristol.ac.uk

(*presenting author)

²University of Bristol, Bristol, UK, Ruza.Ivanovic@bristol.ac.uk

³University of Leuven, Leuven, Belgium,

Tanja.Kouwenhoven@ees.kuleuven.be

⁴NOC, Southampton, UK, M.Gutjahr@soton.ac.uk

⁵SUERC, East Kilbride, UK, r.ellam@suerc.gla.ac.uk

⁶University of Bristol, Bristol, UK, J.Rickli@bristol.ac.uk

During the Late Miocene progressive tectonic restriction of the Mediterranean modified the salinity and volume of Mediterranean Outflow Water (MOW) entering the North Atlantic. This culminated in the Messinian Salinity Crisis (6-5 Ma) when the Mediterranean's salinity fluctuated dramatically from hypersaline levels, resulting in the precipitation of more than 1.5km of evaporite, to brackish water conditions. The aim of this research is to reconstruct the timing and nature of MOW during and immediately prior to the Messinian Salinity Crisis using Nd and Sr isotopes and foraminiferal assemblage data. This information is important both for understanding the evolution of this extreme event in the Mediterranean and for evaluating the controls on Late Miocene circulation in the North Atlantic.

Prior to the formation of the Gibraltar Straits in the early Pliocene, two gateways linked the Mediterranean Sea with the Atlantic Ocean; one through northern Morocco (the Rifian Corridor) and the other through southern Spain (the Betic Corridor). The pattern of circulation through these marine corridors is thought to have varied considerably; anti-estuarine flow in both may have been replaced by a circulation system in which all Atlantic inflow was channelled through the Rifian Corridor, while MOW flowed out through southern Spain. This episode is known as the 'siphon event'. Astronomically tuned Late Miocene successions preserved in these marine corridors provide high resolution age-constraints, allowing these hypotheses for changes in the pattern of water mass exchange to be tested for the first time.

The Nd isotopic composition of present day western Mediterranean seawater (-9.4 ϵ_{Nd}) is significantly different from eastern North Atlantic intermediate water (-11.8 ϵ_{Nd}). We use this Nd isotopic gradient to interpret the origin of water flowing along the bottom of the Rifian Corridor during the Late Miocene. These results are paired with benthic foraminiferal assemblage data and Sr isotope data, which can be used to monitor riverine input and the connectivity of the Mediterranean to the Atlantic. Preliminary results challenge the siphon hypothesis, suggesting that MOW continued to flow through the Rifian Corridor up until the Atlantic-Mediterranean connection was blocked.

Environmental impact of acid mine drainage of Regoufe and Rio de Frades mines (Geopark Arouca, Portugal)

VÁNIA CORREIA^{1*}, PAULO FAVAS^{1,2}, ARTUR SÁ^{1,2}

¹Department of Geology, University of Trás-os-Montes e Alto Douro, Vila Real, Portugal, vfraguito@hotmail.com (*presenting author)

²Geosciences Center, University of Coimbra

In the abandoned mines of Regoufe and Rio de Frades (Arouca Geopark area) a hydrogeochemical study was developed to evaluate the effect of acid mine drainage (AMD) on stream water quality and their ability to self-purification. Previous works demonstrated the occurrence of acid waters in the Regoufe and Rio de Frades mines area.

For this purpose we made two field campaigns to collect water samples, corresponding to the dry and wet periods, which were separated in AMD and stream water, according to the sampling location. The laboratory analyses were performed using current analytical methods (Atomic Absorption Spectrometry, AAS for Ca, Mg, Na and K; coupled graphite furnace AAS for Fe, Mn, Cu, Zn, Cd, Co, Ni, Pb and As; the spectrophotometric method for Cl; SO₄ was analyzed by gravimetry).

The obtained results (Table 1) allow us to discriminate the Rio de Frades mine, mainly by SO₄, Fe and Mg high values, from the Regoufe mine, with Zn, Cd, As e Mn high values, fact that could be explained by the typical mineralization and the oxidation of sulphides of each mine.

This work also shows that the high concentrations of toxic elements, mainly As and Cd, detected in AMD of the Regoufe galleries and tailings, produces a significant contamination of the surrounding aquatic system. In the Rio de Frades mine the major environmental problem is related with the open air sulphide deposits, which are being leached continuously.

Variable	Unit	Stream water			AMD		
		Average	Min.	Max.	Average	Min.	Max.
pH		6.27	5.35	7.10	5.64	4.29	7.50
E.C.	(μ S/cm)	24.75	20.70	36.60	31.13	19.10	58.20
SO ₄	mg/L	3.04	1.52	5.62	5.20	1.16	16.46
Mg	mg/L	0.47	0.35	0.80	0.43	0.18	1.27
Fe	μ g/L	42.59	14.00	100.00	77.77	3.00	321.00
Cd	μ g/L	0.23	0.00	1.25	3.63	0.00	13.31
Zn	μ g/L	17.76	0.00	82.80	174.97	0.00	680.00
Mn	μ g/L	5.57	0.05	15.04	21.68	0.05	104.90
As	μ g/L	6.24	0.85	14.97	65.87	0.76	236.80

Table 1: Summary of chemical composition of AMD and stream waters, from the Regoufe and Rio de Frades abandoned mines.

Perils of paleothermometry using calcium isotopes in coral archives

S.J.G. GALER^{1*}, R. MERTZ-KRAUS², T.C. BRACHERT³,

G. BORNGÄSSER¹, AND H. FELDMANN¹

¹Max-Planck-Institut für Chemie, Mainz, Germany, steve.galer@mpic.de
(*presenting author)

²Berkeley Geochronology Center, Berkeley, USA, rmertz@bgc.org

³Universität Leipzig, Institut für Geophysik und Geologie, Leipzig,
Germany, brachert@uni-leipzig.de

In reconstructing SST paleotemperatures and climate from marine carbonate archives, $\delta^{18}\text{O}$ has proven to be the non plus ultra. A prerequisite, however, is that $\delta^{18}\text{O}$ has itself not varied in open ocean water. This assumption may become problematic due to the effects of polar ice volume, and hydrology in semi-closed basins (runoff and evaporation). Such issues do not arise for Ca isotopes, but attempts at paleothermometry using foraminifera have yielded conflicting results [1-3]. A serious impediment is also the extremely small temperature dependence on $\delta^{44/42}\text{Ca}$ in inorganic and biogenic carbonates of $\sim 0.010\text{‰}/^\circ\text{C}$ [4,5], requiring high analytical precision for it to be at all useful.

Here we explore the potential of $\delta^{44/42}\text{Ca}$ for extracting paleo-SST and seasonality from fossil corals. We studied a pristine 9 Ma-old *Porites* specimen from Psalidha, Crete (Eastern Mediterranean) [6], which was microdrilled to yield a continuous profile with monthly resolution (60 samples) over five annual cycles. The $\delta^{18}\text{O}$ record shows well-developed summer-winter cycles, and implies a slow-down in growth during the winter months. The inter-annual $\delta^{18}\text{O}$ amplitude is $\sim 2.0\text{‰}$ corresponding to SST changes of about 10°C or so [7].

Ca isotopes were measured by TIMS using a ^{43}Ca - ^{46}Ca double spike; internal and external precisions are <0.02 and $\sim 0.04\text{‰}$ (2SD) on $^{42}\text{Ca}/^{44}\text{Ca}$ using 1- μg -sized samples, respectively. $\delta^{44/42}\text{Ca}$, relative to NIST SRM-915a, vary from $+0.20$ to $+0.35$, which are at the lower end of that found in modern corals (see [5]). The absolute SST range of <10 to 20°C inferred from the modern and cultured coral calibration [5] is far too low given that $\sim 14^\circ\text{C}$ is the lower winter limit for *Porites* growth [7]. Since seawater $\delta^{44/42}\text{Ca}$ has not varied much ($<0.1\text{‰}$) over the past 9 Ma [8], this discrepancy is most likely an artifact of slight inter-lab bias. The relative SST amplitude of $\sim 10^\circ\text{C}$ does appear more robust, however, and agrees with that of the $\delta^{18}\text{O}$ record, which is encouraging. Nevertheless, the $\delta^{44/42}\text{Ca}$ and $\delta^{18}\text{O}$ profiles do not match each other particularly well, and the tell-tale seasonality is only partly visible in the $\delta^{44/42}\text{Ca}$ record.

This indicates that Ca isotopes during biomineralization in *Porites* are affected by factors other than just temperature. These factors – such as growth rate, pH, alkalinity, light flux and Mg/Ca – will have to be evaluated carefully. While $\delta^{44/42}\text{Ca}$ in scleractinian coral archives does have much potential as a paleothermometer when $\delta^{18}\text{O}$ fails, more work is needed to understand the mechanisms of isotope fractionation.

[1] Nägler *et al.* (2000) *G³* **1**, 2000GC000091. [2] Sime *et al.* (2005) *Earth. Planet. Sci Lett.* **232**, 51-66. [3] Kasemann *et al.* (2008) *Earth. Planet. Sci Lett.* **271**, 292-302. [4] Gussone *et al.* (2005) *Geochim. Cosmoch. Acta* **69**, 4485-4494. [5] Böhm *et al.* (2006) *Geochim. Cosmoch. Acta* **70**, 4452-4462. [6] Mertz-Kraus *et al.* (2009) *Chem. Geol.* **262**, 202-216. [7] Omata *et al.* (2006) *Global Planet. Change* **53**, 137-146. [8] Griffith *et al.* (2008) *Science* **322**, 1671-1674.

Petroleum system in Sufyan depression of Muglad Basin in Sudan

GAO RISHENG^{1*}, SHI YANLI¹, AND LI ZHI¹

¹Research Institute of Petroleum Exploration & Development,
PetroChina

gaorisheng@petrochina.com.cn (*presenting author)

The Muglad basin in Sudan is located the eastern boundary of Central Africa Strike-slip Fault Zone, is a large Mesozoic petroliferous rift basin. The Sufyan depression is located most north end in this basin. The main structure stale is half graben. The depressions and uplifts arranged in alternative pattern and have different characteristics in the east and the west parts [1].

The Sufyan depression has predominant hydrocarbon forming conditions and a great exploration potential. Lower Cretaceous Abu Gabra Formation is an effective hydrocarbon source rock. Favorable reservoir in this area is the Abu Gabra Formation channel sandbody in delta or fan delta. Upper Cretaceous Darfur Group is the region cap rock. The hydrocarbon trap types have fault anticline, fault nose and fault block etc..

Based on the result of basin modeling, Abu Gabra Formation source rock went into oil generation window at the late stage of Bentiu formaton deposition(97Ma), and reached to oil generation peak at the late stage of Amal formaton (K₃, 56Ma). Hydrocarbons generated from source rock entered into the sandbodies consecutively, and then migrated from the center to the margin of depression ranged in 3000km², the driving force comprised of Formation pressure and buoyancy. According to the history of tectonics evolution, structural type was formed finally in the period of Darfur Group deposition, trap forming period was earlier than hydrocarbon generation peak period. The critical moment of petroleum system was 56Ma, and the duration time of petroleum system ranged from 132Ma to 56Ma, and the preservation started from 56Ma continued to now (Figure 1).

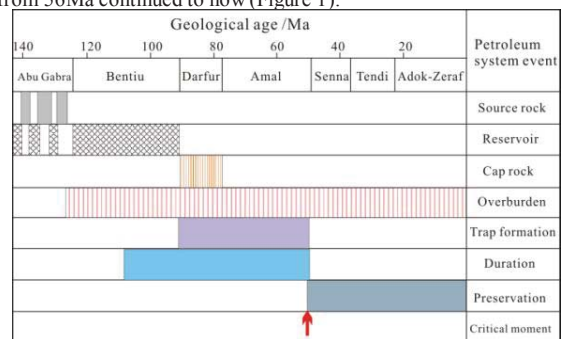


Figure 1: Sketch map showing the petroleum system event in Sufyan depression

The Sufyan depression has two petroleum subsystems vertically, among which Abu Gabra Formation subsystem has favorable assemblage with self generating, collecting and sealing. While the other petroleum subsystem is composed of Abu Gabra Formation source rock, Bentiu Formation channel sandstone reservoir and Darfur Group shale seal. Both they are favorable for exploration. The Central structure belt of the Sufyan depression is most favorable for exploration.

[1] Tong X G *et al.* (2004) *Acta Petrolei Sinica* **25**, 19-24.

U-Pb ages and Sr-Nd-Hf isotopic analysis of accessory phases in carbonatites and phoscorites from the Guli complex, Siberia

MAHDI GHOBADI^{1*}, AXEL GERDES¹, LIA KOGARKO², GERHARD P. BREY¹ AND HEIDI E. HÖFER¹

¹Goethe Universität, Frankfurt am Main, Germany,

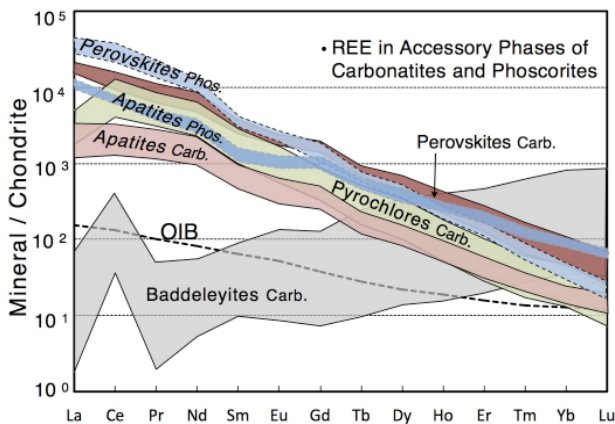
M.Ghobadi@em.uni-frankfurt.de (* presenting author)

²Vernadsky Institute, Moscow, Russia

Introduction

Here we apply Laser Ablation (LA) ICP-MS analysis (spot sizes: 20-60 μm) to four accessory phases from carbonatites and phoscorites of the Guli complex. The aim is to determine the Sr-, Nd-, and Hf-isotopic characteristics as well as the U-Pb ages of the phoscorites and carbonatites through their REE-enriched accessory phases. The advantage compared to the solution-mode bulk analysis is that more data can be acquired in a shorter time span and disturbance due later alteration can be much better resolved.

We analyzed perovskites and apatites from phoscorites and carbonatites plus pyrochlores and baddeleyites from carbonatites. Because of the very high abundances of many trace elements in these phases (Figure below), the Sr and Nd isotopes could be analysed in apatites, perovskites and pyrochlores and Hf in baddeleyites. U-Pb ages were obtained from perovskites, pyrochlores and baddeleyites.



Results and Conclusion

The Sr- and Nd- isotopes of the accessory phases from carbonatites are all identical within error and agree well with literature data obtained from bulk rock samples [1]. Apatites and perovskites of the phoscorites show slightly higher $^{143}\text{Nd}/^{144}\text{Nd}$ and lower $^{87}\text{Sr}/^{86}\text{Sr}$ ratio than those from the carbonatites. The obtained common Pb corrected U-Pb ages also fall in a very narrow range. Baddeleyites, pyrochlores and perovskites from carbonatites yield concordia ages of 250.8 ± 1.4 Ma, 253.9 ± 1.6 Ma and 252.3 ± 1.9 Ma, respectively, while perovskites from phoscorites yield somewhat older ages of 254.4 ± 2.2 Ma. In summary this study shows that apatites, perovskites and pyrochlores are reliable tools for in-situ determinations of Sr-Nd-isotope ratios, baddeleyite is remarkably good monitor for Hf-isotopes and perovskites and pyrochlores can provide reliable U-Pb ages but with a lower accuracy than from baddeleyites.

[1] Kogarko et al. (2006) *A Pb isotope investigation of the Guli massif, Maymecha-Kotuy alkaline-ultramafic complex, Siberian flood basalt province, Polar Siberia Mineralogy and Petrology* **89**, 113-132.

LA-ICP-MS analysis on spinel from chromitites of different tectonic settings: their contrasted minor-and trace-elements compositions

J.M. GONZÁLEZ-JIMÉNEZ^{1*}, W.L. GRIFFIN¹, M. LOCMEIS¹, S.Y. O'REILLY, N.J. PEARSON¹

¹ARC Centre of Excellence of CCFS, ARC National Key Centre of GEMOC, Sydney, Australia

jose.gonzalez@mq.edu.au; griffin@mq.edu.au;

sue.oreilly@mq.edu.au; npearson@mq.edu.au

²ARC Centre of Excellence of CCFS, Centre for Exploration Targeting, Perth, Australia.

marek.locmelis@mq.edu.au

The ratios of Cr, Al, Fe, Mg and Ti in spinels are widely used for determining the nature of parental melts and the geodynamic setting of chromitite formation, as chemistry of spinel is highly sensitive to the geochemical characteristics of its parental melt, which are a function the tectonic setting in which the melt is produced. However, there is a wide overlap in the Cr-Al-Fe-Mg-Ti relationships of spinels in chromitites from different geotectonic settings. We present results of LA-ICP-MS analysis of spinel in chromitites from well-defined and contrasted tectonic settings, including komatiites, layered mafic intrusions and ophiolites (Fig. 1).

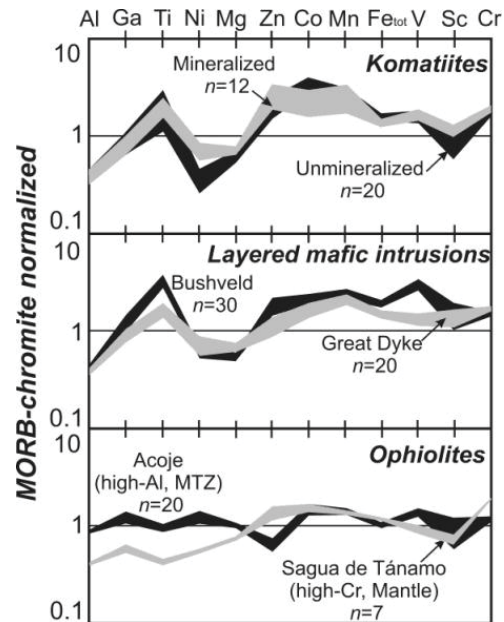


Figure 1. Profiles of major, minor and trace elements in spinel of chromitites from different environments normalized to composition of spinel of MORB [1].

We show that minor- and trace-element (Ga, Ti, Ni, Zn, Co, Mn, V, Sc) patterns of spinel from the three settings studied are clearly distinct. The usefulness of this approach extends to differentiate chromitites generated from different types of melts within a given environment. LA-ICP-MS analysis of chromite is a promising tool for better understanding of the petrogenesis of chromitites.

[1] Pagé & Barnes (2000) *Econ. Geol.* **104**, 997-1018

Nitrogen Cycling Genes and Microbial Diversity from Meke Lake is analogs Mars

YASEMIN GULECAL

¹Istanbul University Department of Freshwater Biology, Istanbul, Turkey, ygulecal@istanbul.edu.tr (* presenting author)

The subsurface of the Earth is one of the major habitats and contains a significant proportion microbial life [1, 2]. However, our overall knowledge about the life forms and biogeochemical processes contained within it is rather scarce, mainly because of the difficulties in approaching this habitat. Recent work has revealed interesting insights into the diversity and resilience of different life forms in analog environments may be revealed and how to recognize biosignatures for subsurface life on other planetary bodies.

Meke Lake is a crater lake, southeast of Karapınar, 8 km. from Karapınar, Turkey. Meke Lake has a circular shape and there is an island in the middle of it which is called Meke. The dept of the lake never exceeds 12 m. The water of the lake comes out from the ground and its water is salty which contains magnesium and sodium sulfate. Meke salty area covers 0.5 km². The lake was formed in a circular shape collapse which had occurred in the first era. And after that, an eruption caused a chimney to rise in the lake. In geology, this rise is called as "Secondary Rise". After this formation volcanic Meke height is formed in the middle of the lake. The special volcanic mess that forms the island has an ability to absorb even the most heavy rain showers. That is the reason why Meke has preserved its shape for thousand years for the Global Warming. The aim of study was to investigate the microbial diversity and their roles of biogeochemical cycling. We have not only used the geochemical analyses but also genetic tools. In addition, this study reports the first microscopic investigations on the microbial communities encountered in the microbial mat Meke Lake.

[1] Whitman et al., 1998. Proc. Natl. Acad. Sci. USA 95: 6578–6583. [2] Roussel et al., 2008. Science 320:1046

Coarse-mode atmospheric particles in a coal mining area of Viet Nam

THI BICH HOÀNG-HÒA^{1*}, RETO GIERÉ¹, VOLKER DIETZE², UWE KAMINSKI², AND PETER STILLE³

¹ Universität Freiburg, Geowissenschaften, 79104 Freiburg, Germany (hoahb@gmail.com) (* presenting author)

² Deutscher Wetterdienst, Research Centre Human Biometeorology, Air Quality Department, 79104 Freiburg, Germany

³ École et Observatoire des Sciences de la Terre, Université de Strasbourg, F-67084 Strasbourg, France

One of the largest coal mining districts of Viet Nam (reserves ~10 Gt) is located near Cam Pha, Quang Ninh province. Exposure to dust is a major challenge for the population living near the open-pit mines, which represent the dominant source of airborne particles [1]. This study focuses on the air quality in Cam Pha, as assessed by monitoring the coarse-mode particle fraction.

The particles have been collected with the passive sampler Sigma-2 on transparent adhesive collection plates for subsequent single-particle analysis by automated optical microscopy. The projected area of individual particles was measured in the size 2.5-80 µm (equivalent diameter). The data shown in Figure 1 represent the averages of two separate measuring campaigns, carried out during fall of consecutive years (7 weeks, Aug-Oct 2009; 6 weeks, Sept-Oct 2010) from three sites in the greater Cam Pha area. Sampling site ST4, located downwind from a major open-pit mine, exhibits the highest particle burden, nearly as high as that observed in Hanoi, but only ~50% of that found in Cairo. ST3 is located on a hill within the town, but not in the direct plume from the mine; its size distribution also has a peak in the 5-20 µm range, but at considerably lower mass concentrations. ST1 represents a background station, located ~10 km from the mines and not affected by pollution, as confirmed by the extremely low mass concentrations and the positive skewed size distribution typical of remote locations. The size distributions for ST3 and ST4 are typical for localities characterized by a local pollution source. The calculated mass concentrations help in monitoring emission levels and in selecting samples for detailed chemical analysis of the particulate pollution.

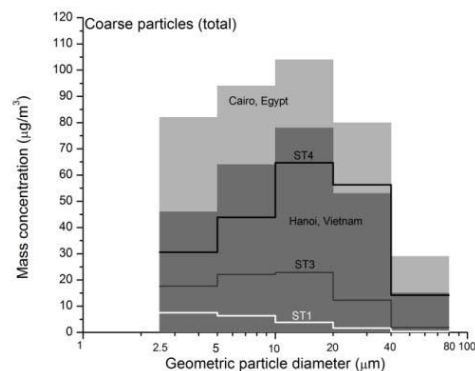


Figure 1: Size distribution of mass concentrations (calculated according to [2]) for coarse particles in the Cam Pha area (ST1, ST3, ST4) and at reference stations in Hanoi and Cairo [3].

[1] Hoàng-Hòa *et al.* (2011) *Min Mag* **75**, 915.

[2] VDI (2012) *VDI guideline* **2119**.

[3] Grobety *et al.* (2010) *Elements* **6**, 229–234.

Dolomite distribution and coarse grained dolomite genesis analysis of Middle Permian in Sichuan Basin

JIANG QINGCHUN^{1*}, YANG XIAOPING¹, BIAN CONGSHENG¹, AND LIU HAITAO¹

¹Research Institute of Petroleum Exp&Dev, Beijing, China, jiangqc@petrochina.com.cn (*)

During the process of investigation the micro-slide of typical wells and the outcrops show that the Permian develop the micro-dolomite, medium-macro crystalline dolomite and leopard dolomite. Porosity and permeability analysis show that reservoir quality of medium-macro crystalline dolomite is best, it can act as the effective reservoir; association with the geology background, multi-geochemical analytic techniques suspect that the medium-macro crystalline dolomite causing by the deep thermal water, which alternate the limestone. Dolomitization fluid is the deep thermal water. The origin evidence of dolomite include six aspects. intercrystalline vugular pore of medium-macro crystalline dolomite was filled by the asphalt. Associated the bury history of typical well, homogenization temperature of fluid inclusions and generation history of source rock show that medium-macro-crystalline dolomite formed very early. At least prior to the Early Jurassic, when the oil generate large scale. After the analysis, origin model of thermal water has been build basing on the typical well of dolomite and the seismic profile.

[1] SCHLAGER, KEIM (2009) Carbonate platforms in the Dolomites area of the Southern Alps—historic perspectives on progress in sedimentology. *Sedimentology*, Volume 56, Issue 1, Pages 191-204

[2] Elizabeth Gusta, K. Dalai (2009) Catalytic Decomposition of Biomass Tars with Dolomites. *Energy & Fuels*, Volume 23, Issue 4, Pages 2264-2272

[3] L. Breesch, R. Swennen, B. Vincent (2010) Dolomite cementation and recrystallisation of sedimentary breccias along the Musandam Platform margin. *Journal of Geochemical Exploration*, Volume 106, Issue 1-3, Pages 34-43

[4] JUDITH A. MCKENZIE (2009) Dolomite Mountains and the origin of the dolomite rock of which they mainly consist: historical developments and new perspectives. *Crisogono Vasconcelos. Sedimentology*, Volume 56, Issue 1, Pages 205-219

[5] H. MIZUOCHI, M. SATISH-KUMAR (2009) Exsolution of dolomite and application of calcite-dolomite solvus geothermometry in high-grade marbles: an example from Skalle vik shalsen, East Antarctica. *Journal of Metamorphic Geology*, Volume 28, Issue 5, Pages 509-526

Impacts of glacial/interglacial cycles on continental rock weathering and CO₂ consumption using Sr/C isotopes in Michigan watersheds

LIXIN JIN^{1*}, SAMUEL B. MUKASA², NIVES OGRINC³, STEPHEN HAMILTON⁴, AND LYNN M. WALTER⁵

¹Department of Geological Sciences, University of Texas at El Paso, El Paso, USA, ljin2@utep.edu (* presenting author)

²College of Engineering and Physical Sciences, University of New Hampshire, Durham, USA, sam.mukasa@unh.edu

³Department of Environmental Sciences, Jožef Stefan Institute, Ljubljana, Slovenia, nives.ogrinc@ijs.si

⁴Kellogg Biological Station and Department of Zoology, Michigan State University, Hickory Corners, USA, hamilton@kbs.msu.edu

⁵Department of Geological Sciences, University of Michigan, Ann Arbor, USA, lmwalter@umich.edu

The upper Midwest USA features glacial-derived till materials enriched in carbonate minerals, but with the uppermost soil layer progressively leached of carbonates in the interval since glaciation. We used C and Sr isotope compositions of soil waters and groundwaters in Michigan watersheds to quantify the relative weathering intensities of the dominant minerals (carbonates from the Michigan Basin, and amphibole, plagioclase and K-feldspar derived from the Canadian Shield), and to elucidate the relationship between the chemical weathering rates and CO₂ consumption fluxes in the soil zones.

The dissolution of plagioclase and amphibole controls shallow soil water ⁸⁷Sr/⁸⁶Sr ratios (0.711-0.713), with minor contributions from K-feldspar weathering. Here respiratory CO₂ was the major source of soil water DIC with little addition from the atmospheric CO₂. Isotopic equilibration between δ¹³C_{DIC} and δ¹³C_{CO2} occurred in an open-system with respect to soil CO₂. In the deeper soil horizons carbonate dissolution dominated soil water chemistry and saturation with respect to calcite and dolomite was attained rapidly. Mass balance calculation showed that large amounts of soil CO₂ were consumed by carbonate dissolution, such that the deeper soil zone may not have been an open system with respect to CO₂. Constant δ¹³C_{DIC} values were observed in these deep soil waters and also in shallow groundwaters of the Huron watershed, due to a rapid kinetics of carbonate dissolution and limited gas-water exchange in the soils., with DIC equally contributed by carbonate minerals and soil CO₂. During the transition from silicate to carbonate weathering, the ⁸⁷Sr/⁸⁶Sr ratios of soil waters move towards the carbonate end-member (~0.709).

Due to the great extent of continental glaciation, Paleozoic carbonate minerals from the Michigan Basin were redistributed widely within the interior of the North America continent. The glacial ice also ground up the ancient Precambrian Canadian Shield, accelerating silicate mineral weathering rates and releasing highly radiogenic Sr from K-feldspar. Both mechanisms lead to elevated weathering fluxes and CO₂ consumption rates after glacial retreat in the Great Lakes Drainage basin.

Insight into the magma source of the Kalkarindji Large Igneous Province.

F. JOURDAN^{1*}, K. HODGES¹, S. TESSALINA¹, M. CHIARADIA²,
L. EVINS³, M. GOLE⁴

¹Curtin University, GPO Box U1987 Perth, WA6845, Australia.

f.jourdan@curtin.edu.au (* presenting author)

²University of Geneva, Rue des Maraichers 13, CH-1205 Geneva, Switzerland.

³Swedish Nuclear Fuel and Waste Management Co, Blekhölmstorget 30, Box 250, 101 24 Stockholm, Sweden.

⁴AusQuest Limited, 8 Kearns Crescent, Ardross WA6153, Australia.

The Kalkarindji large igneous province (LIP) is one of the largest LIPs on Earth, yet, it has received only very little attention (e.g., [1], [2]). This ~510 Ma LIP [3] is located across the Northern Territories and Western Australia and covers a currently known area of $\geq 2.1 \times 10^6$ km² [2] with hints that it stretches as far as the southernmost part of South Australia (equivalent to a total area of $\geq 3 \times 10^6$ km²). The province includes flows, intrusions (dykes and sills) and volcanic tuffs.

We present major, trace and rare earth element analyses obtained on 186 samples from the Antrim and Table Hill areas. A subset of 10 samples representative of both areas was analyzed for Sr, Nd and Pb isotopes and 5 samples were analyzed for Os isotopes. All but one samples are classified as Low-Ti (TiO₂ \leq 2 wt%) basaltic-(trachy) andesite to (trachy) andesite (SiO₂ = 51–63 wt%) and show significant LILE and LREE/HREE enrichment and HFSE depletion (Nb/Nb* = 0.1–0.3). Relatively unfractionated HREEs of the low-Ti rocks suggest a melt extraction from a spinel-bearing lherzolite mantle. The unique high-Ti (TiO₂ = 3.4 wt%) sample analyzed so far shows some HREE fractionation, suggestive of a deeper melt extraction from a garnet-bearing lherzolite source.

Strongly radiogenic initial ⁸⁷Sr/⁸⁶Sr (0.709–0.710) and ²⁰⁶Pb/²⁰⁴Pb (18.11–18.85), with relatively unradiogenic ϵ Nd (–2.1 to –4.2), suggest the involvement of a crustal component in the genesis of the Kalkarindji basalts. Although a co-variation is discernable between ⁸⁷Sr/⁸⁶Sr and Mg#, no correlation is observed between Nd and Pb isotopes vs. Mg#. Furthermore, measured ¹⁸⁷Os/¹⁸⁸Os ratios of 0.1337 and 0.1388 suggest involvement of the sub-continental lithospheric mantle (SCLM) in the genesis of the low-Ti magmas as, for example, previously proposed for the silica-rich Ferrar province [4].

Two models are put forward to account for these geochemical patterns. The first model involves increased temperatures beneath the Gondwana supercontinent, leading to the partial melting of a subduction enriched SCLM. The second model advocates a deep-seated mantle plume that may have assimilated vast quantities of crust during ascent or, alternatively, may have provided the heat required to induce melting of the SCLM. Both models involve a significant contribution from the crust.

[1] Glass & Philips (2006) *Geology* **34**, 461–464. [2] Evins et al. (2009) *Lithos* **110**, 294–304. [3] Jourdan et al. (2012) *34th IGC*, abstract. [4] Molzahn et al. (1996) *EPSL* **144**, 529–545.

Influence of arsenic incorporation on jarosite dissolution rates and reaction products

MATTHEW R. KENDALL^{1*}, ANDREW S. MADDEN¹, MEGAN ELWOOD MADDEN¹ AND QINHONG HU²

¹University of Oklahoma, ConocoPhillips School of Geology and Geophysics, matthew.r.kendall-1@ou.edu (* presenting author), amadden@ou.edu, melwood@ou.edu

²University of Texas at Arlington, Earth and Environmental Sciences, maxhu@uta.edu

Abstract

Jarosite (KFe₃(SO₄)₂(OH)₆) is an environmentally important mineral because it contributes to the natural attenuation of arsenic in some acid mine/rock drainage (AMD/ARD) environments by incorporating arsenate into its crystal structure [1]. However, when solution conditions are altered beyond the stability region for jarosite (e.g., by heavy rain events or remedial action) the mineral will dissolve and potentially release the incorporated arsenic back into the environment. With an abundance of inactive or abandoned mine sites in the United States, it is important to understand the complex geochemical reactions that may enhance or reduce the effects of AMD/ARD.

For this study, arsenojarosite and potassium jarosite were synthesized in the laboratory with varying amounts of incorporated arsenic. X-ray diffraction was used to verify the formation of jarosite, while EMPA and ICP-MS were used to measure the amount of arsenic incorporated into the jarosite. Batch experiments were then undertaken to measure potassium release rates, aqueous arsenic concentrations, and to identify the nanoscale reaction products in pH 2 H₂SO₄, ultra-pure water, and pH 8 TRIS buffered solution. In ultra-pure water, potassium release rates (log r, mol m⁻² s⁻¹) for jarosite containing 0%, 0.6%, 2.1%, and 3.7 wt% arsenic were -9.05 (+/- 0.32), -9.02 (+/- 0.14), -8.78 (+/- 0.06), and -7.71 (+/- 0.07) respectively. Potassium release rates for pH 2 and pH 8 experiments show similar trends but slightly faster dissolution rates. Using TEM, the nanoscale reaction products were identified to be iron (oxyhydr)oxides, predominately aggregates of nanosized (5–10 nm) maghemite crystals. Alteration of aggregate morphology from spherical to “worm-like” segments and decreased particle crystallinity occur with increased arsenic concentrations in ultra-pure water experiments. As arsenic incorporation into jarosite increases, the rate of potassium release also increases. Fluctuations of arsenic concentrations in the ultra-pure water and pH 8 experiments are likely due to sorption/desorption of arsenic onto newly formed iron oxides. These results show that the dissolution of arsenojarosite can have a significant impact on AMD/ARD environments through the release of arsenic to solution or sorbed on the surfaces of nanoparticulate iron oxides, dependent on solution (e.g. pH) conditions.

[1] Slowey, Johnson, Newville, and Brown (2007) *Applied Geochemistry*, **22**, 1884–1898.

Distribution and mobility of Cu, Zn, Pb and As in the stream sediments from the area affected by historical mining and smelting

JAKUB KIERCZAK^{1*}, AND ANNA PIETRANIK^{1†}

¹University of Wrocław, Institute of Geological Sciences, Wrocław, Poland, jakub.kierczak@ing.uni.wroc.pl (* presenting author),
†anna.pietranik@ing.uni.wroc.pl

Potentially toxic metal(loid)s occurring in stream sediments may have both lithogenic and anthropogenic origins. Generally, anthropogenic sources provide larger amounts of metal(loid)s than natural ones. Thus, analysis of chemical composition of stream sediments may be used for the assessment of anthropogenic activities in a given area.

High concentrations of some potentially toxic metal(loid)s have been detected in the stream sediments at the Rudawy Janowickie area (southwestern Poland). The studied site represents a historical industrial centre of Cu mining and smelting. Field observations coupled with chemical and mineralogical analyses revealed that elevated concentrations of metallic pollutants in stream sediments are caused by the presence of smelting wastes (slags) in the immediate vicinity of the three studied streams. The most important contaminants are Cu and Zn with concentrations in stream sediments reaching up to 1500 mg kg⁻¹. Pb and As are also found in elevated amounts comparing to the geochemical background (up to 180 mg kg⁻¹ for Pb and 230 mg kg⁻¹ for As).

The assessment of metal(loid)s contamination in sediments was done using the geoaccumulation Index (I_{geo}) [1] and the Pollution load index (PLI) [2]. Both methods showed that at the sites where the smelting wastes are widespread, the stream sediments are seriously polluted (PLI up to 27 and I_{geo} reaching up to 5 for Cu and As, 4 for Zn and 3 for Pb). The results indicate that the main source of metallic pollution in studied area is represented by historical Cu smelting.

The metal(loid)s mobility estimation in studied sediments was done using the EDTA extraction method [3]. The mobility of the studied elements decreases in order of Pb>Cu>Zn>As. No relationship was observed for the sediment contamination and the mobility of metal(loid)s. With the exception of Zn, whose mobility is inversely proportional to the sediment contamination ($R^2=0.72$, $p<0.05$). It is due the fact that Zn is concentrated in the smelting wastes in phases rather resistant to weathering such as well crystalline silicates and oxides.

Acknowledgements

The work was financed by Polish Ministry of Science and Higher Education grant no. NN307051237.

[1] Müller (1969) *GeoJournal* **2**, 108-118. [2] Tomlinson (1980) *Helgol Meeresunters* **33**, 566-575. [3] Quevauviller (1998) *Trends Anal Chem* **17**, 289-298.

Discovery and characterization of nano Ag and Zn sulfides, and nano TiO₂ particles in sewage sludge, and resulting critical implications for the terrestrial environment

BOJEONG KIM^{1*}, MITSUHIRO MURAYAMA², BENJAMIN P. COLMAN³ AND MICHAEL F. HOHELLA, JR¹

¹Virginia Tech, Department of Geosciences, Blacksburg, VA, USA, bk74@vt.edu (* presenting author)

²Virginia Tech, Department of Materials Science and Engineering, Blacksburg, VA, USA, murayama@vt.edu

³Duke University, Biology Department, Durham, NC, USA, colmanb@gmail.com

The increasing production and extensive, existing and new application of engineered nanoparticles (NPs) for commercial uses will likely increase their release to the environment, yet our understanding of their fate and behavior in the environment is lacking. In the present study, we examined the most likely route for engineered NPs entering the terrestrial environment, i.e., application of sewage sludge products to soils as an amendment, by focusing on Ag-, Zn-, and Ti-containing NPs. Among the commercially available engineered NPs, these are the most widely used to date. First, we examined several sewage sludge products collected as part of the USEPA Targeted National Sewage Sludge Survey. Secondly, we conducted a field-scale mesocosm experiment to investigate the fate and behavior of sewage sludge-born TiO₂ NPs in a terrestrial ecosystem. In both cases, we employed transmission electron microscopy (including scanning and high resolution TEM, as well as detailed selected area electron diffraction) combined with energy dispersive X-ray spectroscopy for direct visualization and thorough characterization of the NPs from the highly complex and heterogeneous sewage sludge matrices. Optimizing sample preparation, along with efficient SEM and TEM surveying techniques, allowed us to perform very extensive searches in order to assure ourselves that we were obtaining representative data.

In all sludges tested, both Ag and Zn are always associated with sulfur. The only sulfides present are α -Ag₂S (acanthite) and ZnS (sphalerite). Sizes range from a few tens to several hundred nanometers, and the particles are most commonly loosely aggregated. The most likely explanation for these findings is that the sulfide crystals are formed in situ in anoxic sewer systems and/or during wastewater treatment under anaerobic conditions. In contrast, we only found oxides of Ti (in all cases TiO₂ rutile) from sewage sludge products in a similar size range as the sulfides. Due to the refractory nature and extremely low solubility of TiO₂, it is unlikely that this phases is modified internally, but important sorption/desorption reactions can take place. Indeed, our investigation in conjunction with the field-scale mesocosms experiments show for the first time that nano-TiO₂ can sorb toxic trace metals like Ag and then enter the terrestrial environment when the sludge products are added as a soil amendment. Thus, it is very important to have adequate knowledge of the nature of mineral phases in the sewage sludge products in order to predict their long term behavior, fate and impact in the terrestrial soil environment.

Organic matter accumulation in Hudson Bay over the Late Holocene

LAUREN KOLCYNski¹, YVAN ALLEAU¹, MIGUEL A. GOÑI^{1*},
GUILLAUME ST-ONGE², TORSTEN HABERZETTL³, PATRICK
LAJEUNESSE⁴

¹Oregon State University, College of Earth, Ocean & Atmospheric
Sciences, mgoni@coas.oregonstate.edu (* presenting author)

²Université du Québec à Rimouski, ISMER & GEOTOP,

guillaume_st-onge@uqar.qc.ca

³Friedrich-Schiller-University Jena, Institute of Geography,
torsten.haberzettel@uni-jena.de

⁴Université Laval, Département de géographie & CEN,
patrick.lajeunesse@ggr.ulaval.ca

Abstract

We have constructed a high-resolution record of organic matter accumulation from combined gravity-piston core sediments collected in the south-eastern region of Hudson Bay. A series of ¹⁴C-dates indicate the combined record extends to ~3500 cal BP and CAT-Scan and multi-sensor core logger data reveal relatively uniform sediments throughout the cores. Organic carbon (OC) and calcium carbonate contents (CaCO₃) of the sediments ranged from 0.4 to 0.6 wt% and 2.5 to 5.5 wt%, respectively, with down core variations that appear related to changes in lithology (e.g., mineral surface area, density and magnetic susceptibility). The carbon-to-nitrogen ratios of the organic matter ranged from 8 to 12 mol:mol, with a steady increase from the bottom of the core suggestive of enhanced contributions from terrestrial sources (higher C:N ratios) over the past 3500 years. Analyses of terrestrial- and marine-derived biomarkers have been completed and these data will be integrated into the bulk measurements to investigate changes in the contribution of allochthonous and autochthonous sources in this region over the late Holocene. We will integrate these signals to evaluate temporal changes in vegetation/fire frequency in the surrounding watersheds and productivity in the overlying water column.

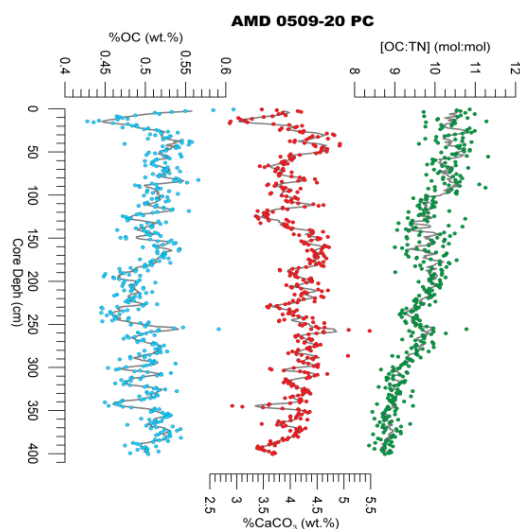


Figure 1: Late Holocene records of organic and inorganic compositions of sediments from a piston core in SE Hudson Bay.

Proton binding at the akaganéite/water interface

PH. A. KOZIN^{*}, J-F. BOILY

Department of Chemistry, Umeå University, Umeå, Sweden,
philipp.kozin@chem.umu.se (*presenting author)
jean-francois.boily@chem.umu.se

Akaganéite is an iron oxyhydroxide mineral, composed of double chains of edge-sharing iron octahedra. These double chains form 2×2 tunnels, stabilized by Cl⁻ ions, receiving hydrogen bonds from bulk hydroxo groups. Cl⁻ ions can easily exchange to aqueous solutions in response to variations in pH and ionic strength [1]. As these variations induce (de)protonation reactions in both bulk and surface sites, buffering capacities of aqueous suspensions of akaganéite nanoparticles are expected to differ considerably from those of other iron oxyhydroxides. This study was consequently devised to probe proton (ad)sorption to the akaganéite surface and bulk.

Potentiometric titrations and zeta potential experiments were carried out on akaganéite nanoparticles equilibrated in solutions of NaCl and NaClO₄. Important differences in suspension pH values are ascribed to proton-chloride uptake to the bulk in NaCl ionic media [2], and to the inability of ClO₄⁻ ions to enter the akaganéite tunnels. The resulting proton uptake data are thereby atypical for iron oxyhydroxides (Fig. 1). Zeta potentials moreover point to a point of zero charge near pH 10 in all ionic media, yet low ionic strength titration data lack the expected sigmoidal-type shape in this region.

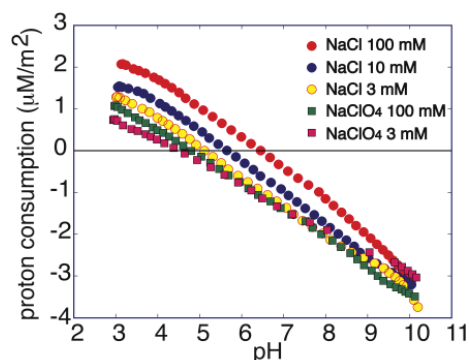


Fig.1 Proton adsorption data of akaganéite nanoparticles, suspended in NaCl and NaClO₄ aqueous solutions.

Our results point to contributions from the akaganéite bulk (hydr)oxo groups on proton uptake reactions. Although akaganéite is not of widespread occurrence in nature, these results underscore the importance of tunnel-like structures in minerals, either as surface defects or inherent features in other minerals (e.g. schwertmannite), on charge development, and thereby surface reactivity.

[1] Reguer et al. (2009) *Corrosion Science* **51**, 2795-2802.

[2] Kim, Grey (2010) *Chemistry of Materials* **22**, 5454-5462.

Geologic Characteristic of Tight Oil Reservoirs of Triassic Yanchang Formation in Huaqing Area of Ordos Basin in China

WANG LAN ZOU CAINENG LI YING

Research institute of Petroleum Exploration & Development,
Petrochina, Beijing 100083, China
(*correspondence: wl2008@petrochina.com.cn)

Ordos basin is a kind of superimposed basin with Cratonic marine facies sediments and terrestrial depression, which is located in central western part of China with an area of approximate 320,000 km² [1]. Ordos basin was once an enormous inland depression basin during the late Triassic, great river and lake delta were developed in a humid environment. Large-area Sand bodies and deep lake facies hydrocarbon source rocks are observed as an interstratification and superimposed layers, and based on this condition, tight sandstone reservoir is formed. Based on the examination of total 600 meters of conventional cores from 30 wells, the characteristics of the tight sandstone reservoirs in Huaqing area have been summarized: (1) The sedimentary characteristics: channels sand bodies and gravity flow sand bodies are widely distributed in Huaqing area of the basin center, it is considered to be one of the characteristics of hinterland depressed basin in China. (2) Weak hydrodynamic deposition can result in the bad separation effect of sand bodies, the relatively high shale contents, the relatively strong diagenesis, and very low porosity & permeability. The strong compaction and cementation not only caused low porosity & permeability, but also the significant heterogeneity. Generally, the permeability is less than 0.001 μm² and porosity is less than 14%. Primary intergranular pores are developed in the deltaic front subaqueous distributary channel. Sandstone and feldspar corrosion cavities are developed in gravity flow sandbody environment. (3) In terms of the reservoir type, the tight sandstone reservoir is the typical lithologic one. Petroleum accumulation is affected mainly by favorable hydrocarbon source rocks and reservoir sand bodies. Tight sandstone reservoirs are formed due to that peak period of large-scale of hydrocarbon migration occurs after compaction, which is one of the forming reasons of the tight sandstone reservoirs. Microcrack under the tectonic stress action can improve the physical properties of the reservoirs.

[1] Yang (2005) AAPG Bulletin, 89 (2) :255-269.

A new chemical isolation method for determining petrogenic and biospheric contributions to riverine particulate organic carbon: Application to the Yangtze River

GEN LI^{1,2*}, XINGCHEN WANG^{1,3}, JUNFENG JI¹,
AND JOSHUA WEST²

¹Department of Earth Sciences, Nanjing University, Nanjing, CHINA; jijunfeng@nju.edu.cn

²Department of Earth Sciences, University of Southern California, Los Angeles, USA; genli@usc.edu
(*presenting author); joshwest@usc.edu

³Department of Geosciences, Princeton University, Princeton, USA; xingchen@princeton.edu

The particulate organic carbon (POC) transported by rivers has an important impact on both the geological and contemporary carbon cycles [1]. Riverine POC is a mixture of (i) radiocarbon-dead petrogenic (bedrock-derived, fossil) OC; (ii) aged biospheric OC associated with refractory soil components; and (iii) recent, labile biospheric OC derived from vegetation [2]. Quantitatively distinguishing between these is critical for evaluating the effect of POC transport on the carbon cycle – for example, erosion and oxidation of refractory soil carbon may represent a source of CO₂ to the atmosphere, while the same may not be the case for transport of POC from recent vegetation. It has remained difficult to differentiate between the components of POC without detailed radiocarbon analyses.

We have developed a chemical isolation method for distinguishing OC components in river sediments. We have tested this method using samples collected from the lower reaches of the Yangtze River, over one year (10/2007-9/2008). Measurements of carbon content before and after partial oxidation allow quantitative separation of the recent, vegetation-sourced OC from the refractory and petrogenic. Analysis of the treated samples by Raman spectroscopy confirmed that the treated material was characterized by graphite. The chemical method was validated by comparing results with the fraction of petrogenic OC determined by binary mixing calculations using radiocarbon content and OC % [3]. Similarity of results suggests that chemical isolation may provide a reliable tool for untangling the various components of riverine POC. Further tests on samples from other localities will help to confirm this.

In the case of the Yangtze River, petrogenic OC comprised ~20% of the total riverine POC over the study period, with a petrogenic flux of ~0.5 Tg C/yr. The fate of this carbon is constrained by data from an offshore core from the East China Sea [4], which potentially indicates the effective preservation of this carbon on the continental shelf.

[1] Berner (1990) *Science* **249**, 1382. [2] Galy & Eglinton (2011) *Nat. Geosc.* **4**, 843-847. [3] Galy et al. (2008) *Science* **322**, 943-945. [4] Yang et al. (2011) *Mar. Chem.* **123**, 1-10.

REE evolution of the Lala IOCG deposit, Sichuan, China

ZEQIN LI^{1,2*}, CHONGJUN HUANG¹, AND JIANGZHEN WANG²

¹ Department of Geochemistry, Chengdu University of Technology, Chengdu, Sichuan 610059, China (*correspondence: zeqinlee@gmail.com)

² State Key Lab. of Geohazard Prevention & Geoenvironment Protection, Chengdu University of Technology, Chengdu, Sichuan 610059, China

The Lala Fe-oxide IOCG deposit is located at Sichuan, South China. The total metal resource is estimated at 200 Mt, with 0.92% Cu, 0.018% Mo, 0.022% Co, **0.25% RE₂O₃**, 0.16 ppm Au, and 1.89 ppm Ag.

Three different paragenetic stages of Cu-Fe have been identified. Stage I is accompanied by enriching of REE. Apatite-bearing REE and a few allanite were formed in this stage. Some purple fluorites and rare monazite and bastnasite are formed in stage II. The purple fluorite usually are rich in REE. Some white fluorites were formed in stage III, which is not enriched in REE.

REE-bearing apatite is the most important REE mineral in Lala. The content of REE-bearing apatite in the ore is 3~11%. It occurs as euhedral to subhedral crystals and sizes 0.1~10 mm. Most of the apatite contains a lot of inclusions of monazite and other REE minerals orientated along C axis of it. They are rich in REE (Fig.1). These apatite formed by metamorphism.

The apatite was altered by metamorphic hydrothermal solution at stage II. The REE-mineral inclusions in some of apatite were partly or fully "cleaned" out. The content of the altered apatite were reduced much. The REE leached transferred into the hydrothermal solution. Then they deposited as monazite and bastnasite. Some enter into purple fluorites. At late stage, a little REE is remained in the system. Thus the white fluorite formed in stage III has a little REE.

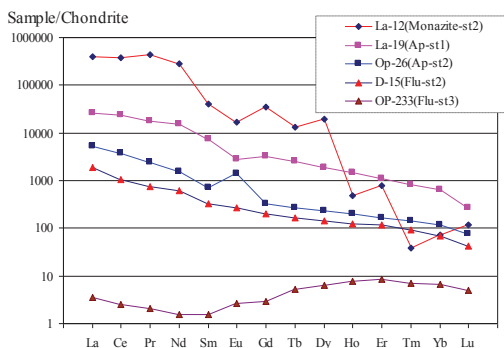


Figure 1 Chondrite-normalized REE patterns of apatite-bearing REE and other minerals in Lala.

The primary REE of the deposit is apatite-bearing REE, which is pyroclastic origin. All of the later REE minerals are sourced from the REE-bearing apatite. REE were redistributed in stage II and III. The new evidence suggests that REE, possibly with other ore-forming elements would be concentrated firstly in the magmatic process during the Kang-Dian Rift development (~1700Ma).

Acknowledgements Support by the National Natural Science Foundation of China (grant: 41072065).

Glacial/Interglacial records of alkenone sea surface temperature in the Japan Sea over the last 170 ka

YANGUANG LIU^{*}, JINXIA CHEN AND XUEFA SHI

First Institute of Oceanography, State Oceanic Administration, Qingdao, China, yanguangliu@yahoo.com.cn (* presenting author)

As a semi-closed marginal sea of the northern Pacific, the Japan Sea (JS) is strongly influenced by the inflow of warm and saline Tsushima Warm Current, the sea-level changes and the East Asian monsoonal (EAM) climate during the late Quaternary.

The uppermost part of ODP site 797 (10.37 m long and spanning the last 170 ka) [1], which located at the south central part of JS, were analysed for C₃₇ alkenones unsaturation index (U^K₃₇) and isotopic compositions of total organic carbon (δ¹³C_{org}). The alkenone sea surface temperature (U^K₃₇-SST) was estimated using the Müller equation [2]. Figure 1 shows that the U^K₃₇-SST oscillated roughly following the glacial/interglacial cycles between 3.8 and 21.5°C with minimum values in MIS (marine isotope stage) 6 and maximum values in MIS 5.3 and MIS5.5. The anomaly high U^K₃₇-SST values during the last glacial maximum (23-18 ka) is a common case in the JS despite this question is not fully interpreted so far. High U^K₃₇-SST recorded in MIS1, MIS5.5, MIS5.3 and MIS5.1 correspond to the higher summer insolation at 65°N [3], stronger summer EAM [4] and higher sea-level [5], revealing a closing connection between the JS sedimentary records and global paleoclimatic proxies. From MIS5.2 to MIS4, the δ¹³C_{org} records of ODP site 797 are not compatible with other proxies imply that the JS experienced different organic geochemical processes from other periods when the JS became semi-isolated to the open sea at the sea level stand of 50 m.

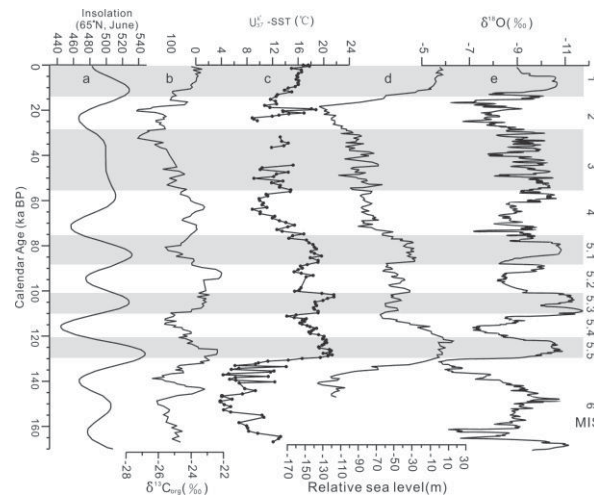


Figure 1: δ¹³C_{org} (b) and U^K₃₇-SST (c) records of ODP site 797 and its linkage to the summer insolation at 65°N (a), relative sea-level changes (d) and δ¹⁸O of speleothem calcite in Sambao and Hulu cave (e)

[1] Tada *et al.* (1999) *Paleoceanography* **14**(2), 236-247. [2] Müller *et al.* (1998) *Geochim. Cosmochim. Acta* **62** (10), 1757-1772. [3] Berger (1978) *J. Atmos. Sci.* **35**, 2362-2367. [4] Waelbroeck *et al.* (2002) *Quat. Sci. Rev.* **21**, 295-305. [5] Wang *et al.* (2008) *Nature* **451**, 1090-1093.

This work was supported by NSFC projects (40606016, 41076038).

Mine hydrochemistry characteristic analysis and recharge tracing based on MSA and GIS: A case in Panyi

LEI MA*, WEIDONG ZHAO, AND XIAOPING ZHOU

School of Resources and Environmental Engineering, Hefei University of Technology, Hefei, China, lei8505@gmail.com

Analysing groundwater hydrochemistry characteristics to understand groundwater recharge, runoff and discharge is an important measure for control and treatment of catastrophic influx of water to coal mines [1-3]. But groundwater is dynamic, as part of the hydro-geochemical cycle and continually undergoing water-rock interaction, and its properties vary in space and time [4-8]. Coupling multivariate statistical analysis (MSA) and GIS is a good method to explore more information from groundwater chemistry. First, categorical principal components analysis (CatPCA) was employed to analyze hydrochemistry characteristics of groundwater, which can reveal relationships between cases, between variables, and between variables and cases^[1]. Then, water samples of coal seam sandstone fracture aquifer were analyzed with factor analysis (FA). The factors were explained according to the results of CatPCA. Next, the water samples with coordinates and factor scores were imported to GIS spatial database. Lastly, spatial distribution of factor scores were drawn by IDW interpolation method.

The results of CatPCA show Cenozoic top aquifer water is distinct from other water, because the aquifer directly receives low-salinity precipitation recharge, while the other groups are high salinity confined water. Water samples of Cenozoic bottom aquifer are close to SO_4^{2-} , total hardness, Ca^{2+} and Mg^{2+} , which shows that the aquifer water has high correlations with these variables. While, the FA results of coal-seam aquifer water show Ca^{2+} , Mg^{2+} , total hardness, SO_4^{2-} , pH are strongly correlated with the first factor, and TDS, K^+Na^+ , Cl^- , HCO_3^- are strongly correlated with the second factor. So, the first factor scores of FA can be explained as the effect sizes of Cenozoic bottom aquifer water.

The spatial distribution of the first factor scores presents high factor scores in the north, while low scores in the south, which implies coal-seam aquifer water is recharged by the Cenozoic bottom aquifer in the north of the area, which agrees well with the geology condition. There is an anticline from northwest to southeast in the area. Because of the lack of aquiclude between coal-seam aquifer and Cenozoic bottom aquifer in the anticlinal axis and pumping in coal-seam aquifer for coal mining, Cenozoic bottom aquifer water has strongly recharged the coal-seam aquifer. Therefore, combining MSA and GIS cannot only analyze vary characteristics of hydrochemistry indexes themselves, but also can analyze vary of some potential information in hydrochemistry. (Grant: 2009HGXC0233)

[1] Ma *et al.* (2011) *Mineral. Mag.* **75**(3), 1375. [2] Qian *et al.* (2011) *J. Hydrol.* **399**, 246-254. [3] Qian *et al.* (2011) *Hydrogeol. J.* **19**, 1431-1442. [4] Lu *et al.* (2011), *Bioresour. Technol.* **69**, 10401-10406. [5] Chen *et al.* (2009) *Journal of Hydrodynamics* **21**(6), 820-825. [6] Qian *et al.* (2009) *Hydrogeol. J.* **17**, 1749-1760. [7] Qian *et al.* (2011) *Hydrol. Process.* **25**, 614-622. [8] Qian *et al.* (2006) *Hydrogeol. J.* **14**, 1192-1205.

The Paleozoic Reservoir Characteristics and Genetic Mechanism of the Basic and Neutral Volcanic Rocks in the West of China

MAO ZHIGUO^{1,2*}, ZHU RUKAI^{1,2}, GUO HONGLI^{1,2}, WANG JINGHONG^{1,2}, AND JIANG HUA¹

¹Research Institute of Petroleum Exploration and Development, Petrochina, Beijing, China

²State Key Laboratory of Enhanced Oil Recovery, Beijing, China (*correspondence: owenmao@126.com)

Background and methods

The significant oil-gas have recently been discovered in the Paleozoic volcanic rocks in sedimentary basins in the west of China, such as Junggar basin and Santanghu basin. These reservoirs were buried at the depth of 3000-4500m with high porosity (5%-30%, average of 12%).

Analyzed cores, rock slices, SEM, image logging, the lithology was composed of basic and neutral volcanic rocks. The reservoir had the complex types and structure of reservoir spaces (Figure 1). The formation and evolution of the volcanic reservoir spaces underwent eruption, condensation, weathering, leaching, burial in the Paleozoic era, and diagenesis, dissolution in the Mesozoic-Cenozoic era.

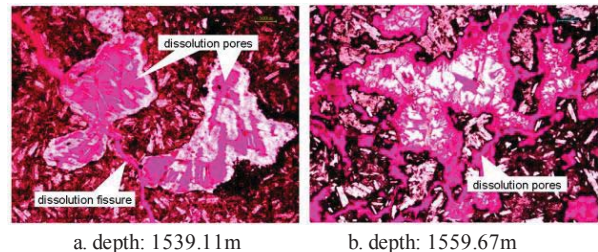


Figure 1: Characters of the Paleozoic volcanic reservoir spaces in the west of China (Well A, andesite, Carboniferous)

Results and Conclusion

It was very meaningful for oil exploration in volcanic rocks.

1) The reservoir spaces are main various types of secondary dissolution pores, such as phenocryst dissolution pores, matrix dissolution pores, amygdale dissolution pores, inter-breccia dissolution pores. These pores are connected by the fissures and cracks.

2) A variety of factors control formation and evolution of the volcanic reservoir spaces. The dissolution of weathering, leaching, and formation fluid is the main reason of the secondary pores development in the basic and neutral volcanic rocks in the west of china. It can increase 5% reservoir spaces for volcanic rocks.

U-Th-REE-Hf-rich phases in marine sediments reflect weathering effect

S. MARCHANDISE^{1*}, E. ROBIN^{1,2}, S. AYRAULT¹

AND M. ROY-BARMAN¹.

¹Laboratoire des Sciences du Climat et de l'Environnement (IPSL/LSCE CNRS-CEA-UVSQ), Allée de la Terrasse, 91198 Gif-sur-Yvette Cedex, France, Sandra.Marchandise@lscse.ipsl.fr (* presenting author)

²CEA-Grenoble, INAC/SP2M/LEMMA, 17 rue des martyrs, 38054 Grenoble cedex 9

The abundance, size and composition of micron-size U-Th-REE-Hf rich phases of marine clayey silt sediments from the Western Mediterranean sea (DYFAMED site) were determined using an automated scanning electron microscope equipped with an energy dispersive spectrometer. The minerals found in the sediment were monazite (mean size $\approx 2,2 \mu\text{m}$), allanite (mean size $\approx 3,1 \mu\text{m}$), florencite (mean size $\approx 1,2 \mu\text{m}$), xenotime (mean size $\approx 4,7 \mu\text{m}$) and zircon (mean size $\approx 2,4 \mu\text{m}$). The size distribution and chemical composition of each phase were used to determine their contribution to the sediment content in U, Th, REE, Y, Zr and Hf.

The detrital fraction of marine sediments is the end product of the erosion of a large variety of crustal rocks. The comparison of the contribution of each mineral to the total trace element content of granites [1] and marine sediments (end product of erosion) provides an integrated view of the effect weathering on accessory minerals. The very low alterability of zircon and xenotime is deduced from their very high contribution (around 100 %) to the Zr, Hf and HREE inventories in both granites and marine sediments and the similar levels of U, Th and REE in zircons and xenotimes from both types of rocks. In contrast, the low contribution of monazite and allanite to the total inventory of U, Th and LREE in marine sediments (whereas these minerals contain most of these elements in granites) implies that monazite and allanite have been strongly weathered. Similarly, the low U and Th content of sedimentary monazite and allanite could be due to the preferential leaching of these elements, or just be related to the nature of the primary unaltered material only. Unlike Th and U, the LREE concentrations of monazite and allanite are identical in DYFAMED and in granites [1]. Therefore, it seems likely that a significant fraction of these minerals initially presents in magmatic rocks are completely dissolved during erosion (in addition to a preferential loss of U-Th in the remaining monazites and allanites). Thorium silicates (thorite and huttonite, ThSiO_4) and uraninite are common in granites but were not detected in the DYFAMED sediments suggesting that they are completely lost during erosion. Florencite, a mineral that can be an alteration product of monazite [2], contains a small fraction of LREE, U and Th but it does not account for the "missing" U, Th and LREE that are not on monazite and allanite. In the case of U, a preferential loss of large zircons during transport can also contribute to the low contribution of accessory minerals in the sediment.

Implications for the U-Th, Sm-Nd and Lu-Hf systematics will be discussed.

[1] Bea (1996) *Journal of Petrology* **37**, 521-552.

[2] Rasmussen (1996) *Am. J. Sci.* **296**, 601-632.

Chromium Speciation in Silicate Glasses and Melts: an in-situ XAS Study

P. M. MARTIN¹, D. R. NEUVILLE², D. TESTEMALE³, M. VILASI⁴
AND C. PETITJEAN⁴

¹CEA, DEN, DEC Cadarache, F-13108 Saint Paul Lez Durance Cedex, France.

²CNRS-IPGP, Géochimie&Cosmochimie, Paris Sorbonne Cité, 1 rue Jussieu, 75005 Paris, France.

³Institut Néel, Département MCMF, 38042 Grenoble, France.

⁴Institut Jean Lamour, BP 70239, 54506 Vandoeuvre, France.

In order to progress in the comprehension and the modeling of how a doping element can modify properties of materials, one of the essential data is the chemical and valence state (its speciation) as a function of manufacturing conditions (temperature, matrix composition, concentration, sintering atmosphere ...). Chromium is widely used in glasses industry. In particular, as coloration agent in packaging design [1], but also in oxides for modifying their properties for either the cast of glasses or the surface of materials put in contact with liquid phases. However, according to temperature, chemical composition and fugacity (or oxygen potential for oxides), the speciation of chromium varies and specific conditions can lead to the stabilization of normally unstable oxidation states (ex: 2+). The challenge is to be able to follow in situ during the material/glass elaboration the evolution of chromium valence.

X-ray Absorption Spectroscopy at chromium K edge is perfectly suited for this application as it allows obtaining both local environment and electronic properties of an element even at very low concentration (~100 ppm). For example, this non-destructive technique has been widely used since ten years to follow the evolution of several elements as a function of temperature [2] in glasses. But, the quantitative determination of the speciation of an element such as chromium using XANES measurements still requires experimental developments.

Here we show our first in-situ XAS results up to 1400°C obtained on sodium silicate glasses and melts on samples initially doped with ~1000 ppm of chromium. Measurements were performed at the MARS beam line of SOLEIL at Cr K edge (5989 eV) in fluorescence mode. In a first time, the evolution of Cr speciation as a function of glasses composition and annealing atmosphere will be presented. In the second time, the in situ evolution of chromium valence as a function of temperature up to 1400 °C will be shown and compared to results already obtained on iron at the same conditions [3,4].

[1] O. Villain, G. Calas, L. Gaiosy, L. Cormier and J.-L.

Hazemann, *J. American Ceramic Society* **90**, 3578-3581 (2007).

[2] D.R. Neuville, L. Cormier, D. de Ligny, J. Roux, A.-M. Flank, P. Lagarde, *American Mineralogist* **93**, 228-234 (2008).

[3] V. Magnien, D. R. Neuville, L. Cormier, B. O. Mysen B.O. and P. Richet, *Chem. Geol.*, **213**, 253-263 (2004).

[4] V. Magnien, D. R. Neuville, L. Cormier, J. Roux, J.-L. Hazemann, D. de Ligny, S. Pascarelli, I. Vickridge, O. Pinet and P. Richet, *Geochim. Cosmochim. Acta.* **72**, 2157-2168 (2008).

Zn-Cl Complexation in Magmatic-Hydrothermal Solutions: Stability Constants from *Ab initio* Molecular Dynamics

YUAN MEI^{1,2*}, DAVID M SHERMAN³, JOËL BRUGGER¹, WEIHUA LIU²

¹School of Earth and Environmental Sciences, The University of Adelaide, Adelaide, SA 5005, Australia,

²CSIRO Earth Science and Resource Engineering, Clayton, VIC 3168, Australia

³Department of Earth Sciences, University of Bristol, Bristol, BS8 1RJ, UK

yuan.mei@adelaide.edu.au (* presenting author)

The speciation of metal complexes in hydrothermal brines plays a key role in controlling the mobility and solubility of minerals in natural and man-made fluids. Experimental measurements of metal speciation is a major challenge, however, and semi-empirical equations of state (e.g., the HKF^[1] model) have been needed to estimate thermodynamic properties of hydrothermal fluids. Now, however, we can apply *Ab initio* (quantum mechanical) molecular dynamics simulations, based on density functional theory, to predict the speciation of metal complexes in hydrothermal fluids as a function of temperature, pressure and fluid composition. Using thermodynamic integration and metadynamics techniques, these simulations can yield stability constants for metal complex formation at conditions that are experimentally inaccessible.

In this study, we investigated the species of zinc chloride complexes via *ab initio* Car-Parrinello Molecular Dynamics (CPMD) simulations for ZnCl₂-NaCl-H₂O system with Cl⁻ concentration of 4 m from ambient to hydrothermal-magmatic conditions. At both 25°C and 350°C, the MD simulations indicate that Zn-Cl complex changed from initial structure octahedral ZnCl(H₂O)₅⁺ to tetrahedral ZnCl(H₂O)₃⁺ after 4 picosecond (ps). However, the ligand change of chloride cannot be observed. Since Zn²⁺ has higher charge, the binding between Zn²⁺ and Cl⁻ is stronger, the ions exchange can be hardly observed via short MD simulation (< 10 ps). Thermodynamic integration is a realistic approach to evaluate entropic properties. To calculate the binding free energy between Zn²⁺ and Cl⁻, thermodynamic integration based on constraint CPMD simulations were conducted by constraining the Zn-Cl bond distances. The constraint systems reached the state of equilibrium within 1 ps. The mean forces of forming Zn-Cl bond at the different distances from 2 Å to 5 Å were calculated over 5 ps, and the change in free energy was derived by integrating the mean force vs distance. The integral gave binding free energies of -6.75 kJ/mol at 25°C, 1 bar and -75.52 kJ/mol at 350°C, 500 bar for reaction Zn²⁺ + Cl⁻ = ZnCl⁺. The predicted logKs of that reaction are 1.18 at 25°C and 6.08 at 350°C, in good agreement with the experimental values (0.20 and 6.87, respectively, from revised HKF model^[1]). Having established our methodology, we will now investigate ZnCl complexation at the extreme temperatures of magmatic-hydrothermal fluids.

[1] Sverjensky et al., (1997) *Geochim. Cosmochim. Acta*, **61**, 1359–1421

Re-Os age of late bornite-chalcopyrite vein ores, Kupferschiefer, SW Poland

S.Z. MIKULSKI¹ AND H.J. STEIN^{2,3}

¹ Mineral Resources Program, Polish Geological Institute - National Research Institute, Poland (stanislaw.mikulski @pgi.gov.pl)

² AIRIE Program, Colorado State University, USA (holly.stein@colostate.edu)

³ PGP, University of Oslo, 0316 Oslo, Norway

The age of the world-class Cu-Ag stratabound mineralization from the southern margin of the Upper Zechstein basin in Poland has been addressed using different geochronological methods. In general the ages of the Kupferschiefer's mineralized samples span from Lower Triassic to Upper Jurassic [1, 3-5, 7-8]. Economic Cu mineralization transgresses sedimentary sequences and is hosted by Kupferschiefer black shale, underlying sandstone (*Rotliegendes*) and overlapping limestone of the Upper Permian marine sequence (*lower Zechstein*). Cu-Ag ores are represented mainly by Cu sulphides such as chalcocite, bornite, chalcopyrite and covellite which are commonly associated with silver admixtures and/or minerals.

Four samples from the Lubin (-610 m b.s.l.) and Polkowice (-740 m b.s.l.) operating mines were acquired for Re-Os analyses. Analyzed samples consist of economic Cu ores characterized by 1-10 mm bornite ± chalcopyrite veinlets in calcareous shale (5-10 cm thick) rich in organic matter. In any single veinlet, bornite and chalcopyrite may occur in variable proportion, and penetrate along shale laminations as fine-grained (1-30 µm in diameter) disseminations and small aggregates (<50 µm). Within macroscopic veinlets where chalcopyrite is present, it forms symmetrical margins to a bornite interior. Bornite, bornite-chalcopyrite and/or chalcopyrite veinlets may cross-cut bedding or be nearly parallel to lamination in black shales. We report a Re-Os isochron age for bornite ± chalcopyrite veinlets that exhibit shallow cross-cutting features to bedding in black shale. A Model 1 regression yields 212 ± 7 Ma, with an initial ¹⁸⁷Os/¹⁸⁸Os ratio of 2.13 ± 0.31 (MSWD = 1.3). The analyzed bornite ± chalcopyrite veinlets have a Re concentration ranging from 5.7 to 12.1 ppb, and a total Os concentration ranging from 27-52 ppt. Significant common Os is present in all of the analyzed samples. The current Model 1 age suggests a higher initial ¹⁸⁷Os/¹⁸⁸Os than our previous result [4]. The origin of the Kupferschiefer mineralization is commonly attributed to multiple flow events of low-temperature oxidizing metalliferous fluids triggered by tectonic activation of basinal sediments [e.g. 2, 6]. Our results strongly suggest that the main Cu-mineralization event took place in the Late Triassic (Norian), ca. 212 ± 7 Ma.

[1] Bechtel *et al.* (1999) *Econ. Geol.* **94**, 261-272. [2] Blundell *et al.* (2003) *Econ. Geol.* **98**, 1487-1495. [3] Jowett *et al.* (1987) *J. Geophys. Res.* **92**, 581-598. [4] Mikulski and Stein (2010) *GCA*, **A708**. [5] Nawrocki (2000) *Econ. Geol.* **95**, 241. [6] Oszczipalski (1999) *Min. Deposita* **34**, 599-613. [7] Pasava *et al.* (2007a) *GCA*, **A763**. [8] Pasava *et al.* (2010) *Min. Deposita* **45**, 189-199.

The work was supported by grant No. N525 393739 from the Ministry of Science and Higher Education to SM.

Mg and Cr isotope compositions of chondrules from primitive chondrites

CHRISTIAN A. MILLER^{1*}, RICHARD W. CARLSON¹, CONEL M. O'D. ALEXANDER¹

¹Carnegie Institution of Washington, Terrestrial Magnetism, Washington, U.S.A., cmiller@dtm.ciw.edu, rcarlson@ciw.edu, alexander@dtm.ciw.edu (* presenting author)

A series of high-precision Pb-Pb and Al-Mg ages indicate an interval of chondrule formation extending about 2 Myr [1,2,3]. Such a lengthy period is difficult to reconcile with models for a turbulent protoplanetary disk that is thoroughly mixed on 10⁴–10⁶ year timescales [4]. Should the spread in Al-Mg ages accurately depict the interval of chondrule formation, then the conditions under which chondrules formed must be revisited; if not, then the observed variability may be due to mixing of older-refractory and younger-volatile reservoirs within chondrules, or by initial ²⁶Al heterogeneity within the protoplanetary disc [5].

Evaluating individual chondrules for both Mg and Cr isotope composition can test these hypotheses. Like Al-Mg, the Mn-Cr chronometer is active during the interval of chondrule formation. Relative age differences between chondrules that are consistent across both chronometers would support a lengthy interval of chondrule formation and initial ²⁶Al and ⁵³Mn heterogeneity. In addition, relative parent-daughter volatilities are reversed in the Al-Mg and Mn-Cr systems [6]. If the Al-Mg chondrule age variability is the result of mixing between refractory and volatile reservoirs, individual chondrules with relatively old Al-Mg ages should have relatively younger Mn-Cr ages.

We present Mg and Cr isotope data from EET 92042 (CR2), ALH 77307 (CO3), Murchison (CM2), and Tieschitz (H3.4).

[1] Amelin *et al.* (2002) *Science* **297**, 1678-1683. [2] Mostefaoui *et al.* (2002) *Meteorit. Planet. Sci.* **37**, 421-438. [3] Kurahashi *et al.* (2008) *Geochim. Cosmochim. Ac.* **72**, 3865-3882. [4] Alexander (2005) *Chondrites and the Protoplanetary Disk*, 972-1002. [5] Larsen *et al.* (2011) *Astrophys. J. Lett.* **735**, L37. [6] Lodders (2003) *Astrophys. J.* **591**, 1220-1247.

Magnetic Properties of Source Clays: Rock Magnetic Implications

MATTHEW A. MILLER^{1*}, SHANNON A. DULIN¹, ANDREW S. MADDEN¹ AND R. DOUGLAS ELMORE¹

¹University of Oklahoma, ConocoPhillips School of Geology and Geophysics, matthew.a.miller-1@ou.edu (*presenting author), shannon.a.dulin-1@ou.edu, amadden1@ou.edu, delmore@ou.edu

Abstract

Paleomagnetic studies have helped derive chronostatic continental positions and determine timing of geochemical events throughout the geologic record. A wide range of rock magnetic studies have identified the magnetic character of rock forming and accessory minerals. Magnetic remanence or the retention of a relict magnetic field by magnetic minerals is the fundamental rock magnetic property used to investigate paleomagnetism. Specifically, the acquisition and decay of an isothermal remanent magnetization (IRM) is often used to make mineralogic assignments in rock samples. Magnetite is often cited as the magnetic phase in sedimentary rocks of varied genetic and diagenetic histories.

This study builds on the work of others indicating the tendency of iron-rich clays to exhibit ferromagnetic behaviour due to antiparallel magnetic spins in unpaired electron shells across Fe²⁺-O-Fe³⁺ bonds [1,2]. IRM saturation and stepwise alternating field (AF) decay experiments have been conducted on four source clays: nontronites NAu-1 and NAu-2, and Montmorillonite STx-1, and Kaolinite KGa-1 in field strengths of 20-2675 mT using an impulse magnetometer for saturation and a 2G Enterprises alternating field demagnetizer in field strengths from 0 to 120 mT for decay. Results of such experiments on clay treated to remove iron oxide contamination indicate a low coercivity, high saturation phase, appropriate for both magnetite and clays with mixed valence structural iron in the dioctahedral layers. Contemporaneous powder x-ray diffraction (XRD) and transmission electron microscopy (TEM) examination of the source clays reveal no Fe₃O₄ component. Therefore, saturation magnetizations obtained in this study vary as a function of variable iron concentration and valence states within the clay, and indicate the uncertainty associated with mineralogic assignment based on magnetic character without traditional petrographic analysis.

[1] Lear and Stucki (1987) *Clays and Clay Minerals*, **35**, 375-378.

[2] Schuette, Goodman and Stucki (2007) *Phys Chem Minerals*, **27**, 251-257.

Ligand effects on Hg^{II} reduction by magnetite

BHOOPESH MISHRA^{1,2*}, TIMOTHY PASAKARNIS³, MAXIM I. BOYANOV², EDWARD J. O'LOUGHLIN², MICHELLE M. SCHERER³, KENNETH M. KEMNER²

¹Illinois Institute of Technology, Chicago, IL, USA

²Argonne National Laboratory, Argonne, IL, USA,

bmishra3@iit.edu (presenting author)

³University of Iowa, Iowa City, IA, USA

Abiotic redox transformations of Hg are important in understanding the fate and mobility of Hg in reducing environments. The presence of complexing ligands significantly modifies the reduction potential of Hg^{II}, influencing its abiotic reduction. We tested the ability of magnetite, a biogenic mineral commonly found in subsurface environments, to reduce Hg^{II} complexed with carboxyl, chloride, and sulfhydryl ligands. These ligands are important constituents of subsurface geomedea. Since the binding constants of Hg-chloro complexes fall between -carboxyl and -sulfhydryl complexes, we further investigated the reduction of the Hg-chloride complex by magnetite containing varying Fe²⁺ stoichiometry (the bulk Fe²⁺/Fe³⁺ ratio, x).

Hg^{II} adsorbed to *Bacillus subtilis* at high and low Hg:biomass ratios (corresponding to Hg complexation predominantly with carboxyl and sulfhydryl groups, respectively) was reacted with magnetite under anoxic conditions, and the solid phase was examined by Hg L_{III} edge XAS. When Hg^{II} was bound predominantly to carboxyl groups, reduction of Hg^{II} to Hg⁰ occurred within 2 h and 2 d at pH 6.5 and 5.0, respectively. When Hg^{II} was bound to sulfhydryl groups, it was not reduced by magnetite after 2 months of reaction at pH 6.5 or 5.0. In the presence of chloride, Hg^{II} was rapidly reduced to Hg⁰ by stoichiometric (x=0.48) magnetite. The reduction of the Hg^{II}-chloride complex by more oxidized forms of magnetite (x=0.38 and 0.28) was kinetically hindered due to the formation of calomel (Hg₂Cl₂) as a stable intermediate reaction product. However, reaction kinetics slowly progressed towards reduced Hg⁰ after 4 months of reaction.

These results suggest that the complexation of Hg^{II} with carboxyl, chloride, and sulfhydryl exhibits a progressively increased inhibition of the reduction of Hg^{II} to Hg⁰ by magnetite. Since Hg is typically present in aquatic and terrestrial systems at low concentrations, binding of Hg^{II} to high affinity sulfhydryl sites on bacteria could have important implications for the potential reduction of Hg^{II} to Hg⁰ and the overall mobility of Hg under Fe-reducing conditions.

[1] Mishra (2011) *ES&T* **45**, 9597-9603.

Multidisciplinary study of an enclave swarm in the Évora granitoid

PATRÍCIA MOITA^{1*}, PEDRO SILVA², JORGE PEDRO³, JOSÉ F. SANTOS⁴

^{1*}HERCULES/ CGE / Dep. Geociências, Univ. Évora, Portugal, pmoita@uevora.pt

²IDL/ ISEL, Lisboa, Portugal

³CeGUL/ Dep. Geociências, Univ. Évora, Portugal

⁴Geobiotec / Dep. Geociências, Univ. Aveiro, Portugal

The enclave swarm of Pomarinho is located in the SW edge of Évora granitoid [1], in the SW sector of the Ossa-Morena Zone (Iberian Variscides). The swarm, with a privileged 3D exposure, was sampled for geophysical, petrographic and geochemical studies in order to better understand the chemical and mechanical processes involved in the genesis of that structure.

The enclaves have tonalitic and granodioritic compositions, whereas the host correspond to a very homogeneous light-coloured granodiorite. Major and trace elements as well Sr and Nd isotopic data suggest a derivation of the enclaves and the host granodiorite from a common primitive melt through magmatic differentiation. The parental melt is related to a mantle source, with no or only small contribution of metasedimentary crustal materials [2].

The tonalitic enclaves have Mg-hornblende [Mg/(Mg+Fe²⁺)=0.56-0.68] and biotite [Mg/(Mg+Fe²⁺)=0.50-0.53], whereas in granodioritic enclaves the biotite [Mg/(Mg+Fe²⁺)=0.47-0.50] is the main mafic phase. Plagioclase of tonalitic enclaves have compositions of An₂₃₋₄₂ with normal zoning whereas plagioclase of granodiorite is more evolved with An₁₃₋₄₄. One granodioritic enclave testifies for a more complex mechanisms once it preserves plagioclases with a widest compositional range (from An₁₈ to An₆₉) in agreement with the role of a more primitive parental melt.

In order to infer the petrofabric, two types of magnetic fabrics were evaluated: anisotropy of magnetic susceptibility (AMS) and anisotropy of anhysteretic remanent magnetization (AARM). AMS results from granite and swarm enclave samples collected along two profiles show very similar results, defining an overall mean tensor with K1 = 179.1°/33.4°, K2 = 315.4°/47.6° and K3 = 73.0°/22.9° for 71 samples from granite and 25 of the enclave. AARM measurements from granite define an ellipsoid with principal axes that share the same orientation of the AMS ellipsoid. In what concerns the enclaves, AARM ellipsoid shows a distinct orientation, with principal axes defined by R1 = 248.7°/31.0°, R2 = 89.0°/57.3° and R3 = 344.4°/9.2°.

The absence of agreement between the orientations of AMS and AARM ellipsoids for samples of the enclave could be related with the presence of single domain magnetite (giving rise to an inverse magnetic fabric) or with the existence of distinct alignments of the paramagnetic and ferromagnetic fractions due to changes of the stress field during their recrystallization.

Funding: Petrochron project (PTDC/CTE-GIX/112561/2009)

[1] Carvalhosa (1983) *Comun. Serv. Geol. Portugal*, **69** (2), 201-208.

[2] Moita, et al., (2011) *Abstract, Hutton Symposium.*, pp: 99-100.

Effects of osteopontin, peptides and amino acids on calcite dissolution

VALENTIN NELEA^{1*}, YUNG-CHING CHIEN¹, JEANNE PAQUETTE², AND MARC D. MCKEE¹

¹Faculty of Dentistry, McGill University, Montreal, Canada, valentin.nelea@mcgill.ca (* presenting author), yung-ching.chien@mail.mcgill.ca, marc.mckee@mcgill.ca

²Department of Earth and Planetary Sciences, McGill University, Montreal, Canada, jeanne.paquette@mcgill.ca

The mineral-binding protein osteopontin (OPN), a prominent component of calcitic eggshell matrix, inhibits calcite crystal growth and modifies its dissolution, but the role of its functional groups in this remains unclear. To study this, the (104) cleaved surfaces of calcite (Iceland spar) were exposed to aqueous solutions containing full-length phosphorylated OPN (P-OPN), mineral-binding peptide fragments of OPN (phosphorylated acidic serine- and aspartate-rich motif [P-ASARM, 18 amino acids], poly-aspartic acid [poly-Asp]), a neutrally charged and nonphosphorylated peptide fragment of OPN, and the amino acids serine (Ser), phosphoserine (P-Ser) and Asp. Atomic force microscopy was used to characterize dissolution and etch pit shapes.

Acidic amino acids (Asp, P-Ser) substantially altered etch pit shape and induced straight steps parallel to [010], which we attribute to the combined influence of two carboxyl groups (Asp) or a carboxyl and a phosphate group (P-Ser). This suggests that closely spaced carboxyl and/or phosphate groups of small biomolecules may match Ca atoms at the step edges along [010]; this matching does not occur, and no [010] steps were formed, for larger peptide fragments (poly-Asp, P-ASARM), or for P-OPN. Steps parallel to [4 2 -1] tend to be induced by amino acids as well as larger peptide fragments. These [4 2 -1] steps form in the presence of both Ser and P-Ser, where amine and carboxyl groups in close proximity cooperate to produce chiral pits. In the case of P-Ser, curved edge steps nearly parallel to [4 2 -1] are additionally induced, an effect that may derive from cooperation among phosphate, carboxyl and amine groups. In the presence of acidic peptides, etch pits lose their straight edges and become rounded, nearly achiral; etch pits show pronounced elongation along the [4 2 -1] direction, suggesting that the acidic functional groups match best with the Ca atomic spacing in that direction. The rounding effects appear to be regulated by phosphate, being more pronounced with an increasing number of phosphate groups on the peptide, and with peptide concentration in solution. Therefore, phosphate groups must bind more strongly to kink sites at step edges than either carboxyl or amine groups. Finally, at increasing concentrations of P-OPN, the pits become nearly circular, suggesting that this larger, highly phosphorylated protein binds to multiple kink sites and becomes less direction-dependent than its constituent smaller peptides; this results in uniform dissolution rates in all directions. *Supported by CIHR and NSERC.*

Vivianite in lake sediment: reactivity, morphological and compositional change

D.W. O'CONNELL^{*1,2}, M. MARK JENSEN^{3,4}, B. THAMDRUP³, R. JAKOBSEN⁴, C. BENDER KOCH², D. POSTMA⁵, H.C. BRUUN HANSEN².

¹CERC Ecohydrology Research Group, University of Waterloo, 2NL 3G1, Waterloo, Ontario, Canada.

(*correspondance: david.w.oconnell@uwaterloo.ca)

²Dept. of Natural Sciences, University of Copenhagen, DK-1871, Copenhagen, Denmark

³Institute of Biology, University of Southern Denmark, DK-5230, Odense M, Denmark.

⁴Inst. of Environment & Resources, Technical university of Denmark, DK-2800, Lyngby, Denmark.

⁵GEUS, DK-1350, Copenhagen, Denmark.

Vivianite [(Fe₃(PO₄)₂.8H₂O)] may precipitate in anoxic lake sediment and potentially play a key role in the control of orthophosphate (PO₄³⁻) equilibrium solution concentrations, thereby reducing P runoff, eutrophication and ultimately the trophic status of lakes. Surprisingly, vivianite's presence and role in the P (and Fe) cycle of predominantly anoxic lake sediments is rarely investigated. Currently large knowledge gaps still remain in relation to our understanding of seasonal redox dynamics on the equilibrium of vivianite with lake porewater. In addition, the effect of sediment depth and seasonally changing redox gradients on vivianite reactivity, structure and morphology are not well understood. In this study, we investigated changes in vivianite equilibria, morphology and composition with sediment depth in a Fe-Si-C rich lake (Ørnsø, Denmark). Speciation calculations on porewater results indicated vivianite to be the limiting phase for PO₄³⁻ solubility in the upper 10cm of winter sediment profiles. In contrast, there was no such correlation between vivianite and PO₄³⁻ solubility in the summer sediment profile, suggesting vivianite formation in this upper sediment section profile to be seasonal. The presence of vivianite and its change in crystallinity with depth were confirmed by X-ray diffraction (XRD). Leaching experiments with HCl and Ascorbic acid (pH 3) were used to investigate the dissolution kinetics of Fe²⁺ and PO₄³⁻ from the various mineral phases within the sediment [1]. The leaching experiments allowed the fractionation of PO₄³⁻ within the sediment profile and suggested the majority of the PO₄³⁻ extracted by HCl (pH 3) was predominantly from vivianite. Although this HCl fraction of PO₄³⁻ is small in relation to the overall PO₄³⁻ sediment pool, its association with vivianite and subsequent PO₄³⁻ mobility is important in terms of lake water quality. Scanning electron microscopy revealed surface pitting of vivianite crystals and Electron dispersive x-ray spectroscopy (EDX) confirmed changes in vivianite elemental composition and suggested along with Fe-oxide reduction, the possible link between Fe-silicate reduction, PO₄³⁻ desorption and subsequent vivianite crystal growth in lower sediment sections.

In conclusion, the data indicates that vivianite equilibrates seasonally with sediment depth and makes an important contribution to PO₄³⁻ mobility in the lake sediment. Vivianite crystals have been shown to undergo pitting due to surface degradation and there are indications from EDX and XRD analysis of composition and structural changes.

[1] Postma, D (2010) *Mobilization of arsenic and iron from red river floodplain sediments, Vietnam*. **74**, 3367-3381.

ORIGIN OF THE CHEMICAL AND U-SR ISOTOPIC VARIATIONS OF STREAM AND SOURCE WATERS IN THE STRENGBACH CATCHMENT (VOSGES MOUNTAINS; FRANCE)

MARIE-CLAIRE PIERRET¹, PETER STILLE¹, JONATHAN PRUNIER², FRANÇOIS CHABAUX¹ (*)

^v Laboratoire d'Hydrologie et de Géochimie de Strasbourg, EOST, Université de Strasbourg et CNRS, 1 rue Blessig 67084 Strasbourg, France [8pt font size]

²GET, Université Paul Sabatier, CNRS et IRD, Observatoire Midi-Pyrénées, 14, avenue Edouard Belin, 31400 Toulouse, France

Major and trace element concentrations as well as ⁸⁷Sr/⁸⁶Sr isotope ratios and (²³⁴U/²³⁸U) activity ratios have been analyzed in water samples from the different springs and brooks of the Strengbach catchment. The obtained data show that, at the scale of such a small and more or less monolithic catchment, the different sources and streamlets can have very different Sr and U isotopic ratios and geochemical signatures (Ca/Na, Mg/Na, Sr/Na ratios). Some of these variations can be related to the existence of small and local lithological variations, and to the hydrothermal overprint of the granitic bedrock, which was stronger on the northern than on the southern slope of the granite. Nevertheless, the data indicate that the chemical compositions of the source waters in the Strengbach catchment are only to a small extent the result of alteration of primary bedrock minerals and rather reflect dissolution/precipitation processes of secondary mineral phases like clay minerals.

The data furthermore show a relatively good relationship between the emerging altitude of sources/springs in each slope of the watersheds, and the intensity of ²³⁴U-²³⁸U activity ratios in the waters. Such a relationship might indicate that U mobilization and ²³⁴U enrichment (consequence of the alpha recoil process) in these waters are controlled by the duration of the water migration along a pathway within the granitic substratum of the watershed: as longer the water pathway within the watershed, as longer the duration of water-rock interaction and hence as stronger ²³⁴U enrichments in the source and spring waters.

Perchlorate in the Great Lakes: isotopic composition and origin

A. POGHOSYAN^{1*}, N. C. STURCHIO¹, Y. GUAN², J. M. EILER², AND W.A. JACKSON³

¹ University of Illinois at Chicago, Chicago, IL, USA; apogho2@uic.edu (*presenting author); sturchio@uic.edu

² California Institute of Technology, Pasadena, CA, USA; yunbin@gps.caltech.edu; eiler@gps.caltech.edu

³ Texas Tech University, Lubbock, TX, USA; andrew.jackson@ttu.edu

Concentrations and stable isotopic compositions of perchlorate were investigated in the five Laurentian Great Lakes. Samples were collected during monitoring cruises in 2007-2009 of the U.S. EPA's *RV Lake Guardian* as well as at the water supply intake of Marquette, MI on the southern shore of Lake Superior. Concentrations of perchlorate were measured by IC/MS/MS at 24 locations, including one or two depth profiles in each lake. Concentrations (µg/L) are: Superior, 0.06 ± 0.01; Michigan, 0.10 ± 0.01; Huron, 0.11 ± 0.01; Erie, 0.08 ± 0.01, and Ontario, 0.09 ± 0.01. Concentration with depth is nearly constant in all lakes, indicating well-mixed conditions.

Perchlorate was concentrated aboard ship by passing 15,000 to 80,000 L of lake water through 1-L cartridges containing bifunctional anion-exchange resin. In the laboratory, perchlorate was eluted from the resin, purified, and precipitated as a >99% pure crystalline phase. Milligram amounts were recovered from each lake for stable isotope ratio analysis. Chlorine and oxygen isotopic analyses were performed at Caltech using the Cameca 7f-GEO SIMS instrument, following validation of the SIMS method with analyses of USGS-37 and -38 KClO₄ isotopic reference materials. Preliminary results for Great Lakes perchlorate indicate a relatively narrow range in δ³⁷Cl values (+3.3 to +4.6 ‰) and a wider range in δ¹⁸O values (-4.6 to +4.2 ‰), with a geographic trend of increasing δ¹⁸O from west to east.

The preliminary isotopic data indicate that the perchlorate is dominantly of natural origin, having isotopic composition resembling that of perchlorate from pre-industrial groundwaters in the western USA [1]. Mass balance indicates that substantial perchlorate biodegradation or uptake may occur in Lake Erie. Additional SIMS measurements are in progress to refine Δ¹⁷O values and AMS measurements to determine ³⁶Cl/Cl ratios. These additional data will enable us to better constrain possible source(s), mixing proportions, and possible isotopic exchange or fractionation processes within the lakes, as well as to obtain better estimates of the regional atmospheric deposition flux of perchlorate.

[1] Jackson, W.A., J.K. Böhlke, B. Gu, P.B. Hatzinger, and N.C. Sturchio (2010) *Environ. Sci. Technol.* **44**, 4869-4876.

Metallogenic age and tectonic settings of Hongtoushan Cu-Zn deposit in Liaoning province, China: Evidences from zircon

Y. QIAN^{1,2*}, F.Y. SUN¹, AND B.L. LI¹

¹College of Earth Sciences, Jilin University, Changchun, China, qianye@jlu.edu.cn (* presenting author)

²State Key Laboratory of Continental Dynamics, Northwest University, Xi'an, China

Hongtoushan Cu-Zn deposit is located in northern Liaoning province in North China Craton, which is the only one Archean VMS deposit in China. The immediate ore-hosting rocks in the deposit are biotite plagioclase gneiss and amphibolite which were subjected to amphibolite facies metamorphism. The geological and geochemical data [1] reveal that original rocks of the ore-hosting rocks are calc-alkaline tholeiite-andesite-dacite series and formed in island-arc tectonic settings.

In order to determine the metallogenic age and tectonic background of the deposit, we have made the cathodoluminescence (CL) images and LA-ICP-MS U-Pb dating of the zircons from the ore-hosting rocks. In CL images, there occur relatively fine oscillatory zoning within the zircon center, while it gradually vanishes toward its edge. It is suggested that the zircons are of magmatic origin and suffered metamorphic superimposition [2]. Zircons from the biotite plagioclase gneiss have U-Pb ages of 2521-2580Ma, with the upper intercept age of 2552Ma (MSWD=0.84, n=24). Correspondingly, zircons from the amphibolite have the upper intercept age of 2550Ma (MSWD=0.78, n=16).

Based on geological data and zircon U-Pb dating, it has been concluded that the forming age of Hongtoushan Cu-Zn deposit is 2550Ma. During that time, drifting of ancient continents caused the subduction of the oceanic crust, which resulted in the submarine volcanism. In the intermittent period of volcanism, the hot ore-bearing fluids as black smoker were mixed with cold seawater and formed the Hongtoushan VMS deposit. During the subsequent arc-continent collision, the deposit was subjected to the metamorphism and deformation.

[1] Zai, Yang (1984) *Geological Rev.* **30**, 523-525. [2] Hoskin, Black (2000) *J. metamorphic Geol.* **18**, 423-439.

Effect of ionising radiation on *Serratia* phosphatase activity and radionuclide phosphate biomineralization

J. C. RENSHAW^{1*}, M. PATERSON-BEEDLE¹, B. C. JEONG², C. H. LEE³, W. H. KIM³, S. HANDLEY-SIDHU¹ AND L.E. MACASKIE¹

¹ The University of Birmingham, Edgbaston, B15 2TT, UK, j.c.renshaw@bham.ac.uk*

² Myong-ji University, San 38-2, Na Dong, Yongin-Si, 3005-600, South Korea

³ Korea Atomic Energy Research Institute, P.O. Box 105, Yusong, Daejeon 3005-600, South Korea

Introduction

Serratia sp. shows promise for the biomineralization and co-removal of radionuclides [1]. *Serratia* sp. can form metal phosphates using glycerol 2-phosphate (G2P); this bioprocess removes key radionuclides, such as U, Pu, Co, Sr, and Cs from aqueous wastes [2-5]. The G2P is cleaved via an atypical phosphatase enzyme, and liberated phosphate precipitates with metal on the bacterial cell surface [6]. The efficacy of this process for radionuclide removal will depend on the radiotolerance of the phosphatase enzyme.

Experimental

To test the radiotolerance of *Serratia* sp. and of the purified phosphatase enzyme, individual suspensions were irradiated using a ⁶⁰Co gamma source [7]. The phosphatase activity of both the cells and the enzyme were compared against activity in non-irradiated controls. Using a simulated radioactive waste *Serratia* sp. was allowed to biomineralize and remove U, Cs, Sr and Co from solution.

Results and Conclusions

Radiostability testing using ⁶⁰Co gamma source showed high cell lethality and that the purified enzyme lost its activity within a few hours. In contrast whole-cell phosphatase retained 80% of its activity, and in the presence of a radioprotectant (mercaptoethanol) full activity was retained beyond an accumulated dose of >1.3 MGy. By a process of co-crystallization ¹³⁷Cs⁺ and ⁸⁵Sr²⁺ were effectively removed from a simulated waste with high background Na⁺ concentration. In terms of radiotolerance it would be feasible to use whole cells of *Serratia* sp. for the remediation of nuclear waste since blockage of column filters by accumulated metals (several fold to excess over the bacterial dry weight) would occur before the onset of radio-inhibition.

[1] Macaskie L.E. et al. (1994) *FEM Microbiol. Rev.* **14**, 351-367.

[2] Paterson-Beedle M. et al (2010) *Hydrometallurgy* **104**, 524-528. [3] Lloyd J.R. et al (2000) *Environ. Sci. Technol.* **34**, 1297-1301.

[4] Macaskie L.E. et al (1996) *Nuclear Energy*, **35**, 257-271.

[5] Paterson-Beedle M. et al (2006) *Hydrometallurgy*, **83**, 141-145.

[6] Thackray A. et al (2004) *J. Mater. Sci. Mater. Med.* **15**, 403-406.

[7] Paterson-Beedle M. et al *Biotech. Bioeng.* In press

The relevance of SGD as a source of chemical compounds to a Mediterranean bay

VALENTÍ RODELLAS^{1*}, JORDI GARCIA-ORELLANA¹, ANTONIO TOVAR-SANCHEZ², GOTZON BASTERRETXEA³, PERE MASQUÉ¹, ESTER GARCIA-SOLSONA⁴, ANTONI JORDI³, DAVID SÁNCHEZ-QUILES², JOSÉ M. LÓPEZ⁵

¹Institut de Ciència i Tecnologia Ambientals & Dep. Física. Univ. Autònoma de Barcelona, Spain, Valenti.Rodellas@uab.cat

²Department of Ecology and Marine Resources. IMEDEA (CSIC-UIB), Balearic Islands, Spain

³Department of Global Change Research. IMEDEA (CSIC-UIB), Balearic Islands, Spain

⁴Laboratoire d'Etudes en Géophysique et Océanographie Spatiales (LESBOS/OMP), Toulouse, France

⁵Instituto Geológico y Minero de España (IGME), Oficina de proyectos de Palma de Mallorca, Balearic Islands, Spain

Background

Submarine groundwater discharge (SGD) plays an important role as a source of terrestrial pollutants, trace metals, nutrients and other compounds to the coastal environment. Palma Bay (Balearic Islands, Spain) is an important Mediterranean touristic destination, and the demographic concentration in the coastline together with the intensive agricultural practices have resulted in enhanced loads of nutrients and other compounds in groundwaters. As no permanent surface flows are present in Palma Bay and diffusive SGD occurs over most of the year, SGD becomes the most relevant pathway to deliver terrestrial compounds to its coastal waters.

In this work, Ra isotopes and ²²²Rn have been used to evaluate the significance of SGD in Palma Bay and its associated input of dissolved nutrients and trace metals to the coastal sea. Measurements of Chl_a were also conducted in bay waters with the purpose of establishing potential linkages between SGD and primary production.

Results and discussion

Eddy diffusion coefficients were calculated using short-lived Ra isotopes. In conjunction with ²²⁶Ra activities, SGD fluxes to the Palma Bay were estimated to be on the order of 30000 m³·d⁻¹, comparable to a figure of 21000 m³·d⁻¹ based on continuous ²²²Rn measurements. The agreement between both estimates and the local hydrological water budgets, together with the low salinities measured in nearshore porewaters, indicates that freshwater discharge is the main component of SGD fluxes. Our findings show that diffusive discharge of nutrient-rich (e.g. NO₃ up to 300 μM) and mostly fresh groundwater is the main source of nutrients to Palma Bay. Conversely, the correlation between salinity and trace metal concentrations measured in shoreline porewaters suggests that inputs of trace metals via fresh SGD are minimal, and that the microtide and wave-driven seawater that re-circulates through the beach aquifer represents the main mechanism to supply these compounds to the bay. Nutrient fluxes derived from SGD likely sustain the high coastal productivity of Palma Bay observed in summer, as derived from the relationships between the distributions of Ra isotopes and Chl_a-based biomass.

Automated sample purification: Radiogenic and non-traditional metal isotopes in the 21st century

STEPHEN ROMANIELLO¹, GWYNETH W. GORDON^{1*}, DAN WIEDERIN², M. PAUL FIELD² AND ARIEL D. ANBAR^{1,3}

¹School of Earth & Space Exploration, Arizona State University, Tempe, AZ, USA, gwyneth.gordon@asu.edu*

²Elemental Scientific, Inc., Omaha, NE, field@icpms.com

³Department of Chemistry, Arizona State University, Tempe, AZ, USA, anbar@asu.edu

Isotope Analysis in a New Age

In 1931, Harold Urey predicted different vapor pressures for hydrogen isotopes would lead to fractionation. By 1940, Nier developed a mass spectrometer to accurately and precisely determine the relative abundance of different isotopes. Beginning in the 1960's, gas-source MS led to the emergence of light stable isotopes as a powerful tool in hydrology, paleothermometry and climate science. The use of gas-source GC-IRMS proliferated in the 1980's and 1990's with the development of automated sample preparation and introduction systems (EA, TC-EA, TOC, etc.).

In parallel with these developments, radiogenic isotope systems reached high levels of measurement precision using TIMS. However, TIMS analyses are not amenable to automated sample introduction. Automated sample preparation has seen limited use because the rate of TIMS measurement, rather than rate of sample preparation, is usually the bottleneck in routine applications.

In recent years, many TIMS applications have migrated to MC-ICP-MS. This technology also opened the way to new types of isotope analysis, particularly "non-traditional" stable isotopes which have found use in (paleo)environmental, archeological, and biomedical research. As with TIMS, high precision isotope MC-ICP-MS analyses still require extensive purification to isolate elements from natural matrices, eliminating interferences (polyatomic and isobaric) and minimizing matrix suppression effects. In contrast to TIMS, however, automated sample introduction is possible with MC-ICP-MS because the ion source is at atmospheric pressure. Additionally, the utility of an automated preparation system would be high because of the enhanced rate of sample throughput in MC-ICP-MS vs. TIMS. In addition to increasing sample throughput and reducing personnel costs, an automated sample preparation and introduction system for MC-ICP-MS analyses could reduce the need for expensive laminar-flow hood space and cleanlabs, as well as expand the use of high-precision isotope analyses in fields such as anthropology, forensics and food authentication where such facilities may be unavailable.

Working toward the vision of automated sample preparation and introduction, we are developing protocols for automated ion exchange purification for isotopic analysis using the new prepFast-MCTM offline unit from ESI. This automated low-pressure ion exchange chromatography system can process up to 60 samples unattended. This highly flexible system allows sample loading, multiple acid washes, conditioning and elution cycles necessary to isolate elements of interest. The final eluent is automatically collected, dried and reconstituted for isotopic analysis. Initial methods and results will be presented.

Heavy Isotopes and Archeology

JOAQUIN RUIZ*¹, DAVID KILICK², ALYSON THIBODEAU^{1,2}
AND TOM FENN².

¹University of Arizona, Department of Geosciences, Tucson, Arizona
jruiz@email.arizona.edu (*presenting author)

²University of Arizona, School of Archeology, Tucson Arizona
85718,

Heavy isotopes were first applied to the provenance of archaeological materials (lead metal, lead glasses) in the 1960's. Experiments in the early 1970's showed that smelting and other metallurgical processes did not produce measurable fractionation of lead isotopes, and thus established lead isotope analysis as a technique for tracing the provenance of non-ferrous metals like silver and copper through the traces of lead that they contain. From the perspective of the present, many of the studies conducted from the 1970's through the mid-1990's were flawed because they did not attempt to make use of geological knowledge about the evolution of lead isotopic ratios. The precision of measurement by TIMS was also insufficient to distinguish between potential sources of metals in some of the regions (e.g. Britain) where much of the work was done. The development of MC-ICPMS, with its much greater precision, has revived the use of lead isotopes in archaeology.

Strontium isotopes have been used in archaeological since the late 1980's, almost always to study human migration through strontium isotopic ratios in teeth, often paired with oxygen isotopic ratios. This has been one of the most successful applications of isotopes in archaeology and its use has soared since 2000.

In this talk we present applications of high-precision lead and strontium isotopic analysis to provenance analysis of several inorganic materials. These include: the sources of lead for lead-glazed ceramics in Pueblo 4 pottery in the southwestern USA; the sources of archaeological turquoise in the southwestern USA and Mexico; and the regions of manufacture of glass trade beads during the Islamic era.

Geochemical Investigations of Metals Release From Submerged Coal Fly Ash

JENNIFER SEITER^{1*}, ANTHONY BEDNAR¹, BRANDON LAFFERTY¹, RYAN TAPPERO², CYNTHIA PRICE¹, MARK CHAPPELL¹

¹Engineer Research and Development Center, US Army Corps of Engineers, Vicksburg, MS, US,
Jennifer.M.Seiter@usace.army.mil (*presenting author)

Anthony.J.Bednar@usace.army.mil,

Brandon.Lafferty@usace.army.mil,

Cynthia.L.Price@usace.army.mil

Mark.A.Chappell@usace.army.mil

²National Synchrotron Light Source (NSLS), Brookhaven National Laboratory, Upton, NY, US, rtappero@bnl.gov

Introduction:

The Tennessee Valley Authority commissioned the U.S. Army Engineer Research & Development Center to geochemically characterize the fly ash spilled in the Emory River at the Kingston Fossil Plant. The study focused on naturally occurring metals found in the fly ash material. The purpose was to distinguish any transformations that may have occurred during its prolonged submersion in the river that would promote release of metals during cleanup dredging operations.

Methods:

Solid and liquid-state analytical techniques were used to characterize the As and Se in collected ash samples from the spill site. Synchrotron based-techniques μ -X-ray Fluorescence mapping, μ - and bulk-X-ray Absorption Spectroscopy (XAS) and μ -X-ray Diffraction were used to identify elemental associations and As/Se species present both before and after fly ash submersion. Data were collected at beamline X27A and X11A at the NSLS. High Performance Liquid Chromatography interfaced to Inductively Coupled Plasma Mass Spectrometry was used to quantify arsenic and selenium species in the dissolved phase. Preliminary ash selenium and arsenic stabilities were determined using extended elucitrate tests under oxic and anoxic conditions. Potential photooxidation of As and Se in Emory River and dredge cell water were tested using a cell photo reactor.

Results and Conclusions:

Bulk X-ray absorption spectroscopy determined that fly ash manganese species were reduced from Mn(IV) to Mn(II) while Fe species were changed nominally during its residence time in the Emory River. XAS showed that Se transformed from mostly selenite (Se(IV)) in the original ash storage pile to organoselenium (Se(-II)) or thiol-bound species from prolonged submersion. The As in all fly ash samples were determined predominantly as arsenate (As(V)) species with a small component of reduced arsenite (As(III)) species. Ash chemical stability studies showed small (ppb) releases of metals through dissolution, but negligible changes in Se and As speciation. Photooxidation studies demonstrated the potential oxidation of As, and Se along the dredge cell in the presence of dissolved Fe. These results indicate that As and Se species were relatively stable, but undergoing kinetically slow transformations with increased time of submergence in the Emory River.

Thermal Effects of SEM Analysis on (U-Th)/He Ages: Examples from Durango Apatite

JINGNAN SHAN^{1*}, KYOUNGWON MIN², NOURI ABDELKADER³

¹University of Florida, Department of Geological Sciences, Gainesville, USA, jnshan@ufl.edu (* presenting author)

²University of Florida, Department of Geological Sciences, Gainesville, USA, kmin@ufl.edu

³University Oum El-Bouaghi, Material Sciences Department, Algeria, nouiri_kader@yahoo.fr

Scanning electron microscopy (SEM) provides a convenient way to identify appropriate mineral phases and describe their petrographic features for (U-Th)/He dating. However, there has been a concern regarding the electron-beam induced thermal effect on phosphate samples because He diffusion in phosphate is known to be highly sensitive to temperatures. In this contribution, we aim to assess whether the SEM analysis can cause any detectable effects on the apatite (U-Th)/He ages through two independent approaches: (1) determining single-grain (U-Th)/He ages of Durango apatites examined under different SEM analytical conditions, and (2) estimating SEM-induced temperature rise by simulating the random walk behavior of electrons within the apatite samples.

Two batches of Durango apatite fragments were prepared for (U-Th)/He dating. The first batch was composed of four groups, each group containing 3 small (<90 µm), 3 medium (90-150 µm) and 4 large (150-250 µm) fragments. Fragments for the second batch were selected from an identical size range (150-250 µm) and divided into four aliquots. All fragments were examined and chemically mapped under variable analytical conditions, then used for the determination of (U-Th)/He ages. The (U-Th)/He ages of the first batch ranged from 29.97 ± 1.80 Ma (2σ) to 33.44 ± 2.20 Ma. The calculated weighted means of the four groups were 30.90 ± 1.10 Ma, 31.34 ± 0.77 Ma, 30.89 ± 0.80 Ma and 30.72 ± 0.84 Ma. Ages from the second batch were from 28.68 ± 0.99 Ma to 33.10 ± 1.56 Ma, with the weighted means of four aliquots being 31.23 ± 0.88 Ma, 30.20 ± 1.20 Ma, 30.80 ± 1.00 Ma, and 30.50 ± 1.10 Ma. All ages are in good agreement with the reference ages for the Durango apatite: $^{40}\text{Ar}/^{39}\text{Ar}$ age of 31.44 ± 0.18 Ma [1], (U-Th)/He age of 31.02 ± 2.02 Ma [1] and Pb/Pb LA-ICP-MS age of 30.6 ± 2.3 Ma [2]. These results combined with isothermal heating modeling suggest the homogeneous T of the samples during the SEM analysis should be lower than 190 – 285 °C.

To confirm these results, a hybrid method, Monte Carlo and molecular dynamic, has been employed to calculate the temperature rise under similar SEM analytical conditions. For the maximum beam current of 1000 pA, the simulated surface temperature increase is calculated as ~160 °C. Furthermore, the elevated temperatures decreases rapidly with depth, and essentially there is no effective temperature rise at ~1 µm from the apatite surface. These results indicate that the SEM electron beam leads to only a minor T increase near the grain surface, not causing any detectable diffusive He loss.

[1] McDowell et al. (2005) *Chemical Geology* **Volume 214**, 249-263.

[2] Chew et al. (2010) *Chemical Geology* **Volume 280**, 200-216.

Geochemical mapping and statistical analysis of the Bafq region, Iran: Implication for the mineral exploration

M.R. SHAYESTEHFAR^{1*}, F. ZANDIEH²

¹Associate Professor of Mining Engineering Department, Shahid Bahonar University of Kerman, Iran, shyeste@uk.ac.ir (*)

²PhD. Student of Mining Engineering Department, Shahid Bahonar University of Kerman, Iran, zandifar62me@yahoo.com

Introduction

The Bafq region of Saghand-Golpayegan-Bafq is a roughly 2500 km² area in the central part of Iran, and is one of the most important metallogenic provinces. This area is located in the Precambrian region of the Central Iranian Formation, which is known as the Morad Formation in Iranian stratigraphy.

The aim of the work was to detect and map geochemical anomalies by using univariate and multivariate analysis of 400 stream sediment samples from Bafq region.

Methods

Samples were analyzed for 13 elements using Xray Fluorescence, XRF and Inductively Coupled Plasma Mass Spectrometry (ICP-MS and AES) equipment techniques. In univariate analysis for plotting geochemical distribution of variables, two different procedures were used to identify anomalous geochemical data: the boxplot method and the Median Absolute Deviation (MAD) on Log-transformed data and in multivariate analysis ,after removing outliers data using Mahalanobid Distances (MD), Principal Component Analysis (PCA) and Cluster Analysis were applied on Log-transformed data and PCs maps were drawn.

Results and discussion

The [median±2MAD] method delivers the lower threshold rather than the boxplot procedure but they are the most easily understood robust approaches [1]. Thirteen geochemical regional element distribution maps using fence values (obtained from [median±2MAD] and upper and lower inner fence of boxplots) were prepared. Five factor maps were also obtained with respect to our investigation. Mineral prospective regions were known such as Cu-anomaly in northwest of the 1:100,000 Bafq Sheet which is located on the reddish sandstone. Iron anomalies are also detected in two regions: northeast and center of the 1:500000 Chahdoogh Sheet and in the near of Choghart Mine.

Conclusion

The 1:100,000 Bafq sheet is interesting in terms of petrology, geochemical anomalies, tectonics, and different variables such as Fe, Ti, V, Pb, Zn and Cu. It is very important to provide a database for this region that can be used as a framework for future exploration programs and for detecting metal anomalies that may indicate potentially valuable mineral deposits.

[1]Reimann, Filzmoser, Garrett (2005) *Science Of The Total Environment* **346**, 1-16.

Biogeochemical consequences of the Palaeoproterozoic Great Oxidation Event: case study from the North China Craton

ZHENGBING SHE^{1,2*} AND DOMINIC PAPINEAU²

¹Faculty of Earth Sciences, China University of Geosciences,

Wuhan, China, zbshe@gmail.com (* presenting author)

²Department of Earth and Environmental Sciences, Boston College, Chestnut Hill, MA, USA, dominic.papineau@bc.edu

Oxygenation of the atmosphere in the Paleoproterozoic concurred with major perturbations in global biogeochemical cycles. While the causes and interconnections of these perturbations are still unclear, the consequences of the changes are equally uncertain. Recent discoveries of negative $\delta^{13}\text{C}_{\text{org}}$ excursion in the Onega Basin (Shunga) of Fennoscandia and the contemporary Francevillian Basin of Gabon have suggested oxidation of massive amounts of organic matter due to increased redox states. Was the Shunga-Francevillian excursion a global phenomenon? In order to address these questions, we investigated the Palaeoproterozoic Hutuo Group (2.14–1.85 Ga) in the North China Craton. The Hutuo Group is a >10-km-thick volcano-clastic and carbonate sequence that has undergone only lower greenschist facies metamorphism. It consists of, in ascending order, a fining-upward clastic succession, a carbonate-mudrock succession with well-developed stromatolites and a coarsening-upward molasse sequence. The Hutuo Group is unusual because it contains the earliest known records of red beds and stromatolites in the North China Craton and possibly hosted eukaryotic microorganisms. Diverse stromatolite morphotypes, ranging from small domical, conical, and columnar forms to bioherms with diameters up to 4 meters, are extensively developed. Petrographic and Raman microspectroscopic studies of the stromatolitic dolostones showed wide presence of finely disseminated carbonaceous material and clusters of organic-walled coccoidal cells that likely represent degraded microfossils. Raman spectra display features of disordered carbonaceous material, which yielded a maximum peak metamorphic temperature of 350°C ($\pm 50^\circ\text{C}$). Carbon isotopes of carbonates yielded $\delta^{13}\text{C}_{\text{carb}}$ values between +1.1‰ and +3.1‰, whereas acid-insoluble carbonaceous material had $\delta^{13}\text{C}_{\text{org}}$ values between -29.5‰ and -19.9‰. These data, together with previous studies, document a generally decreasing trend of $\delta^{13}\text{C}_{\text{carb}}$ values from +3‰ to 0‰ followed by a negative excursion to -3‰, which is also coeval with an abrupt decline of stromatolites. In addition, preliminary data suggest the possibility of a 10‰ decrease in $\delta^{13}\text{C}_{\text{org}}$ values. Although our preliminary data do not show carbon isotope excursions comparable to those of Fennoscandia and Gabon rocks, similar patterns might be preserved in North China. These might reflect oxidative geobiological processes in distinct environments after the Great Oxidation Event, including and expansion of stromatolite-forming microbial communities, massive production and recycling of organic material and redox changes in ocean chemistry.

Geochemistry and stratigraphic correlation of pyroclastic rocks in Songliao basin, NE China

Y.J. SHEN*, R.H. CHENG

College of Earth Sciences, Jilin University, Changchun, China,

shenyj@jlu.edu.cn (* presenting author), chengrh@jlu.edu.cn

Pyroclastic rocks and lava of the first member of Yingcheng formation crop out well in the east margin of the Songliao basin, NE China. The location of the ancient crater has been determined by the lithology and lithofacies association in this volcanic rock formation. While pyroclastic sediments on the volcano slope are difficult to compare only by their lithology as a result of discontinuous accumulation and occurrence of pyroclastic rocks around the crater.

To compare the pyroclastic rocks strata and resume the accumulation on volcano slopes, in the studied area, two profiles of pyroclastic rock in Yingcheng formation (I and II) around the crater have been researched in detail. The strata in profile I can be divided into 18 layers according to the grain size, color and lithology of rocks, and the profile II into 10 layers. 28 samples are collected, each one corresponding to each layer, the first 18 samples (B1-B18) are from profile I, and other 10 samples from the profile II. Major elements in these samples are analyzed.

Major element compositions in the pyroclastic rocks have such three common features as following: ①The inflection point of the major element curve is corresponding to changes of both lithology and grain size; ②Contents of Al_2O_3 and K_2O in the rock are inversely related to that of SiO_2 ; ③Content of Na_2O change little and unaffected by the particle size, but it increases in the point where the lava appeared.

On the volcano slope, native ingredients and post-diagenetic changes of pyroclastic rocks in the same layer are similar. Then contents of major elements in pyroclastic rocks can be used in the stratigraphic correlation of pyroclastic rocks on the volcano slope. As showed in the Fig.1, curves of major elements content in the profile I can be divided into two different sections. SiO_2 content is showing as a decreasing trend in the lower section (samples B1-B10) and weak changes in the upper section (samples B11-B18). While contents of Al_2O_3 and K_2O have an increasing trend in the lower stage and minor serrated fluctuations in the upper stage. In the profile II, however, from the sample B19 to the sample B28, SiO_2 content decreases as a whole, while those of Al_2O_3 and K_2O increase.

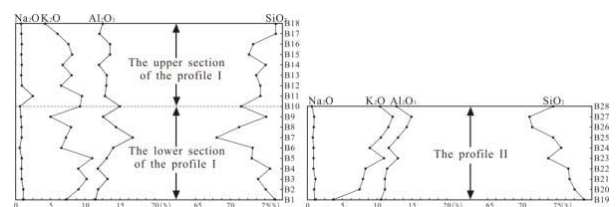


Figure 1: Changing curves of major element contents in pyroclastic rocks from different profiles

By this way, we can draw a conclusion that the profile II is corresponding to the lower section of the profile I.

This research was financially supported by the National Natural Science Foundation of China (Grant 40972074).

The characteristics of volcanic abiogenic hydrocarbons reservoir in Songliao Basin, China

SHENGGUANG ZHUO^{1*}, XIANBIN WANG², AND GUIFANG YANG³

¹Northeast University at Qinhuangdao, China.
zoe200200@163.com (* presenting author)

²Key Lab, CAS, Lanzhou, China, xbwang@lzb.ac.cn

³Northeast Petroleum University at Qinhuangdao, China,
y2000-@163.com

Introduction

The natural gas reserves of Xushen gas field in Songliao Basin, China, is about Hundreds of millions m³, and the reserves of volcanic reservoirs is 89.8%[1], generally the nature gas has abiogenic alkane gases characteristics[2].

Volcanic lithofacies and volcanic genesis

Cretaceous Yingcheng formation is rich in volcanic rock in Songliao Basin, China. Volcanic lithofacies consist of eight types. Such as fallout facies, effusion facies, base surges facies, pyroclastics flow facies, lahar facies, eruption-sedimentary facies, sub-volcanic rock facies and subexplosive breccia facies. The lithology of volcanic rock is mainly middle acid volcanic rock (dacite, rhyolite, middle acid brecciated tuff and tuff), belonging to the calc-alkali series of subalkaline series.

Volcanic reservoir condition

The eruptive and overflow facies have better reservoir condition that has largely been affected by volcanic condensation diagenesis, tectonism, solution and fluid activity, and the volcanic rocks reservoir commonly with the porosity of 6.3%~10.8% and permeability of about $0.55 \times 10^{-3} \mu\text{m}^2 \sim 122.0 \times 10^{-3} \mu\text{m}^2$. The most of effective reservoir are the upper phase or external phase of volcanic facies belts, usually being layers or thin layers of 10~20m.

The pore types of volcanic reservoir

The pores of volcanic reservoir could be classified into four types: ① primary pores of original rocks, ② diagenetic pores, ③ diagenetic fractures, ④ secondary tectoclasts and weathered fractures.

Conclusion

Diagenetic pores and diagenetic fractures of volcanic reservoir are the most effective reservoir space which were formed in volcanic eruption process of cooling and after cooling.

[1] Zhengshun Xu et al (2006), *Petroleum Exploration and Development* **33(5)**, 521-531. [2] Xianbin Wang et al (2009), *Sci. in China D*, **52(2)**, 213-226.

Water vapor sorption on iron oxyhydroxides

XIAOWEI SONG^{*}, JEAN-FRANÇOIS BOILY

Department of Chemistry, Umeå University, Sweden,
xiaowei.song@chem.umu.se (* presenting author)

Iron oxyhydroxide (FeOOH) surfaces are populated with distinct types of hydroxyl functional groups acting as reaction centres with respect to gases, solvents and solutes. Molecular resolution of these reactions is thereby required to develop a fundamental understanding the role of mineral surfaces in the atmosphere, pedosphere, lithosphere as well as hydrosphere.

In this work water vapor sorption reactions on three FeOOH polymorphs (α , β , γ) are probed by Fourier transform infrared spectroscopy. O-H stretching vibrations of surface hydroxyls are monitored with water loadings. These measurements provided clues to hydrogen bonding patterns adopted by physi- and chemi-sorbed water molecules. The water bending region moreover transformed from gas-like to water-like features with loadings increasing from vacuum to 20 Torr. These modes were used to develop thermodynamic adsorption model predicting water uptake on the different FeOOH polymorphs considered in this work.

Molecular dynamics simulations were used to suggest possible interfacial water structures at the FeOOH/gaseous water interface. Hydrogen bonding populations, patterns, strengths and dynamics were also extracted from these simulations. This work opens a path for understanding water structure as well as condensation reactions on these important mineral particles.

Minor and trace element abundance of Cr-spinel from forearc mantle and abyssal peridotites.

FABIO STERN^{1*}, KEIKO HATTORI¹, BENOIT SAUMUR¹
AND SIMON JACKSON²

¹University of Ottawa, Department of Earth Sciences
fster095@uottawa.ca (* presenting author)

khattori@uottawa.ca
bmsaumur@gmail.com

²Natural Resources Canada, Geological Survey of Canada
Simon.Jackson@NRCan-RNC.gc.ca

We examined chemical compositions of Cr-spinel in forearc mantle peridotites from the Marianas, Himalayas, Bay of Island Ophiolite Complex (BOIC) in Newfoundland and the northern ultramafic belt in Dominican Republic. The origin of the Himalayan peridotites is similar to that of the Mariana samples; both represent refractory peridotites in a mature stage of subduction zones whereas BOIC and Dominican Republic samples represent an infant stage of subduction zones. To characterize the spinel compositions from forearc mantle peridotites, spinel in abyssal peridotites from Dominican Republic was also examined.

Cr-spinel is commonly rimmed by magnetite, but the cores of Cr-spinel have low YFe³⁺ (<0.10) and similar compositions among different grains in individual samples. Therefore, the cores are considered to be primary. Cr-spinel grains contain high Cr# in the Himalayas (0.60-0.76) and Marianas (0.68-0.73) compared to those from the BOIC (0.40-0.64) and Dominican Republic (0.20-0.39) in abyssal peridotites; 0.47-0.66 in forearc mantle peridotites).

Nickel concentration in Cr-spinel from all locations range from 276 to 2166 ppm; showing a broad positive correlation with Mg#, confirming their coherent behaviour in the mantle. High Ni contents (887–2166 ppm) are found in spinel in abyssal peridotites from Dominican Republic and low contents (317-470 ppm) are found in forearc mantle peridotites from the Himalayas. The correlation suggests that S was low in all locations during partial melting.

The Cr-spinels in all samples have significant amounts of Co (272-777 ppm), with an average of 405 ppm. Cobalt has a strong inverse correlation with Mg# and a positive correlation with Cr#. Co contents are low (295-367 ppm) in abyssal peridotites from Dominican Republic and high (574-777 ppm) in forearc mantle peridotites from the Himalayas, suggesting that Co is compatible in spinel in the mantle during partial melting.

Manganese has the widest range of concentration among the minor elements from 938 to 5535 ppm. It shows a positive correlation with Fe²⁺ suggesting Mn also resides in the octahedral site. Cr-spinel in abyssal peridotites from Dominican Republic shows low Mn contents (938–1446 ppm) whereas the Himalayan Cr-spinel shows high contents (2432-5535 ppm).

Our data document very large variations in minor and trace element abundances in spinel compared to major elements; some elements, such as Ti and Ni, show variations greater than one order of magnitude, and the trace and minor element abundances provide distinct geochemical signatures reflecting tectonic settings of the host rocks.

Compositionally stratified magmas at Merapi volcano, Indonesia

JOHN STIX¹, OLIVIER NADEAU^{2*}, ANTHONY WILLIAMS-JONES¹

¹McGill University, Earth & Planetary Sciences,
stix.john@mcgill.ca

²UQAM, Science de la terre et de l'atmosphère,
nadeau.olivier@uqam.ca (* presenting author)

Silicate melt inclusions are commonly used to study magmatic systems because these minuscule droplets of melt are entrapped by crystals growing in magma chambers and thus represent snapshots of an evolving magma. In the present study, major and volatile elements were analyzed in melt inclusions by electron microprobe and secondary ion mass spectrometry, respectively. Water and CO₂ concentrations were used to estimate the pressure at which the inclusions were trapped. The composition of the melt varies with depth with more mafic melt inclusions trapped at deeper levels and more evolved melt inclusions at shallower levels. The varying concentrations of H₂O, CO₂, S and Cl in the melt allowed us to calculate the composition of the fluid that would degas from the magma, in either an open or a closed system. This composition was compared to that of gas samples collected at Merapi in 1977, 1994 and 2006. The model H₂O, CO₂ and S concentrations are similar to the measured concentrations of these gases, whereas the modeled Cl concentration is considerably higher (~6.1 mol.% HCl versus ~0.9 mol.% HCl).

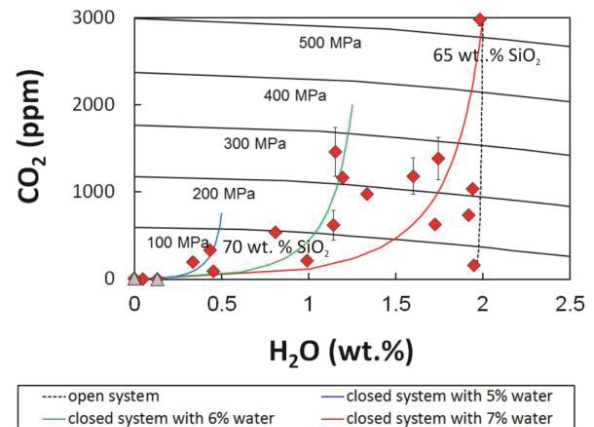


Figure 1: Concentration of CO₂ and H₂O in silicate melt inclusions (red diamonds) and matrix glasses (grey triangles). Error bars are shown when greater than the diameter of their symbols.

In the light of these results, a new model is proposed for the structure and dynamics of the magmatic-hydrothermal system beneath Merapi volcano. Within the upper 18 km (3.5 km/100 MPa) of the crust underlying the volcano, the magmatic-hydrothermal system is compositionally stratified, with a volatile-saturated melt having a SiO₂ concentration of ~65 wt.% at 18 km depth and 70 wt.% in the near-surface lava dome. With injection of magma from below, lava erupts at the surface maintaining the system in a 'steady-state'. As this magma rises, it degasses a hydrothermal fluid. Sinks for Cl (groundwater and crystallizing chloride-bearing minerals) may explain the anomalously low measured Cl concentration of the gas.

Nanoparticle tracer transport through heterogeneous porous media

SASI SUBRAMANIAN^{1*}, LAWRENCE CATHLES²

¹The KAUST-Cornell Center for Energy and Sustainability and Cornell University, Department of Earth & Atmospheric Sciences, Ithaca, USA, sk772@cornell.edu (* presenting author)

²Cornell University, Earth & Atmospheric Sciences, Ithaca, USA, lmc19@cornell.edu

Introduction

Nanoparticles have a diffusion constant at least an order of magnitude greater than inert chemical tracers such as KBr, and this means that they can potentially be used to measure the degree to which subsurface flow occurs through fractures. Laboratory experiments shown in Figure 1a illustrates how fracture flow can be detected by passing water containing both KBr and 5-10nm carbon nanoparticle tracers through a portion of the subsurface (or in this case laboratory apparatus). When the fluid and tracers are injected into a permeable core channel (fracture) at the rate of one core pore (fracture) volume every 5 days, the KBr tracer has time to diffuse into the surrounding halo much more than the particle tracer and arrives much sooner in the effluent (Fig 1a). When the flow is fast (1 core pore volume injected in a few minutes), neither tracer has time to diffuse into the halo and both arrive in the effluent simultaneously (Fig 1b).

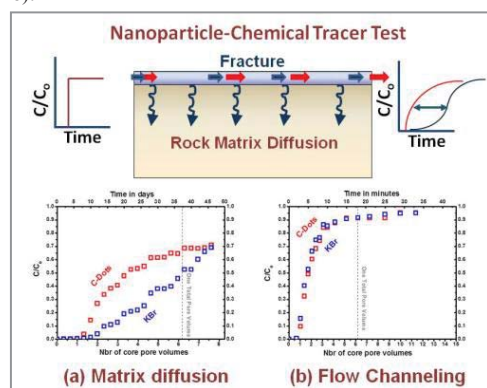


Figure 1 Water containing carbon nanoparticles and KBr tracers is injected into a rectangular core open to a thin slit (rock matrix halo) into which the tracers can diffuse. (a) Plot of concentration of the tracers in the effluent when injection is at a very slow rate. (b) When the injection is rapid (in minutes rather than days) neither tracer has time to diffuse into the halo and both emerge together.

We have carried out this kind of experiment in apparatus of 4 different designs (Hele Shaw slit as in Figure 1, beadpack rectangular Hele Shaw style cell, and two cylindrical beadpack columns with a permeable coarse bead central core). Interpretation required models that take into account the flow in the halo as well as the core, and include dispersion. All experiments could then be interpreted in a consistent fashion. This success suggests that it may be possible to assess the extent of fracture-controlled flow in the subsurface by combining non-sticking nanoparticles with an inert chemical tracer. The key is to develop nanoparticle tracers that do not aggregate or stick to any mineral surface.

Arsenic mobilization from contaminated aquifer sediments by chemical amendments for accelerated remediation

JING SUN^{1*}, STEVE CHILLRUD², BRIAN MAILLOUX³, AND BENJAMIN BOSTICK⁴

¹Columbia University, New York, U.S.A.

jingsun@ldeo.columbia.edu

²Lamont-Doherty Earth Observatory, Palisades, U.S.A.

chilli@ldeo.columbia.edu

³Barnard College, New York, U.S.A. bmaillou@barnard.edu

⁴Lamont-Doherty Earth Observatory, Palisades, U.S.A.

bostick@ldeo.columbia.edu

Pump-and-treat (P&T) is a widely used option for plume containment and aquifer clean up of various environmental hazards in contaminated aquifers, including arsenic (As)—a well known carcinogen. However, remediation of As contaminated groundwater by conventional P&T can often be impeded by slow sustained desorption of As from aquifer solids. Chemical amendments which either compete with arsenate/arsenite for sorption sites or dissolve As hosts such as iron (Fe) minerals, can positively increase As mobility and shorten the timescale of remediation.

Our previous work [1] on oxidized (orange colored) aquifer sediments from Vineland Chemical Company Superfund site (NJ) have showed that both phosphate ($\text{NaH}_2\text{PO}_4 \cdot \text{H}_2\text{O}$) and oxalic acid ($\text{C}_2\text{H}_2\text{O}_4 \cdot 2\text{H}_2\text{O}$, a small organic acid) can substantially enhance release of As from solids where solid-phase As concentrations were between 20 and 100 mg/kg. Conventional P&T also has recently been chosen as the best remediation strategy for Dover Municipal Landfill site (NH). The Dover site is quite different from Vineland from multiple perspectives: 1. The aquifer sediments have much lower As concentrations (2.4–13 mg/kg), 2. They are generally reduced (gray colored), and 3. The As contamination is probably of natural origin. In 24-hour laboratory batch extraction experiments, phosphate mobilized up to 24% of the solid-phase As in Dover sediments (1 mM–1 M phosphate) and oxalic acid mobilized up to 49% (1 mM–100 mM oxalate). The addition of chemical amendments, therefore, appears to potentially improve the P&T operation efficiency in different As-contaminated sites, with a range of pHs and redox potentials. Additionally, oxalic acid is more effective at mobilizing As at lower concentrations than phosphate. At the same time, the results on the two sites suggested that As and Fe solid-phase speciation can strongly impact the extents of As removal induced by chemical amendments, as confirmed by synchrotron-based As XANES and Fe EXAFS spectroscopy. In order to determine optimal amendments for improving P&T, how the initial pH of oxalate solution (pH=1–3) as well as the presence of other ions impact batch extractions were also examined. Our data indicated that Fe dissolution and thus As mobilization were generally encouraged in high acid solutions and when ferrous Fe were added.

[1] Wovkulich (2010) *Applied Geochemistry* **25**, 1500-1509.

Competition Between Direct Electron Transfer and Electron Shuttling Pathways During Microbial Fe(III) Respiration

MARTIAL TAILLEFERT^{1,*}; JUSTIN BURNS², SENG K. WEE², AND THOMAS J. DICHRISTINA²

¹School of Earth and Atmospheric Sciences, Georgia Institute of Technology, Atlanta, USA, mtaillef@eas.gatech.edu (* presenting author)

²School of Biology, Georgia Institute of Technology, Atlanta, USA, thomas.dichristina@biology.gatech.edu

Several mechanisms have been proposed to explain how metal-reducing bacteria transfer electrons to solid terminal electron acceptors, yet the competition between the different pathways has not been extensively investigated. In this study, the direct contact and the electron-shuttling mechanisms involved in the anaerobic respiration of different iron oxides by *Shewanella oneidensis* are compared to determine whether these pathways are complementary or competitive. Kinetic studies were conducted with the wild-type and a mutant strain of *S. oneidensis* lacking an outer membrane porin required for secretion of proteins postulated to be part of the terminal reductase complex. A mathematical model was also developed that accounts for the parallel reduction of iron oxides by the outer membrane terminal reductase and the reduction of exogenous electron-shuttling compounds. The model is calibrated using a suite of independent experiments with the two different *S. oneidensis* strains and the different iron oxides to investigate the competition between these two pathways.

Multi-period Petroleum Accumulation And Adjustment In Carbonate Reservoirs Of Sinian Dengying Formation In Central Sichuan Basin

WANG RUIJU *, WANG ZECHENG, JIANG HUA, LIU WEI, LI YONGXIN

Research Institute of Petroleum Exploration and Development, Petrochina, Beijing, China

(*correspondence: wruiju@petrochina.com.cn)

Background and methods

Sinian Dengying Formation is an important exploration domain in the Sichuan Basin with abundant gas, especially, gas show was found in GGS-1 well on the slope of paleo-uplift in 2011. In fact, sinian carbonate reservoir is also the oldest reservoir in China. The formation and distribution of those reservoirs were major controlled by high energy sedimentary facies, dissolution and faults. Karst weathering crust reservoir in the Dengying Formation in Upper Sinian was distributed quasilayered. The gas was complex accumulated in multi-layer. Those reservoirs were composed of carbonate rocks with low porosity and low permeability, and buried in 4500~6500m depth with intensive heterogeneity. The spatial distribution of effective reservoirs controlled the occurrence of hydrocarbon and accumulated in large area, which showed an integral enrichment characters in paleo-uplift. Through the biomarker correlation study in reservoir soluble bitumen and extracts of source rocks, detailed gas-source rock correlation indicates that gases were mainly originated from both Cambrian source rocks and Sinian source rocks. However, the natural gases were major oil-crack gases from paleo-oil-reservoirs and kerogen crack gas.

Closely associated with the evolution of paleo-uplift, the thermal evolution of source rock organic matter, sedimentary burial history and pale temperature, the paleo-uplift area experienced three stages of hydrocarbon accumulation. The first stage occurred in the Late Caledonian tectonic cycle and a small quantity of the crude oil began to originate from lower Cambrian source rocks. The second stage occurred in the Late Hercynian and Indosinian tectonic cycle which was the most important hydrocarbon charging stage, the abundant oils and gases were made and charged into paleo-traps. The third stage occurred in the late Himalayan tectonic cycle, oil crack gases in paleo-uplift began to generated and adjusted into new traps formed during tectonic periods, while kerogen crack gas in depth, charged into reservoirs along faults, then formed complex gas reservoirs which is now occurred in Central Sichuan Basin.

Results and Conclusion

Carbonate reservoirs of Sinian Dengying Formation in Central Sichuan Basin show very good perspective, and its formation was very complicated.

- 1) The reservoir experienced three periods petroleum accumulation and adjustment at least, which controlled by structure action.
- 2) the natural gases were major oil-crack gases from paleo-oil-reservoirs and kerogen crack gas.

Comparative study of the Ni-laterite profiles under the tropical and subtropical climatic conditions: Examples from Indonesia and China

WEI FU^{1,2*}, HUJIE NIU² AND XIAORONG HUANG²

¹Key Laboratory of Geological engineering in Guangxi, China(fuwe@glite.edu.cn)

²Department of Earth Sciences, Guilin University of Technology, Guilin, China(fuway59@163.com)

Ni-laterite is widely studied from a single deposit perspective. Little attention, however, is directed to understanding what is the difference between the Ni-laterite profiles occurred over similar parent rocks but under different climatic conditions. We present two ideal examples for comparative study. One is from Kolonodale area under tropical climatic condition (eastern Sulawesi, Indonesia), and the other is from Yuanjiang area under the subtropical climatic condition (Yunnan, China). We compared these two profiles based on field geological, mineralogical and geochemical investigations, aiming to provide new details to understanding the role of climate on the genesis of Ni-laterite.

Preliminary study shows some noticeable results as following: (1) The dominant petrographic face in Kolonodale laterite profile is characterized by a thick limonite layer, but a thick saprolite layer in Yuanjiang. The limonite/saprolite thickness ratio between them is distinguished; (2) The Ni-bearing minerals in Kolonodale profile composed of abundant new formed secondary minerals, in particular "garnierite", but little in Yuanjiang profile, where the inherited mineral (serpentine) is the main Ni-bearing component; (3) The redistribution of elements during the laterization process occurred actively in Kolonodale, but exhibiting lower-level activities in Yuanjiang. Typical geochemical indicators show significant differences, such as the depletion coefficient of Mg (up to 0.006 in Kolonodale vs up to 0.077 in Yuanjiang), the residual concentration coefficient of Fe (up to 7.4 in Kolonodale vs up to 7.7 in Yuanjiang), and the secondary enrichment coefficient of Ni (up to 12.5 in Kolonodale vs up to 5.0 in Yuanjiang).

There is trend of increasing in the thickness of the limonite layer, the content of new formed secondary minerals, and the intensity of the element redistribution when the climate changed from the subtropical to tropical environment. These above-mentioned results indicate that the climate play crucial role in controlling the degree of laterite process of ultrabasic rocks, which is positively correlated with the supergene Ni mineralization.

This work was funded by the National Natural Science Foundation of China (Grant No: 41102051) and Natural Science Foundation of Guangxi, China (Grant No: 0991083).

Fluid Inclusion Study on the Duobaoshan Porphyry Copper Deposit, Heilongjiang, China

WEI H^{1*}, XU JH¹, ZENG QD², LIU JM² AND CHU SX²

¹ Resource Engineering Department, University of Science and Technology Beijing, Beijing, China ronghaiwei@163.com

² Institute of Geology and Geophysics, Chinese Academy of Sciences, Beijing, China

Geological Settings

The Duobaoshan porphyry Copper deposit, located in Nengjiang county of Heilongjiang province, China, is the largest porphyry deposit in the Central and northern Daxinganling. Ore bodies are hosted in Hercynian granodiorite pluton underlying Ordovician Duobaoshan formation[1]. Hydrothermal alteration in the central core of the ore bodies is dominantly sericitization, from where it grades outward, one side into a poorly mineralizing potassic halo, and the other side into widespread propylitic alteration[2]. Four ore-forming stages are recognized: (I) potassic and silicic stage; (II) silicification-molybdenum stage; (III) phyllic-copper mineralizing stage; and (IV) carbonate-quartz stage.

Fluid Inclusions and Isotope Compositions

Fluid inclusions are abundant in quartz of various stages. Stage I is characterized by aqueous, and CO₂-rich inclusions, and stage II is dominated by aqueous, CO₂-H₂O, daughter mineral-bearing inclusions. Stage III is also characterized by aqueous and CO₂-H₂O inclusions, whereas stage IV is simply aqueous. Homogenization temperatures and salinities for each stage are shown in figure 1. Estimated trapping pressures for stage I, II, III are 110-160MPa, 58-80MPa, and 8-17MPa, corresponding trapping temperatures are 375-650°C, 310-350°C, 210-290°C.

The δD and δ¹⁸O values of fluids range from -82.2 to -101.5 per mil and 2.0 to 8.1 per mil respectively, which indicates a evolution process from magmatic hydrothermal fluid to a mixing magmatic and meteoric fluid. The δ³⁴S values of sulfides mainly range from -1.6 to -4.6 per mil, suggesting predominantly source of deep magma chamber.

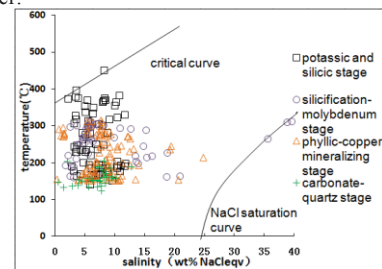


Figure 1: Temperature-salinity diagram of fluid inclusions for the Duobaoshan porphyry Copper deposit

Conclusion

The ore-forming fluid generally belongs to H₂O-CO₂-NaCl fluid system, and mixing, immiscibility and boiling action of ore-forming fluid play a significant role for metallic sulfide deposition.

[1] Wang XC *et al* (2007) Chinese Journal of Geology **42**(1), 124–133. [2] Du Q (1980) Acta Geologica Sinica **4**, 310–323.

Mantle depletion couples Pd and Pb in monosulphide solid solution

NADINE WITTIG¹ AND REINER KLEMD²

¹National High Magnetic Field Laboratory, 1800 E. Paul Dirac Drive, Tallahassee, FL 32310, USA. (wittig@magnet.fsu.edu)
²GeoZentrum Nordbayern, Schlossgarten 5a, 91054 Erlangen, GER

Although Cr-diopsides are typically used to characterize the Pb content and isotope composition of the lithospheric mantle, peridotite sulphides have been proposed to (a) dominate the Pb budget of the upper mantle despite their minute modal abundance (0.01%) and (b) prevent this element from becoming incorporated in the Earth's crust due to the assumed high Pb compatibility in monosulphide solid solution (MSS [1]).

We present *in-situ* LA-ICP-MS measurements of platinum-group element (PGE) and Pb abundances from MSS (n = 28) found in 7 off-cratonic Middle Atlas lherzolite xenoliths in order to test these hypotheses.

These MSS have correlated, but highly variable PGE and Pb concentrations on cm-scale (Pb = <1 to 140ppm; Os = <1 to 600ppm). The MSS are categorized as residual ($[Pd/Ir]_N < 1$) and melt-like ($[Pd/Ir]_N > 1$) species, however, these different PGE systematics are not affiliated with textural occurrence (interstitial vs inclusions). Residual and melt-like MSS have distinctly different $[Os/Pb]_N$, with the former having lower Pb abundances at a given Os concentration. The whole rock PGE systematics [2] appear to result from mixing of the distinct MSS groups analysed here.

Given the well known behaviour of PGE during mantle melting, i.e. the removal of Pt and Pd relative to I-PGE, we may couple Pb to PGE melting theory. In $[Pd/Ir]_N$ - $[Os/Pb]_N$ space, the residual MSS adhere to the depleted mantle evolution if an MSS/melt Pb partition coefficient of ca. 5000 is assumed. In this scenario, melt-like MSS are also well affiliated with the evolution of the corresponding melts. These observations strongly suggest that Pb in MSS behaves similar to Pd and is overall less compatible than previously thought.

Previously determined Cr-diopside U, Th, Nd and Pb abundances and Pb isotopes systematics ($^{206}Pb/^{204}Pb > 19.6$ [3]), together with the MSS Pb concentrations allow simple whole rock mass balancing calculations for the Middle Atlas continental mantle root. Using the highest measured Pb abundances from residual and melt-like MSS, an excess of 93% of the Pb budget is hosted in ortho- and particularly clinopyroxene. To eliminate the extremely high clinopyroxene Nd/Pb (25-260) on the whole rock scale, the associated MSS are required to carry 16x higher Pb concentrations than seen in these xenoliths. Alternatively, the clinopyroxene would need approximately 7x higher Pb than found in the most enriched samples. The Pb component hosted in MSS is also insufficient to appreciably affect the Pb isotopes systematics of the whole rock peridotite, even if the least radiogenic $^{206}Pb/^{204}Pb$ possible (<13) is assigned to the constituent MSS.

Our MSS study implies that mantle melting efficiently extracts Pb from the mantle, rendering a high Pb MSS repository with unradiogenic Pb isotopes implausible to cause the Pb deficit, i.e., Pb paradoxes seen in Earth's geochemical reservoirs.

[1] Hart and Gaetani (2006) *CMP* **152**, 295-308.

[2] Wittig et al. (2010) *Lithos* **152**#, 15-26.

[3] Wittig et al (2010) *GCA* **74**, 1417-1435.

The Triassic lacustrine deposits in the vicinity of maximum flooding surface and oil black shales in Ordos basin, China

YINYE WU^{1*}, LUOFEI WU², TING YUE³, TIANSHU ZHANG¹

¹Research Institute of Petroleum Exploration and Development, PetroChina, Beijing, China, wyy@petrochina.com.cn

²School of Earth and Space Sciences, Beijing University, Beijing, China, wlf_133@sina.com

³China University of Mining and Technology, Beijing, China, yueting200612@163.com

Background and methods

Ordos basin in China with Mesozoic lacustrine shale and siliciclastic reservoirs have new oil discoveries in unconventional resources exploration in recent years. The sedimentary microfacies and diagenetic phase of shales and siltstones are main factors influencing reservoir quality. A detailed study on that domain will be efficient measures for predicting favorable depositional belts and relatively higher quality oil shale belts and silty permeable reservoirs on the background of low porosity and low permeability.

There are 28 lines of outcrops studied and 200 photographs taken on Ordos basin included Yanhe Triassic profile, Linyou-Chenshuihe Triassic profile, Lonxian-Putuohe Triassic and Jurassic profile and Congxin-Nahe Triassic profile and so on. Also there are 20 pieces of siltstones and sandstones sampled and made into thin section for observation.

In view of stacking pattern of parasequence and lacustrine area changes, the Yanhe formation of late Triassic in Ordos basin went through mainly three times of transgression and regression to lead to form multiple deltaic sediments and three sets of source rocks and oil shales in the vicinity of maximum flooding surface. In Yanhe Triassic profile, the shallow lake shale of Chan 7 member can be interpreted as maximum flooding surface, on which there develop mouth bar of deltaic front. Based on above depositional evolution features, most siltstone and sandstones of the fluvial-deltaic distributary channel with crossbedding are sediments formed during early transgressive systems tract period or regressive systems tract period[1].

In thin section observation, siltstones and sandstones from Yanhe Triassic profile have a lot of laumontite cements appeared in the northern and east-northern Ordos basin, originated from provenance full of volcanic materials such as volcanic debris and ash and feldspar minerals. Sometimes laumontite and calcite are appeared in the same visual field of thin section that may imply multi-phase products. Therefore, the key to form high quality reservoirs in Ordos basin is secondary pores of feldspar dissolution, laumontite dissolution and calcite dissolution discovered in different area of Ordos basin.

Conclusions

The distribution of oil shales are controlled by sedimentary facies during transgressive period, but siltstones and sandstones are influenced mostly by diagenetic process. The main sedimentary environments of oil black shales are shallow lake and moderately deep lake in the vicinity of maximum flooding surface.

Key words: unconventional resources exploration, lacustrine facies, delta, black shale, siliciclastic reservoir, Triassic, Ordos basin

***About the first author:** YinYe Wu was born in 1964, and received his PhD degree in petroleum geology from China University of Petroleum(Beijing) in 1992. Now he is a research professor with his research interests in sedimentology and petroleum geology.

[1] Catuneanu. (2009) *Principles of Sequence Stratigraphy*, 165-233.

ZIRCON U-Pb GEOCHRONOLOGICAL AND Hf-O ISOTOPE EVIDENCE FOR CRUSTAL GROWTH AND REWORKING OF A COMPLEX COLLISION OROGEN: AN EXAMPLE FROM THE QINLING-DABIE OROGEN, CENTRAL CHINA

YUANBAO WU^{1*}, HAO WANG¹, ZHENGWEI QIN¹

¹ State Key Laboratory of Geological Processes and Mineral Resources, Faculty of Earth Sciences, China University of Geosciences, Wuhan 430074, China, *Correspondence: yuanbaowu@cug.edu.cn

The formation and evolution of collision orogen is a prominent feature of convergent plate margins, and is generally a complex process including oceanic crust subduction and accretion, continent-continent collision, and final orogenic collapse. Ascertaining continental crust growth and reworking during these processes are crucial for understanding the generation and rearrangement of continental crust on the Earth. Zircon U-Pb ages, Hf and O isotope compositions can be used to distinguish between crustal reworking and generation in different orogenic processes. The Qinling-Dabie orogen marks the suture between the North and the South China blocks in central China, which has experienced oceanic crust subduction and accretion from the late Cambrian to the late Carboniferous, continent-continent collision in the Triassic, and final orogenic collapse in the Cretaceous. An integrated study of zircon U-Pb ages, and Hf and/or O isotope compositions was carried out for igneous or meta-igneous rocks. The results indicate that juvenile magmatic input occurred during the oceanic crust subduction and accretion, and was enhanced during extension and back-arc rifting. While during continent-continent collision and subsequent orogenic collapse, crustal reworking is the main mechanism without significant crustal growth due to the thickened continental lithosphere. Therefore there are quite different styles of crustal growth and reworking from accretionary through collisional to collapse processes of a complex collisional orogen.

Examination of the Biogeochemical processes of the trace metals Mn and Cu and reactive oxygen species in the Tropical North Atlantic

K. WUTTIG^{1,*}, M. I. HELLER², T. WAGENER³, P. STREU⁴ AND P. L. CROOT⁵

¹ Helmholtz-Zentrum für Ozeanforschung Kiel (GEOMAR), Kiel, Germany (kwuttig@geomar.de) (*)

² USC, Los Angeles, USA (miheller@usc.edu)

³ Institut Méditerranéen d'Océanologie (MIO), UMR CNRS – Univ. Aix-Marseille - IRD, Marseille, France (thibaut.wagener@univmed.fr)

⁴ Helmholtz-Zentrum für Ozeanforschung Kiel (GEOMAR), Kiel, Germany (pstreu@geomar.de)

⁵ National University of Ireland - Galway, Galway, Ireland (croot.peter@gmail.com)

Mn and Cu are both redox active trace metals required for a range of critical biological processes in marine organisms. Mn is the active metal centre in several redox enzymes, most notably in Photosystem II where it converts H₂O to O₂, and in the Mn family of Superoxide dismutases (SODs) which are used as an intracellular defence against reactive oxygen species (H₂O₂ and O₂⁻). Cu is widely known to be toxic to most species of phytoplankton, and in particular to pico-phytoplankton, in part because it competitively inhibits Mn uptake and once inside the cells is implicated in the production of reactive oxygen species (ROS). However recent studies have suggested that Cu, in the form of multi-copper oxidases, is essential for the uptake of iron by phytoplankton.

The distribution and speciation of Mn and Cu, contrast markedly in the surface ocean, as Cu(II) is found as strongly organic complexes while Mn(II) is mostly present as the free ion. The higher oxidation states of Mn(III/IV) are poorly soluble and react with H₂O₂ to form Mn(II), this redox cycle is completed by slow (chemical or biologically mediated) oxidation of Mn(II) to form MnO₂. However the two metals are strongly linked through the competition for metal binding sites in phytoplankton uptake systems and through common redox processes involving ROS.

In this presentation we will examine a series of datasets collected during 3 recent cruises in the oligotrophic Eastern Tropical North Atlantic (M80/1, M83/1 and MSM17/4) showing the importance of redox processes in the euphotic zone and the Oxygen Minimum Zone (OMZ) on Cu and Mn speciation and reactivity with ROS species including O₂⁻ and H₂O₂. Here we use the collected data to identify the respective contributions of Mn and Cu to ROS cycling in the upper ocean and the implications this has to the residence time for dissolved Mn and Cu in this region.

Enrichment of fluid-mobile elements in forearc mantle peridotites in the Sulu UHP belt, China

ZHIPENG XIE¹, KEIKO HATTORI², JIAN WANG^{1*}

¹College of Earth Sciences, Jilin University, Changchun, Jilin, 130061, PR China, dapeng841216@163.com, wangjian304@jlu.edu.cn (*presenting author)

²Department of Earth Sciences, University of Ottawa, Ottawa, Canada, khattori@uOttawa.ca

The Sulu ultrahigh pressure (UHP) belt represents a northern margin of the Yangtze Craton that was subducted below the North China Craton, to a depth greater than 150 km after the collision of the two continents in mid Mesozoic time. The peak metamorphic condition is estimated to be ~ 700 C and > 4.0 GPa (Ernst et al., 2007). The rocks in the Sulu UHP belt are well exposed in the southeastern part of the Shandong Peninsula. They are mostly granitic gneisses and eclogites, but minor volumes of ultramafic rocks are common in the belt. This study examined ultramafic rocks from Yangkou Bay and the Suoluoshu-Hujialin area. Ultramafic rocks form lenticular to rounded bodies within UHP rocks with some in the Hujialin area larger than 5 km in length.

Primary silicate minerals are pervasively hydrated to form serpentinites except for dunite samples in Hujialin. Relict olivine in Hujialin dunite has high Mg (Fo = ~ 92) and NiO contents (0.35-0.4 wt%) and the compositions of olivine and spinel plot in the refractory forearc mantle field in the olivine-spinel mantle array of Arai (1994). The bulk rock compositions show low moderately incompatible elements, such as Ca, Al, V and Ti, and plot in refractory mantle peridotites. Furthermore, high Ir-group PGEs (13 to 22 ppb in total) in bulk rocks and high Cr# (0.66-0.8) in spinel confirm that these ultramafic rocks are residual peridotites after extensive partial melting. High values of Cr# compared to those for abyssal peridotites suggest that they originated from the wedged mantle overlying the subducted Yangtze Craton below the North China Craton. These ultramafic rocks including dunite with relatively low loss on ignition (~ 6.6 wt%) show a prominent enrichment of fluid-mobile elements, such as Sb (20-200 times the primitive mantle value) and Pb (8-100 times the PM value). The enrichment pattern is similar to forearc mantle serpentinites elsewhere reported by Hattori & Guillot (2007). The degrees of the enrichment are comparable to the Himalayan serpentinites, and greater than forearc mantle serpentinites from the Dominican Republic and Marianas. The data suggest that the enrichment of fluid-mobile chalcophile elements is prevalent in mantle wedge peridotites and the degrees of enrichment are greater in continental subduction zones than oceanic subduction zones. This difference likely reflects the compositions of subducted material. Shallow water sediments on the margins of continents are commonly enriched in fluid-mobile elements and readily release them to the overlying mantle.

This research was jointly supported by a grant from the NSERC of Canada to KH and grants from the National Natural Science Foundation of China (Nos. 41173034, 90814003).

[1] Ernst et al. (2007) *Geol Soc Am Sp. Pap* 433, 27-49.

[2] Arai (1994) *Chem Geol.* 111, 191-204.

[3] Hattori & Guillot (2007). *Geochem. Geoph. Geosys.* 8, Q09010.

To Explore Ore-forming Processes of Sphalerite by Fe-Ca-Zn Three Components Coupling System

D. XU^{1,4*}, Q. CHENG^{2,4}, S. XIE^{3,4}, Z. YUAN^{2,4}

¹ School of Economics and Management in China University of Geosciences, Wuhan, China, xdy@cug.edu.cn (*presenting author)

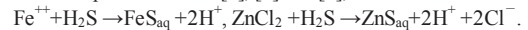
² Faculty of Resources in China University of Geosciences, Wuhan, China, qiuming@cug.edu.cn

³ Faculty of Geosciences in China University of Geosciences, Wuhan, China, tinaxie2006@gmail.com

⁴ State Key Laboratory of Geological Processes and Mineral Resources, China University of Geosciences, Wuhan, China, xdy@cug.edu.cn

Vectoring towards mineral deposits: integrated spatial analysis of geochemical and other mineral exploration datasets

In exploring the complexity of the nonlinear dynamic system of sphalerite ore-forming processes, two components Fe and Zn were considered in previous work [1], [2] and [3], as in



Recently, the contents of 22 elements on each of 307 points on an intersection of a sphalerite hand sample were measured, in situ. As we considering the spatial distribution features of elements related to the forming of sphalerite within only one forming procedure, against-logarithm-of-Calcium transformation was suggested. We found statistically

$$N\left(\frac{C(X)}{\log(C(Ca))} > r\right) \propto r^{-\alpha},$$

where $N(\cdot)$ is the number, $C(X)$ is the content of element X , r is the scale of the content and α is the fractal exponent.

The discovery implies that the dissolution and the recrystallization of CaCO_3 in the forming process of sphalerite play positive and negative feedback roles either in the limitation of the host space or in the reaction and diffusion processes of related components. Therefore, Fe-Ca-Zn three components coupling system was put forward to study the complicated nonlinear dynamic phenomena in the forming processes of sphalerite. The Cellular Nonlinear Network (CNN) method [3] was applied to simulate the diffusion-reaction processes, and the Diffusion limited Aggregation (DLA) models [4] were applied to explore the coupling rule of the host space limitation by the dissolution and recrystallization of CaCO_3 and the chemical reactions in the forming of sphalerite.

In this study, significant discoveries were obtained, such as zonations of FeS and ZnS in an intersection space perpendicular to the axes of the calcite crystal, bifurcations of the mole fraction of FeS on the sphere surface of sphalerite crystallites, and fractal oscillations of the radiuses of sphalerite crystallites.

This work was financially supported by NSFC (Nos. 40972205, 40872195, 40525009), National High-tech R&D program of China (2009AA06Z110) and Project of China Geological Survey (Nos. 1212010633910, 1212011121101).

[1] D. Xu et al. (2010) *Computers & Geosciences* 36 895-901. [2]

S. Katsev et al. (2001) *Physics Letters A* 292 66-74.

Mo isotope of Early Cambrian black shales and associated polymetallic Ni-Mo-(PGE-Au) mineralization in South China

XU LINGANG^{1*}, BERND LEHMANN², MAO JINGWEN¹,
THOMAS F. NÄGLER³ LIU MIN¹

¹ Institute of Mineral Resources, Chinese Academy of Geological Sciences, Beijing, China, xulingang@sina.com (*presenting author)

² Technical University of Clausthal, Clausthal-Zellerfeld, Germany, lehmann@min.tu-clausthal.de

³ University of Bern, Bern, Switzerland, naegler@geo.unibe.ch

Molybdenum is a redox-sensitive element and its isotope fractionation occurs during Mo removal from seawater to marine sediments under a wide range of environmental conditions and provides basic information on the paleo-redox conditions of the ocean-atmosphere system [1]. In south China, the transgressive Early Cambrian black shale sequence of the Niutitang Formation occurs across the Yangtze Platform for about 1600 km-long. An unusual organic carbon-, phosphate- and sulfide-rich polymetallic Ni-Mo-(PGE-Au) ore layer is locally distributed in the lowermost part of the black shale sequence [2]. This black shale sequence and peculiar polymetallic sulfide ore layer may be relevant to understand the Early Cambrian ocean-atmosphere system.

We studied a stratigraphic profile of the Niutitang Formation (Dingtai profile), and three polymetallic Ni-Mo-(PGE-Au) sulfide ore deposits (Dazhulishui, Maluhe and Sancha), and introduced a periodic replenishment model for strong variability of $\delta^{98/95}\text{Mo}$ values (from -1.56 to 1.71 ‰). Based on the isotope geochemical features, the Dingtai profile can be classified into three intervals. In the interval 1 of the Dingtai profile which hosts the polymetallic Ni-Mo-(PGE-Au) sulfide ore layer, black shales are represented by heavy $\delta^{98/95}\text{Mo}$ values (1.40 \pm 0.44 ‰). The average $\delta^{98/95}\text{Mo}$ value of stratigraphically equivalent sulfide ore is 1.20 \pm 0.16 ‰. We infer that the redox conditions of Early Cambrian seawater in South China during interval 1 were euxinic and that the Yangtze Platform was relatively well connected to the open ocean. The black shale sample with the heaviest $\delta^{98/95}\text{Mo}$ value of 1.71 \pm 0.05 ‰ would represent the Mo isotope composition closest to the coeval Early Cambrian global seawater. Black shales from interval 2 and 3 are characterized by highly variable $\delta^{98/95}\text{Mo}$ values. The lowermost interval 2 is characterized by heavy $\delta^{98/95}\text{Mo}$ values (1.26 \pm 0.05 ‰), generally in the same range as in interval 1, indicating that the basin was relatively well connected to the open ocean. However, the sharp decrease in $\delta^{98/95}\text{Mo}$ down to -0.14 \pm 0.03 ‰ at 4.3 m is likely to reflect major Mo influx from continental material. After that episode, the restricted basins once again connected to the open ocean, leading to Mo components dominantly from the open sea. The heavy $\delta^{98/95}\text{Mo}$ values in the uppermost interval 2 (1.07 \pm 0.03 ‰ and 1.06 \pm 0.04 ‰ at 8.8 m and 10.3 m, respectively) indicate that the water column during this period is still euxinic. The lower part of black shale interval 3 is generally characterized by light $\delta^{98/95}\text{Mo}$ values, with fluctuant $\delta^{98/95}\text{Mo}$ values upwards indicating that terrigenous Mo influx was dominant during the early period of interval 3. The periodically restricted basin situation could be caused by marine transgression/regression episodes, i.e. fluctuating seawater level possibly helped by the local karstic paleotopography. Global sea level change is likely related to the continental reconfiguration during the Early Cambrian and repeated transgressive episodes on the Yangtze Platform are indicated by paleogeographical studies and by relics of evaporitic sedimentation.

[1] Siebert *et al.* (2003) *Earth Plan. Sci. Lett.* **211**, 159-171. [2] Lehmann *et al.* (2007) *Geology* **35**, 403-406.

Origin and evolution of the largest continuous tight gas field in China

YANG ZHI^{*}, WU ZHEN-ZHEN, CAO FENG, LI QI-YAN

Research Institute of Petroleum Exploration & Development, PetroChina, Beijing, China

petroyangzhi@yahoo.com.cn (* presenting author)

Sulige giant gas field is the largest continuous tight gas field in China. This giant gas field is located in north-central Yishan Slope in Ordos Basin, with areas 30 thousand square kilometers, proven reserves over 2 trillion cubic meters, and yearly production over 10 billion cubic meters. The target strata of the field is in the Lower Permian tight sandstones, with the burial depth from 2500m to 4200m, per-well production 10-20 thousand cubic meters per day, and reserves abundance 120-150 million cubic meters per square kilometers.

The coupling relationship between reservoir's diagenesis and gas-charging is the key in the origin and evolution of the continuous tight-gas reservoirs.

The sequent process of compaction, quartz cementation and carbonate cementation causes the sandstone reservoirs tight gradually. The reservoirs were compacted strongly and the grain contacted closely, and the porosity reduction by mechanical compaction mainly functioned within the stage when the burial depth is shallower than 2500-3000 meters. Quartz overgrowth and carbonate cements are ubiquitous, reducing the pores sharply. The siliceous cementation appeared earlier than the carbonate cementation, as the carbonate cements normally developed outside the overgrowth quartz. According to the homogenization temperature of fluid inclusions in the overgrowth quartz, generally from 90 to 140 centigrade temperature, the quartz cementation formed from the late Triassic to early Cretaceous time. For the carbonate cements, mainly ferrocalcite, ferroan dolomite, and ankerite, the homogenization temperature is generally from 120 to 150 centigrade temperature, corresponding to the stage from the Middle Jurassic to Early Cretaceous. Moreover, both $\delta^{13}\text{C}$ and $\delta^{18}\text{O}$ of carbonate cements, within the range of -15.7‰~-6.9‰ and -19.8‰~-14.4‰, respectively, show negative values, indicating a significant effect of hot organic fluids. When the gross porosity reduced to less than 10%, corresponding to the Early Cretaceous time, the reservoir was too compacted to have buoyancy force work, let alone the differentiation of fluids. On the other hand, the coal measures generated and expelled a great part of gas during 140-95 Ma, and at that time the thermal event happened, followed by the tightness event. Although the heterogeneity of the reservoirs was obvious, gas-generation-caused overpressure drove the gas through micro-fractures upward. Besides, coal-bearing source rocks contact the shallow delta sand closely in large dimensions. It shows the macro pattern of down-generating and up-preserving, so it is easier for the expelled gas to migrate upward to the reservoirs. Although, the basin was uplifted and evolved into a low temperature and low pressure basin, micro-fractures were well-developed, and the gas reservoirs were modified after the Early Cretaceous, it still remained the previous pattern formed during the main gas-charging stage.

In conclusion, the giant field has two important formation elements.

(1) Sandstone reservoirs became tight prior to gas expulsion from the source rocks, forming the continuous gas deposit; (2) coal measure strata and shallow delta sand-bodies interbedded with each other on a large scale.

The success of Sulige giant gas field, is of great importance for China's unconventional petroleum resources. It breakthroughs the traditional paradigm of trap exploration for conventional reservoirs, and extends new exploratory provinces to the whole basin.

Geochemical peculiarities of Las Cruces deposit (Iberian Pyrite Belt)

LOLA YESARES^{1*}, JOSÉ MIGUEL NIETO¹, REINALDO SÁEZ¹,
GABRIEL RUIZ DE ALMODÓVAR¹ AND JUAN CARLOS VIDEIRA²

¹Huelva University, Geology Department, Spain,

lola.yesares@dgeo.uhu.es (* presenting author)

²Cobre Las Cruces S.A., Spain,

The Las Cruces (LC) massive sulfide deposit is located on the eastern end of the Iberian Pyrite Belt (IPB). It is buried underneath sediments belonging to the Neogene-Quaternary Guadalquivir basin. This disposition has conditioned the postdepositional evolution of the LC deposit, including the particular geochemical features of the weathering profile. The orebody is mainly characterized by a thick supergene profile which includes the gossan and the underlying Cu-rich secondary ore. This cementation zone replaces most of the primary ore, and constitutes the present mining project which involves the exploitation of 17.6 Mt at 6.2 % Cu. In addition, there are about 2Mt of gossan, as a feasible resource of Au, Ag and Pb.

Two main facies are distinguished in the primary deposit: polymetallic and Cu-rich ores. Polymetallic ore is comprised of 20.7 Mt with average grades of 4.2 % Zn, 2.0 % Pb and 0.8% Cu. Cu-rich ore consists of 4.5 Mt with mean grades of 1.0% Zn, 0.3% Pb and 3.3 % Cu [1]. Silver, Hg and As are mainly concentrated in the polymetallic ore with average values of 42 ppm [1], 52 ppm and 3500 ppm respectively, whereas Bi is mainly associated with the Cu-rich ore showing mean concentrations of 750 ppm. Gold concentration is similar in both ore types with average grades of about 0.5 ppm [1]. Regarding the supergene profile, Cu and Zn are entirely depleted in the gossan, whereas the cementation zone is highly enriched in Cu, even reaching peak values up to 39.3%. Lead and Bi are highly enriched in the gossan with mean grades of 4.5% [1] and 315 ppm respectively, and achieving local maximum values of 44.5% Cu and 375 ppm Au. Gold, Ag and Hg are also enriched in the gossan, showing average concentrations of 5 ppm Au, 115 ppm Ag [1] and 52 ppm Hg. These values strongly increase downwards in the gossan profile. In addition, gossan shows uncommon Fe depletion (15% Fe) as compared with primary sulfides (38% Fe). It is also remarkable the high carbonate content in the LC gossan, giving C_{tot} values higher than 10%.

The LC primary ore shows a geochemical zoning very similar to other VHMS deposits, including IPB massive sulfides deposit [2]. However, the geochemical features of the LC supergene profile differs from usual models [3]. These peculiarities are a consequence of the geological evolution of the area, involving, first the orebody uplifting and later burial below the carbonate-rich sedimentary pile. As a consequence LC deposit was subjected to substantial changes in the hydrochemistry of water-rock interactions. Current peculiar geochemical features of the LC weathering profile occurred due to changes in the redox front, along with processes of interaction with alkaline fluids produced by the circulation of meteoric fluids through the sedimentary pile.

[1] Doyle et al. (2003) *Irish Association for Eco. Geo.*, 381–390.

[2] Marcoux et al. (1996) *Mineralium Deposita*, **31**, 1-26.

[3] Thornber. (1985) *Chemical geology*, **53**, 279-301.

The application of red mud in the treatment of waste water

YU LI-JING¹ AND FENG YOU-LI^{2*}

¹ Henan Polytechnic University, Jiaozuo, P.R.China,
yulijing@hpu.edu.cn

² Henan Polytechnic University, Jiaozuo, P.R.China,
fengyouli@hpu.edu.cn(* presenting author)

1 The physical and chemical properties of red mud

The refining of bauxite to alumina by the Bayer process produces a waste product often referred to as 'red mud'. The density of red mud is $2.70 \text{ g/cm}^3 \sim 2.89 \text{ g/cm}^3$. Its specific surface area is $64.09 \text{ m}^2/\text{g} \sim 186.9 \text{ m}^2/\text{g}$. The cation exchange capacity of red mud is $0.2079 \text{ mg/g} \sim 0.5781 \text{ mg/g}$. The fresh red mud contains water-solubility ion $\text{Na}^+ > \text{K}^+ > \text{Ca}^{2+} > \text{Mg}^{2+}$.

2 Application of red mud in waste water treatment

With red mud as raw material, after washing, acid-washing, roasting activation, it can produce good water treatment agent. It can absorb not only Cd^{2+} , Zn^{2+} , Cu^{2+} , Ni^{2+} , Cr^{6+} , Pb^{2+} heavy metal ions in waste water, but also F^- , As^{3+} , As^{5+} , PO_4^{3-} nonmetal ions. In addition, red mud can absorb a amount of radioactive elements such as Cs, Sr, U, Th. The red mud grain has good absorbing ability to Cu^{2+} , Pb^{2+} , Zn^{2+} , Ni^{2+} , Cr^{6+} , Cd^{2+} heavy metal ions. The red mud can remove Ni^{2+} , Cu^{2+} , Zn^{2+} 100%, 68% and 56% respectively. Prilling red mud has good adsorption capacity to Cu^{2+} , Pb^{2+} , Cd^{2+} , the most adsorption capacity is $\text{Cu}^{2+} > \text{Pb}^{2+} > \text{Cd}^{2+}$. The reason of high adsorption capacity of red mud to heavy metal attributes to the surface activity of oxide. The activated red mud using HCl can absorb the fluoride in water and the eliminating efficiency for F^- is 82% [1].

The experiment shows that the heat-treated ($200 \text{ }^\circ\text{C} \sim 800 \text{ }^\circ\text{C}$) and acid-treated (HCl) have good absorption to As in water, when As mass concentration is 10 mg/L and the red mud is 20 g/L, the eliminating efficiency is 96.52% within 1 hour at $25 \text{ }^\circ\text{C}$ [2].

Results and Conclusions

Red mud can not only restore environment, but apply in material synthesis. So, there is a future market to develop the function of red mud, it can treat waste water. It has many advantages such as lower costs, simple technology and using waste to treat waste.

[1] Cengeloglu et al. (2002) *Separation and Purification*,

Technology, **28**, 81-86. [2] Altundogan, et al. (2002) *Waste Management*, **22**, 357-363.

Metallogenic age and Tectonic settings of Sirehong Skarn Cu deposit in Xinjiang, China: Constraints of Zircon U-Pb dating

X. F. YU^{1,2*}, F. Y. SUN², Z. Q. HOU¹ AND J. CHEN²

¹ Institute of Geology Chinese Academy of Geological Science, Beijing, China, xfyu@jlu.edu.cn (*presenting author)

² College of Earth Sciences, Jilin University, Changchun, China

The Sirehong deposit, located in the west segment of the Western Kunlun in Xinjiang, is a newly discovered skarn Cu deposit in northwest China. Ore-bearing strata mainly consist of Carboniferous metasandstone, biotite-quartz schist and interbedded marble. Ore bodies in this deposit mainly lie in the contact zone between the diorite porphyrite and marble, and the ore-hosting rocks are dominated by skarn. The fact that some high-temperature skarn minerals as magnetite occur in the contact means that skarn alteration is closely related to the mineralization.

To determine the metallogenic age and tectonic settings of this deposit, zircons from the metallogenic diorite porphyrite have been researched by CL imaging and LA-ICP-MS U-Pb dating. Zircons in CL images are light and have wide oscillatory zonings. High contents of U ($151.86 \sim 1317.72 \times 10^{-6}$), Th ($84.28 \sim 340.56 \times 10^{-6}$), and ratios of Th/U ($0.34 \sim 0.83$, most over 0.40) imply these zircons belong to typical magma-derived ones [1]. U-Pb ages of zircons from the diorite porphyrite change from 239Ma to 244.2Ma, with an upper intersection age of $239.8 \pm 1.51.5$ Ma (MSWD=1.1, n=17).

It can be concluded that the metallogenic diorite-porphyrite in Sirehong skarn Cu deposit was emplaced in 239.8 ± 1.5 Ma and caused by the Triassic magmatism. The metallogenesis had closely spatio-temporal relationship with the diorite porphyrite. Namely, in the early Indosinian period, the subduction of Qiangtang plate to Tarim plate induced closing of the Paleo-Tethys Ocean, which resulted in a series of acid-intermediate magmatic rocks in the studied area [2]. The magmatic hydrothermal solution carrying a lot of ore-forming material, when arrived at the contact zone between diorite porphyrite and marble wall rock, resulted in the Cu mineralization. Moreover, there happens not only an important magmatic event in Triassic period, but also an associated polymetallic mineralization.

This research was supported by basic research grants from Jilin Province (No. 201115034).

[1] Wu and Zheng (2004) *Chinese Science Bulletin* **49**(15), 1554-1569. [2] Bi (1999) *Science in China (series D)* **29**(5), 398-406.

Wallrock alteration and fluid inclusion study on the Dongping gold deposit, Northern Hebei, China

ZHANG GUORUI¹, XU JIUHUA¹, WEI HAO¹, SONG GUICHANG², ZHANG YABIN², AND ZHAO JUNKANG²

¹ Resource Engineering Department, University of Science and Technology Beijing, Beijing, China, zgr0819@126.com

² Chongli Zijin Mining Co., Ltd, Chongli, Hebei, China

Ore Geology

The Dongping gold deposit, situated in northern Hebei Province, China, occurs in the Hercynian Shuiquangou alkaline complex near the south flank of Shangyi-Chongli fault [1]. Gold-bearing ore bodies were emplaced in the Yanshanian, and potassic alteration is the most important for gold mineralization [2]. Alterations and mineralization of the Dongping gold deposit can be divided into four stages: (I) feldspar-quartz veins stage; (II) pyrite-white quartz stage; (III) sulphides-smoky gray quartz vein stage; and (IV) late carbonate stage. Zonation is clear in altered fractured ore-controlling rocks, and five zones from unaltered syenite of footwall to centre of ore body can be distinguished.

Fluid Inclusions

Fluid inclusions in various vein quartz of the Dongping gold deposit can be divided into three types [3]: 1) CO₂-rich inclusions, including L_{CO2}-L_{H2O} two phase inclusions and L_{CO2}-V_{CO2}-L_{H2O} three phase inclusions under room temperatures; 2) aqueous inclusions (L-V); and 3) one-phase inclusions. Type 1 and 2 inclusions are commonly seen, while type 3 is scarcely. The homogenization temperatures and salinities of L-V and CO₂-rich inclusions in quartz veins of different stages for the Dongping gold deposit are summarized in table 1. The result shows that ore-forming fluids belong to H₂O-CO₂-NaCl fluid systems, and are characterized by CO₂-rich, low salinities, mesothermal to hypothermal fluids.

Table 1: Fluid inclusion characteristics from the Dongping deposit

Stage	Dongping				Zhuanzhilian	
	L-V		H ₂ O-CO ₂		L-V/H ₂ O-CO ₂	
	Th/°C	Sal./%NaCl _{eqv.}	Th/°C	Sal./%NaCl _{eqv.}	Th/°C	Sal./%NaCl _{eqv.}
I	220~359	1.1~3.1	346~383	/	/	/
II	217~372	1.1~5.7	241~397	2.2~6.2	220~416	12.9~20.8
III	158~350	0.7~5.5	215~378	3.0~6.0	195~415	9.1~17.9
IV	151~249	0.9~8.3	/	/	/	/

Conclusion

Gold-rich quartz veins were formed in hypothermal fluids ($T > 300^\circ\text{C}$, up to higher than 400°C) and deep portion (pressures higher than 70~160MPa). It is more reasonable to consider the gold deposit in the Dongping area as intrusion-related gold deposits, based on geological setting, hydrothermal alteration, ore mineral assemblage, and characteristics of fluid inclusions.

[1] Yang (1997) *Geology and Prospecting*, **33**(6), 12-16. [2] Jiang & Nie (2000) *Geological Review*, **46**(6), 621-627. [3] Roedder (1984) *Reviews in Mineralogy*, **12**, 1-644.

Photochemical Vapor Generation for effective mercury removal and trapping

ZHANG RUO XI*, ZHANG YONG

Chengdu University of Technology, Sichuan, China
(*correspondence: zhangruoxi06@cdu.cn)

It is of great concern about the technique for mercury removal from water because of its highly toxic, bio-accumulative and non-degradable natures. There are many techniques have been used to realize this purpose with satisfactory results. However, these techniques are usually limited by their disadvantages including high cost, time consumption, producing secondary pollution.

Therefore, a novel system has been developed to effectively remove mercury from micro-pollution water and further efficiently trap the generated Hg^0 . Meanwhile, the escaped Hg^0 was online monitored to ensure no mercury emission to the environment. The system consisted of two photo-reactors and a commercial atomic fluorescence spectrometer (AFS), Hg^0 generated from the first photo-reactor when mercury solution containing organic compounds exposed to UV light. The Hg^0 was separated from liquid phase in a gas-liquid separator (GLS) and swept to the second photo-reactor by air or argon gas, and was then photo-oxidized for trapping on the surface of the quartz tube. The escaped mercury from over-saturated absorption quartz tube was monitored by AFS for early-warning of mercury leak. The factors affecting the efficiencies of cold vapor generation, transport, collection and monitoring were carefully investigated. Under the optimized conditions, both the efficiencies of mercury removal and collection were nearly 100% in the range of 2–100 $g.L^{-1}$. Moreover, the design of this system also decomposed the organic compounds and made a decrease of chemical oxygen demand (COD) as mercury was removed from the micro-pollution water. It should be noted that the collected mercury could be partly liberated from the inner surface of quartz tube when the UV lamp of second photo-reactor was turn off.

The results indicate that this system provide a safe, green, complete, simple and fast yet inexpensive method for mercury removal from micro-pollution water.

Our research also proved that even without the use of argon gas, use of air still allows the mercury ions degradation in water. We also found that, volatile mercury vapor in the atmosphere can be converted to HgO after illumination by nature light and enriched in solid. It can be said that, the study simulated mercury from water migration and transformation to gas phase then to the solid phase process in nature which added the original way of mercury migration and transformation.

Characteristics, Genesis and Accumulation of the Western Slope Heavy oil in Songliao Basin, China

TIANSHU ZHANG^{1*}, ZHAOYUN WANG¹, YINYE WU¹, TAILIANG FAN², YANLI LIU³

1Research Institute of Petroleum Exploration and Development, Petrochina, Beijing, China, zhangtianshu@petrochina.com.cn (*presenting author), wzy@petrochina.com.cn, wyy@petrochina.com.cn

2School of Energy Resources, China University of Geosciences (Beijing), Beijing, China, fantl@cugb.edu.cn

3Research Institute of Petroleum Exploration and Production, SINOPEC, Beijing, China, liuyanli@pepris.com

The western slope heavy oil in Songliao Basin China prospects well. This study demonstrated the characteristics and genesis of the western slope heavy oil, and the relationship between sequences, microfacies and heavy oil accumulation, and delineated targets for exploration. Detailed information has been acquired by study on group composition, isotopes, chromatography, GC-MS, oil-source correlation, 2700m long cores, thin sections of rocks, logging data of 134 wells, and seismic data. The conclusions are as follows.

Firstly, the western slope oil was long-distance migrated, enduring biodegradation and water washing oxidation [1]. It has the characteristics of relatively low density, medium viscosity, richness in non-hydrocarbon and low content of asphalt. The analyses of GC and GC-MS reveal biodegradation and multiple filling of oil. The 25-norhopane series are absent in the biodegraded oil.

Secondly, source rocks of the western slope oil are mainly the Qing lacustrine mudstones of central depression. The carbonate isotopic values of western slope oil are -29‰ ~ -32‰, that of kerogen are -22‰ ~ -24‰ of Jurassic coal rocks and are -27‰ ~ -31‰ of Qing and Nen mudstones. The source rocks have low maturity, and calculated R_o values are 0.75% ~ 0.95%, based on the index of methyl-phenanthrene and methyl-dibenzene-thiophene.

Thirdly, K-Ar chronology data of reservoir bed authigenic illite of four wells, Ta20, Du66, Fu42 and Lai24, are 56Ma, 45Ma, 35Ma and 35Ma respectively. The above well locations are from east to west successively. Therefore, the oil migration has three stages.

Fourthly, delta front subaqueous distributary channels, mouth sand bars, and lacustrine sand bars are oil-saturated in the vicinity of sequence transform boundaries [2]. Oil accumulates in the transition zones, from a sequence transform boundary to a flooding surface. Oil migration and accumulation is controlled by unconformities, where oil-bearing property is excellent.

Fifthly, microfacies dominate the capability of catching, and enriching oil. Subaqueous distributary channels and mouth sand bars, more easily catch oil through unconformities and faults, but are easily washed due to the shape of strata and range of traps, and consequently form heavy oil reservoirs.

Key words: Songliao Basin, western slope, heavy oil, genesis, microfacies, accumulation

[1] Larter et al. (1996) *Nature* **383**, 593-597. [2] Emery et al. (1996) *Sequence Stratigraphy*, 134-177.

A method to estimate fluid saturation in 2-D three-phase system

YANHONG ZHANG^{1*}, SHUJUN YE¹ AND JICHUN WU¹

Department of Hydrosociences, Nanjing University, Nanjing, China,
yhzhang618@gmail.com

Two-dimensional flow chamber is one of the most important tools for studying multi-phase fluid migration in laboratory. Light transmission techniques with Charge Coupled Device (CCD) camera have been used with two-dimensional flow chamber to monitor the migration of nonaqueous phase liquid (NAPL). A method was firstly developed by Niemet and Selker (2001) to predict liquid saturation of water/gas system in 2D laboratory systems containing translucent porous media by light transmission intensity[1]. However, there is no existed model to relate fluid saturation in NAPL/water/gas three-phase system with light transmission intensity. Three flow cells, similar to Ye et al. (2009) [2], were set up to study the infiltration of NAPL. TCE was selected as NAPL and dyed with red oil O. Two kinds of physically based light intensity-saturation (LIS) models were developed to predict the fluid saturation in three-phase system and verified by the experimental data. LIS models were based on assumptions and simplifications concerning pore geometry, wettability and drainage. For a specified two-dimensional flow cell, the liquid saturation was related only to variation in light intensity which caused by infiltration of TCE. Liquid saturation and its total volume were calculated by LIS models with light intensity observed. Compare to the experimental data, the results showed that the root mean squared errors (RMSEs) were from 2.3% to 20%. It demonstrates that LIS models are applicable in three-phase system. The method allows continuous, quantitative and dynamic full field mapping of the NAPL saturation as well as monitoring saturation variations of water and air during NAPL flow.

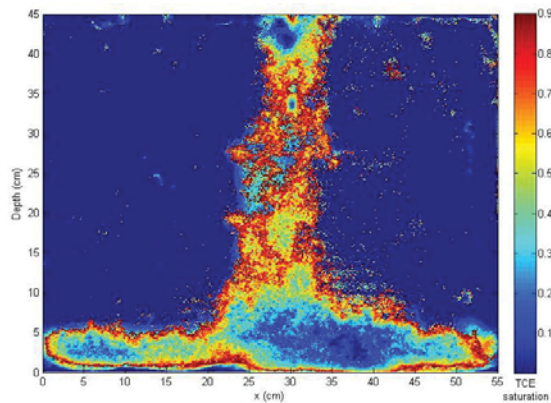


Figure 1: The distribution of TCE saturation in the flow cell in NAPL/water/gas three phase system

Acknowledgements

Funding for this research from 973 Program No. 2010CB428803, from NSFC No. 40872155, 40725010 and 41030746, and also from Fundamental Research Funds for the Central Universities No.020614300003 is gratefully acknowledged.

[1] Niemet & Selker (2001) *Adv. Water Res.* **24**, 651-666. [2] Ye, Sleep & Chien (2009) *J. Contam. Hydro.* **103**, 48-57.

Hydrocarbon Accumulation in Nano-pores

ZOU CAI-NENG^{*}, HU SU-YUN, YANG ZHI, TAO SHI-ZHEN, HOU LIAN-HUA, YUAN XUAN-JUN, ZHU RU-KAI, JIA JIN-HUA, WU SONG-TAO, WANG LAN, GAO XIAO-HUI

Research Institute of Petroleum Exploration & Development,
 PetroChina, Beijing, China

Yangzhi2009@petrochina.com.cn (* presenting author)

The reserves and production of unconventional petroleum increase quite fast in recent years. It proves that nano-pores can also store prolific petroleum resources in tight reservoirs, just as conventional reservoirs do. Global petroleum exploration is shifting its focus from milli- and micro-pores in conventional traps to nano-pores in unconventional reservoirs.

Nano-pore-throat networks develop well and compose the main interconnected storage space for tight reservoirs. The diameters of the main tight reservoirs in Sichuan Basin and Ordos Basin in China range in 20-500 nanometers, those of the source rocks 20-200 nanometers, the tight sandstones 100-500 nanometers, and the shale gas reservoirs 100-200 nanometers.

Nano-pores petroleum reservoirs can play multiple roles, including source, reservoir, and cap rocks. In nanometer pore-throat networks, oil and gas is not significantly affected by hydrodynamic force, with no oil-gas-water differentiation, low-velocity non-Darcy flow, and no unified oil-gas-water contacts or pressure system. Oil and gas are retained and absorbed greatly in tight reservoirs near source rocks. The nano-pores remain prolific petroleum resources in China. Tight gas develops mainly in the Ordos, Sichuan, and Tuha Basin, with prospecting areas of 270 thousand square kilometers and the total resources of 9-12 trillion cubic meters. Shale gas reservoirs occur mainly in the Palaeozoic marine strata, and their exploration and development have been launched with prospecting areas of 630-900 thousand square kilometers and the total resources of 30-100 trillion cubic meters.

Nano-pore hydrocarbon accumulation breakthrough the traditional cut-off threshold for conventional reservoirs and the paradigm of trap exploration. The petroleum reserves do not include the estimated resources from nano-pores, more than 1/3-1/5 of the present reserves, which would be exploited by improved technology in the future. For example, there are 3 trillion cubic meters reserves in the Sulige area of Ordos Basin, north-central China, theoretically 4 trillion cubic meters additional resources from nano-pore reservoirs. Further revolutions by theory innovation, technique progress and cost reduction, will promote these nano-pore hydrocarbon accumulation in tight reservoirs near the source rocks to become actual commercial energies.

-A-

Aacharya, Sabita161
 Abbas, Zareen161
 Abdelkader, Nouiri.....194
 Adkins, Jess.....163
 Ahlberg, Elisabet161
 Aja, Stephen.....162
 Alessi, Daniel.....165
 Alexander, Conel187
 Alleau, Yvan.....181
 Allegre, Claude.....162
 Almodovar, Gabriel R.....205
 Amaach, Nouredin.....162
 Amrani, Alon163
 Anbar, Ariel D.....192
 Andersen, Morten170
 André-Mayer, Anne-Sylvie.....163
 Arndt, Nicholas T.173
 Atkins, Amy164
 Ayrault, Sophie.....185

-B-

Bagnoud, Alexandre.....164
 Bargar, John.....165
 Basterretxea, Gotzon.....192
 Bednar, Anthony.....193
 Bernier-Latmani, Rizlan164, 165
 Bi, Xianwu165
 Bian, Congsheng.....166, 178
 Boily, Jean-Francois.....181, 196
 Borngasser, Gerlinde.....175
 Bostick, Benjamin198
 Bouchez, Julien172
 Bouvier, Laura166
 Boyanov, Maxim.....188
 Brachert, Thomas175
 Brey, Gerhard176
 Brugger, Joel186
 Bruun Hansen, Hans Christian189
 Burdige, David169
 Burns, Justin.....199

-C-

Cable, Jaye.....169
 Cadoux, Anita.....167
 Cai, Jing.....168
 Caineng, Zou.....182
 Campbell, Kate.....165
 Cao, Feng.....204
 Carlson, Hans.....170
 Carlson, Richard.....187
 Carvalho, Maria do Rosario.....167
 Cathles III, Lawrence M.....198
 Cerrato, Jose.....165
 Chabaux, Francois.....190
 Chai, Sheli.....168
 Chai, Yuan168
 Chappell, Mark193
 Chauvel, Catherine.....173
 Chen, Bin.....168
 Chen, J.....206
 Chen, Jin Xia183
 Chen, Youwei165
 Cheng, Qiuming169, 203
 Cheng, R.H.....195

Chevis, Darren169
 Chiaradia, Massimo179
 Chien, Yung-Ching189
 Chillrud, Steve198
 Chirita, Paul171
 Chu, ShaoXiong.....200
 Clark, Iain170
 Coates, John170
 Cogez, Antoine162
 Colman, Benjamin180
 Condon, Daniel170
 Constantin, Cristina.....171
 Cordeiro, Cristina.....171
 Correia, Vania174
 Croot, Peter L202
 Cuney, Michel163

-D-

Dalleska, Nathan.....163
 Dannhaus, Nadine.....172
 Davis, James165
 Debaille, Vinciane173
 Dekas, Ann.....163
 Demichelis, Raffaella.....172
 Dichristina, Thomas J.....199
 Dietze, Volker.....177
 Dong, Shaohua.....165
 Duchemin, Claire173
 Dulin, Shannon.....187
 Durand, Cyril.....163

-E-

Eglinger, Aurelien163
 Eiler, John190
 Ellam, Rob174
 Elmore, R. Douglas187
 Elwood Madden, Megan179
 Evins, Lena179

-F-

Fan, Tailiang.....207
 Favas, Paulo171, 173, 174
 Feldmann, Heinz175
 Feng, You-li205
 Fenn, Tom.....193
 Fernandes, Paula.....167
 Feybesse, Jean-Louis163
 Field, M. Paul192
 Flecker, Rachel174
 Fox, Patricia.....165
 Fraguito, Vania.....174

-G-

Gale, Julian D.172
 Galer, Stephen175
 Gao, Lina.....168
 Gao, Risheng175
 Gao, Xiao-Hui.....208

Garcia-Orellana, Jordi.....192
 Garcia-Solsona, Ester192
 Gerdes, Axel176
 Ghobadi, Mahdi.....176
 Giammar, Daniel165
 Giere, Reto177
 Gole, Martin179
 Goni, Miguel181
 Gonzalez Jimenez, José Maria.....176
 Gordon, Gwyneth.....192
 Griffin, William L.176
 Gu, Zhidong166
 Guan, Yunbin190
 Guifang, Yang.....196
 Gulecal, Yasemin177
 Gutjahr, Marcus.....174

-H-

Haberzettl, Torsten181
 Hamilton, Stephen.....178
 Handley, Kim165
 Handley-Sidhu, S.....191
 Hattori, Keiko197, 203
 Heller, Maija I.....202
 Hellstrom, John.....170
 Henderson, Gideon.....170
 Hoang-Hoa, Thi Bich.....177
 Hochella, Michael.....180
 Hodges, Kyle.....179
 Hou, Lian-Hua.....208
 Hou, Z.Q.....206
 Hu, Qinrong179
 Hu, Ruizhong165
 Hu, Su-Yun208
 Hu, Xiaoyan.....165
 Huang, Chong.....183

-I-

Ivanovic, Ruza174

-J-

Jackson, Andrew190
 Jackson, Simon.....197
 Jakobsen, Rasmus189
 Janot, Noemie.....165
 Jeong, B.C.....191
 Jesus, M. Rosario167
 Ji, Junfeng.....182
 Jia, Jin-Hua208
 Jiang, Qingchun166, 178
 Jin, Lixin178
 Johannesson, Karen.....169
 John, Seth.....163
 Jordi, Antoni.....192
 Jourdan, Fred179

-K-

Kaminski, Uwe	177
Kelly, Roger	169
Kemner, Kenneth	188
Kendall, Matthew	179
Kierczak, Jakub	180
Killick, David	193
Kim, Bojeong	180
Kim, W.H.	191
Klemm, Reiner	201
Koch, Christian	189
Kogarko, Lia	176
Kolczynski, Lauren	181
Kouwenhoven, Tanja	174
Kozin, Philipp	181

-L-

Lafferty, Brandon	193
Lajeunesse, Patrick	181
Lan, Wang	182
Le Mouel, Jean-Louis	162
Lee, C.H.	191
Lehmann, Bernd	204
Lewin, Eric	162
Lezama-Pacheco, Juan	165
Li, B.L.	191
Li, Gen	182
Li, Qi-yan	204
Li, Zeqin	183
Li, Zhi	175
Liu, Ankun	168
Liu, Haitao	166, 178
Liu, JianMing	200
Liu, Weihua	186
Liu, Yan Guang	183
Liu, Yanli	207
Locmelis, Marek	176
Long, Philip	165
Lopes, Ana Rita	167
Lopez, Jose M.	192

-M-

Ma, Lei	184
Macaskie, L.E.	191
Madden, Andrew	179, 187
Mailloux, Brian	198
Mao, Jingwen	204
Mao, Zhiguo	184
Marchandise, Sandra	185
Mark Jensen, Marlene	189
Martin, Jonathan	169
Martin, Philippe	185
Mason, Andrew	170
Masque, Pere	192
Mattielli, Nadine	173
McHugh, Cecilia	162
McKee, Marc	189
McLean, Noah	170
Mei, Yuan	186
Melnyk, Ryan	170
Mertz-Kraus, Regina	175
Meynadier, Laure	162
Mikulski, Stanislaw Z.	186
Miller, Christian	187
Miller, Matthew	187
Min, Kyoungwon	194
Min, Liu	204

Minarik, William	166
Mishra, Bhoopesh	188
Missenard, Yves	167
Moita, Patricia	188
Moran, S. Bradley	169
Mukasa, Samuel	178
Murayama, Mitsuhiro	180

-N-

Nadeau, Olivier	197
Naegler, Thomas	204
Naren, Gaowa	161
Nelea, Valentin	189
Neuville, Daniel	185
Nieto, Jose Miguel	205
Niu, Xiaolu	168
Noble, Stephen	170
Nordholm, Sture	161

-O-

O'Connell, David	189
Ogrinc, Nives	178
Ohashi, Hironori	161
Okaua, Yoshihiro	161
O'Loughlin, Edward	188
O'Reilly, Suzanne Y.	176
Orphan, Victoria	163

-P-

Papineau, Dominic	195
Paquette, Jeanne	189
Pasakarnis, Timothy	188
Paterson-Beedle, M.	191
Peacock, Caroline	164
Pearson, Norman J.	176
Pedro, Jorge	188
Peng, Jiantang	165
Petitjean, Carine	185
Pierret, Marie-Claire	190
Pietranik, Anna	180
Pik, Raphael	166
Pinti, Daniele	166
Poghosyan, Armen	190
Postma, Dieke	189
Pratas, Joao	171, 173
Price, Cynthia	193
Prunier, Jonathan	190

-Q-

Qian, Ye	191
Qin, Zhengwei	202

-R-

Raiteri, Paolo	172
Renshaw, Joanna	191
Richards, David	170
Rickli, Joerg	174
Robin, Eric	185
Rodellas, Valentí	192
Roden-Tice, Mary K.	166
Romaniello, Stephen	192
Roy-Barman, Matthieu	185
Ruiz, Joaquin	193

-S-

Sa, Artur	174
Sajez, Reinaldo	205
Sanchez-Quiles, David	192
Santos, Jose	188
Saumur, Benoit	197
Scherer, Michelle	188
Schlegel, Michel	171
Schwyn, Bernhard	164
Seiter, Jennifer	193
Sessions, Alex	163
Shan, Jingnan	194
Shang, Linbo	165
Shaw, Samuel	164
Shayestehfar, Mohamadreza	194
She, Zhenbing	195
Shen, Y.J.	195
Shengguang, Zhuo	196
Sherman, David	186
Shi, Xue Fa	183
Shi, Yanli	175
Silva, M. Catarina R.	167
Silva, Pedro	188
Song, Guichang	206
Song, Xiaowei	196
Stein, Holly J.	186
Stern, Fabio	197
Stille, Peter	177, 190
Stix, John	197
St-Onge, Guillaume	181
Streu, Peter	202
Stubbs, Joanne	165
Sturchio, Neil	190
Stylo, Malgorzata	165
Subramanian, Sasi	198
Sun, F.Y.	191, 206
Sun, Jing	198
Suvorova, Elena	165
Suzuki, Katsuhiko	168

-T-

Taillefert, Martial	199
Tao, Shi-Zhen	208
Tappero, Ryan	193
Tessalina, Svetlana	179
Testemale, Denis	185
Thamdrup, Bo	189
Thybodeau, Alyson	193
Tovar-Sanchez, Antonio	192
Tremblay, Alain	166

-V-

Vanderhaeghe, Olivier	163
Videira, Juan Carlos	205
Vilasi, Michel.....	185
von Blanckenburg, Friedhelm.....	172

-W-

Wagener, Thibaut.....	202
Walter, Lynn	178
Wang, Hao	202
Wang, Hongjun.....	166
Wang, Jian.....	203
Wang, Jiangzhen	183
Wang, Lan.....	208
Wang, Ruiju	199
Wang, Xingchen.....	182
Wang, zecheng.....	166
Wang, Zhaoyun.....	207
Wee, Seng K.....	199
Wei, Fu	200
Wei, Hao	200, 206
West, Joshua	182
White, Christopher	169
Wiederin, Dan	192
Williams, Kenneth.....	165
Williams-Jones, Anthony	197
Wittig, Nadine.....	201
Wittmann, Hella	172
Woodhead, Jon	170
Wu, Jichun	208
Wu, Luofei	201
Wu, Song-Tao.....	208
Wu, Yinye	201, 207
Wu, Yuanbao	202
Wu, Zhen-zhen	204
Wuttig, Kathrin.....	202

-X-

Xianbin, Wang	196
Xie, Shuyun	203
Xie, Zhipeng.....	203
Xu, Anna.....	166
Xu, Deyi	203
Xu, JiuHua	200, 206
Xu, Lingang	204
Xu, Zhaohui.....	166

-Y-

Yang, Xiaoping	178
Yang, Zhi.....	204, 208
Ye, Shujun	208
Yesares, Lola	205
Ying, Li.....	182
Yokoyama, Takushi.....	161
Yu, Li-jing	205
Yu, X.F.	206
Yuan, Xuan-Jun.....	208
Yuan, Zhaoxian	203
Yue, Ting.....	201

-Z-

Zandieh, Farzaneh.....	194
Zeng, QingDong.....	200
Zhang, Chao.....	168
Zhang, Guorui.....	206
Zhang, Ruoxi.....	207
Zhang, Tianshu	201, 207
Zhang, Yabin	206
Zhang, Yanhong.....	208
Zhang, Yong	207
Zhao, Junkang.....	206
Zhao, Weidong.....	184
Zhou, Xiaoping.....	184
Zhu, Ru-Kai.....	208
Zou, Cai-Neng	208